Characterizing groundwater recharge processes in a semiarid mountain-front using stable isotopes, hydrochemistry and heat as a tracer (Ourika basin, Tensift, Central Morocco)

Houssne Bouimouass

THÈSE DE DOCTORAT D'AVIGNON UNIVERSITÉ

École Doctorale ED536

Agrosciences et sciences

Spécialité / Discipline de doctorat :

Hydrogéologie

Laboratoire UMR EMMAH

Présentée par

Houssne Bouimouass

Characterizing groundwater recharge processes in a semiarid mountain-front using stable isotopes, hydrochemistry and heat as a tracer (Ourika basin, Tensift, Central Morocco).

Soutenue publiquement le 14/01/2021 devant le jury composé de :

Abdelghani CHEHBOUNI, DR, IRD, UM6P, Benguerir, Maroc	Président
Bouabid El MANSOURI, PES, FS, UIZ, Kenitra, Maroc	Examinateur
Christian LEDUC, DR, UMR G-EAU, IRD, Montpellier, France	Examinateur
Lahoucine HANICH, PES, FST, UCA, Marrakech, Maroc	Examinateur
Sarah TWEED, CR, UMR G-EAU, IRD, Montpellier, France	Examinatrice
Younes FAKIR, PES, FSS, UCA, Marrakech, Maroc	Directeur de thèse
Marc LEBLANC, PES, UAPV, Avignon, France	Co-directeur de thèse
Mounia BENRHANEM, Ingénieure principale, ABHT, Marrekech, Maroc	Invitée

Remerciements

Le temps est venu de remercier toutes les personnes qui ont contribué de près ou de loin à la réalisation de ce travail tout au long de ces quatre années.

Cette thèse a été menée au sein du laboratoire GEOHYD (laboratoire Géosciences Semlalia depuis 2019) et l'UMR EMMAH, et n'aurait pu aboutir sans les supports financiers du CNRST, l'université Cadi Ayyad, Avignon université et de l'IRD.

Je tiens tout d'abord à faire part de ma plus profonde reconnaissance aux Professeurs Younes Fakir et Marc Leblanc, les deux directeurs de cette thèse, pour leur implication dans cette étude, leur grande disponibilité, leur gentillesse et leurs nombreux conseils. Merci d'avoir partagé vos connaissances et vos expériences, et surtout de m'avoir donné le courage et la motivation d'aller au bout de cette aventure.

Je tiens également à exprimer toutes mes gratitudes envers les membres de jury pour l'intérêt qu'ils ont porté à mon travail en acceptant d'évaluer cette thèse. Le président M. Abdelghani Chehbouni, Directeur de recherche à l'IRD. Les rapporteurs : M. Christian Leduc, directeur de recherche à l'IRD du Laboratoire G-EAU à Montpellier. Pr. Bouabid El Mansouri, professeur à l'Université Ibn Tofail, laboratoire Géosciences et ressources naturels. Pr. Lahoucine Hanich, professeur à l'université Cadi Ayyad. Mes sincères remerciements à Dr. Sarah Tweed, chargée de recherche à l'IRD et Mme. Mounia Benrhanem, ingénieure principale à l'ABHT m'avoir honoré de leur accord à examiner cette thèse. Les discussions et vos recommandations m'ont aider pour améliorer la qualité de ma thèse.

J'adresse un grand merci à l'équipe du laboratoire d'hydrogéologie d'Avignon de l'UMR EMMAH, qui m'ont accueilli durant deux visites au sein de leur laboratoire. Merci à Milanka Babic et Roland Simler pour les analyses isotopiques hydrochimiques de mes échantillons.

Les résultats acquis au cours de cette étude étant en une grande partie issue de prélèvements et mesures sur le terrain, ces travaux n'auraient pas pu être réalisés sans la collaboration des propriétaires des puits. Je tiens à remercier la faculté des sciences Semlalia pour leur support logistique lors des campagnes de terrain.

Les campagnes d'échantillonnage ont été menées pendant trois ans parfois sous la pluie, sous le soleil de Marrakech et sa chaleur qui peut atteindre 45 °C. Ces sorties de terrain ont parfois tourné en balades amusantes avec ma mobylette à travers les pépinières verdoises de Ghmat,

les champs de pommes dans la vallée de l'Ourika et les paysages blanchâtres dans la vallée enneigée de l'Oukeimden.

Je voudrais également remercier mes camarades thésards et les stagiaires avec qui j'ai partagé des moments inoubliables de la vie doctorante, les discussions quotidiennes intéressantes ainsi que les déjeuners et les pauses café : Younes, Radouan, Jamal, Youssef, Mariam, Malak, Hassan, Abdelkhalek …

Enfin et surtout, je pense à mes proches et ma famille. Je remercie mes parents pour leur soutien constant. Mes parents, des paysans modestes, n'ont jamais mis les pieds à l'école mais qui croyait au rêve de leur fils ainé à devenir le premier docteur de leur petit village. Je tiens à remercier tous mes amis et amies pour leur soutien pendant les bons moments et les périodes plus difficiles.

Résumé

La recharge au niveau des piémonts constitue une source importante de recharge naturelle des eaux souterraines dans les zones arides et semi-arides. Le bassin du Tensift, au centre du Maroc, héberge la plaine du Haouz et l'aquifère alluvial du Haouz dont l'extension spatiale dépasse 6000 km^2. L'eau souterraine est la source d'eau principale pour les activités agricoles, industrielles et pour l'alimentation en eau potable. Cette ressource est considérablement affectée par la surexploitation et le changement climatique. La détermination des sources et processus de la recharge, en particulier au niveau des piémonts, est primordiale pour la gestion efficace des ressources en eau. Malgré son importance, la dynamique de la recharge au niveau des piémonts du Haut-Atlas, comme dans d'autres zones semi-arides autour du globe, reste peu étudiée. L'objectif de la présente étude est d'investiguer, de près, les sources de recharge dans le piémont du Haut-Atlas, en se focalisant sur l'infiltration au niveau des oueds. L'étude est basée sur la combinaison de plusieurs types de données : prélèvements des seguias, piézométriques, isotopiques, hydrochimiques, teneur en eau des sédiments et température des sédiments récoltés sur le terrain. Ces données ont été analysées qualitativement et quantitativement par modélisation. Les données piézométriques et isotopiques (^{18}O et ^{2}H) ont été utilisés pour comparer la recharge naturelle et la recharge induite par irrigation dans le piémont du Haut-Atlas. L'évolution piézométrique a montré que la recharge induite par l'irrigation traditionnelle dépasse celle induite par l'infiltration au niveau des oueds. Cela est en accordance avec la distribution spatiale des signatures isotopiques qui montre l'influence du captage des eaux par Séguias, en période d'écoulement normal sur la recharge des eaux souterraines. L'évolution hydrochimique des eaux souterraines dans la zone d'étude est influencée par les interactions eau/roches, la dissolution des minéraux carbonatés et des évaporites, l'hydrolyse des silicates et les échanges ioniques entre l'eau et les sédiments. L'influence de l'irrigation par les eaux de surface sur la recharge des eaux souterraines et les pratiques agricoles dans la zone d'étude ont préservé la bonne qualité de ces eaux et leur adéquation à l'utilisation domestique. La teneur en eau et la température des sédiments mesurés sur un site expérimental dans le lit de l'oued Rheraya, pendant une année entière, ont été utilisés pour caractériser la dynamique de l'infiltration et de la recharge des eaux pendant les périodes d'écoulements. Ces données sont aussi exploitées pour le calage d'un modèle du transport d'énergie dans le milieu poreux pour calculer les taux d'infiltration. Pendant toute l'année, la recharge totale calculée est de 425 mm/m^2. La recharge est principalement induite par les crues et elle est contrôlée par la saisonnalité, l'état antérieur de saturation des sédiments, la durée des

événements, puis la hauteur du niveau de l'eau. Les résultats de cette étude peuvent être incorporé dans les schémas futurs de la gestion et de la préservation des ressources en eau dans le bassin de Tensift.

Mots clés : Sources de recharge, Eau souterraine, Traçage environnemental, Piémont, Semi-aride.

Abstract

Mountain-front recharge is the recharge of groundwater occurring in the piedmonts of high-elevation mountains often receiving more precipitation due to orographic effects. This type of recharge is the major source of groundwater replenishment in many semi(arid) basins. The Tensift basin in central Morocco hosts the large alluvial plain of Haouz with its vast phreatic aquifer of more than 6000 km^2. Groundwater in the Haouz plain is the main source of water for the socio-economic activities in the area. This groundwater originates from the adjacent High-Atlas ranges. Despite the importance of mountain-front recharge for the socio-economic development in the area, it was never investigated with care but only incorporated in a very limited regional-scale studies providing highly speculative conclusions. The aim of the present study is the close investigation of recharge sources in the mountain-front area of the High-Atlas of Marrakech at the local scale, with an emphasis on infiltration within wadi channels. Hydrophysical data (piezometry, sediment water content and heat), hydrochemical (major ions) and environmental tracers (stable isotopes of water) from field campaigns and experiments were used in this study. The data acquired was analyzed by analytical methods and modeling (heat transport modeling). Coupled groundwater fluctuation measurements and environmental tracers (^{18}O, ^{2}H, and major ions) were used to identify and compare the natural mountain-front recharge to the anthropogenic irrigation recharge. Within the High Atlas mountain front of the Ourika Basin, Central Morocco, the groundwater fluctuation mapping from the dry to wet season showed that recharge beneath the irrigated area may be higher than recharge along the streambed. A conceptual model of seasonal groundwater recharge sources in the study area was established. These findings highlight that irrigation practices can result in the dominant mountain front recharge process for groundwater. The hydrochemical evolution of groundwater in the mountain-front area is controlled mainly by water-rock interactions through mineral dissolution, silicate weathering and ion exchange. The strong relationship between groundwater and mountain water, enhanced by traditional irrigation, and the ecological agriculture practiced in the area preserved the excellent quality of groundwater. Streambed water content and temperature were continuously logged over a year for the Rheraya intermittent wadi. Over the entire year, the calculated total potential recharge based on heat transfer modeling was 425 mm/m^2. During winter and spring when the alluvium has a higher water moisture, this recharge is predominantly generated by floods. Normal streamflow generally generates low infiltration but contributes to wetting the sediment. During the summer, brief flashfloods over dry sediment result in shallower and slow wetting from infiltration, despite of their higher peak streamflow.

Results from this study can be incorporated in future management schemes for the water resources preservation in the Tensift basin.

Keywords : Recharge sources, Groundwater, Environmental tracing, Mountain-front, Semiarid.

Summary

Chapter 1: Introduction

I. General background

Since the dawn of history, freshwater has been and still the key driver of human civilization. As for primitive human societies always settled near water, water is strongly linked to the development of all modern societies. Water is crucial for food security, poverty reduction and sustainable development. Groundwater constitutes the second important reservoir of freshwater in the world after ice caps (Gleick, 1996), and it is also considered as the predominant water resource for human survival and social development in the World (Holland et al., 2015). Groundwater is used in drinking water supply to human agglomerations, agriculture and industry (Aeschbach-Hertig and Gleeson, 2012). However, this precious resource is experiencing severe depletion and quality deterioration (Taylor et al., 2009), due to several factors such as population growth, agricultural development, industrialization and climate change (Vörösmarty et al., 2010; Arnell and Lloyd-Hughes, 2014), especially in arid and semiarid areas (Custodio, 2002; Massuel et al., 2013; Baudron et al., 2014).

Arid and semiarid areas cover 30% of the global terrestrial surface area and are expanding (Dregne, 1991). In addition to groundwater issues mentioned above, arid and semiarid areas are characterized by low precipitation and high evapotranspiration, resulting in low annual diffuse rainfall recharge of aquifers (Izbicki et al., 2000; Walvoord et al., 2002). However, high elevation mountains when present can often receive greater precipitation as rainfall and snow due to orogenic effects. They could supply their mountain fronts (piedmonts) by consistent amounts of streamflow that generally generate significant arid and semi-arid groundwater recharge, called Mountain Front Recharge (Blasch and Bryson, 2007; Wahi et al., 2008; Liu and Yamanaka, 2012; Martinez et al., 2017; Bresciani et al., 2018).

Recently in warming climate, the snowfall portion of precipitation in less likely to occur in mountains, and the precipitation regime tends to shift from snow to rain (Knowles et al., 2006). Arising the question of the potential influence of this shift on surface water resources, Berghuis et al. (2014) have showed that this shift is causing a decrease in mean streamflow. By analyzing data of 420 catchments located across the contiguous United States for the period 1948–2014, they found that higher fraction of precipitation falling as snow is associated with higher mean streamflow, compared to catchments with marginal or no snowfall. Furthermore, they showed that the fraction of each year's precipitation falling as snowfall has a significant influence on the annual streamflow within individual catchments. A change in streamflow regime in headwater catchment due to the change of precipitation regime will have a significant impact

on the water resource availability and on the socio-economic context of the downstream communities (Malek et al., 2020).

In order to set efficient management strategies to face these many challenges threatening water resources availability in arid and semiarid areas, a good understanding of groundwater recharge processes in mountain fronts is as mandatory as urgent.

As the case for the whole North Africa, Morocco is characterized by arid to semiarid climate with high inter-annual variability and several periods of below average precipitation (Hertig and Jacobeit, 2008a). The conjunctive effect of population growth, industrial development and the agricultural flourishment have dramatically increased the pressure on water resources during the last two decades (Kadi and Ziyad, 2018). The Tensift basin is one of the main hydraulic basins of Morocco hosting the Haouz plain, one of the biggest plains of Morocco. With no perennial rivers, one dam and one artificial channel bringing water from the adjacent Oum Er Rbia basin, the majority of agricultural and drinking water supplies relies on groundwater pumping. Groundwater within the plain experience severe depletion of 2 m/year (Fakir et al., 2015). Tensift basin is bordered to the south by the High-Atlas Mountains which is often referred to as the water tower for the Haouz plain (Jarlan et al., 2015).

II. Scientific background

II.1. Mountain front recharge (MFR)

Mountain front recharge (MFR) is defined by Wilson and Guan (2004) as recharge from (i) subsurface inflow from the mountain bedrock to the basin floor, via faults and fractures, or via the porous matrix of weathered bedrock aquifers; (ii) infiltration from streambeds to underlying aquifers near the mountain front (Simmers, 2003; Viviroli et al., 2003). This type of focused groundwater recharge is considered a major source of recharge in many arid and semi-arid regions (Shanafield and Cook, 2014), and is induced by perennial (Schmadel et al., 2010), intermittent or ephemeral streams (Niswonger et al. 2008). This terminology considers the subsurface inflow from the mountain block called mountain block recharge (MBR) as a component of MFR, however, recent studies have adopted a new terminology addressing MFR and MBR as two separated components under the mountain system recharge (MSR) (Bresciani et al., 2018). Here we adopt the terminology of Wilson and Guan (2004) and address MBR as a part of MFR.

Despite the importance of mountain front recharge for arid and semi-arid groundwater resources, there remain significant challenges in distinguishing its different sources and their

specific contribution. This is particularly the case in irrigation areas, where the groundwater recharge may also include inflow from irrigation leakage (herein referred to as irrigation recharge) that is often a redistribution of both local- (pumping from alluvial aquifers) and mountain- (floods and streamflow generated from rainfall or snowmelt) derived water.

Mountain front areas are globally important regions for irrigation (Van Steenbergen et al., 2011; Bresciani et al., 2018; Cody, 2018). Water budget analyses and water resources management in these areas need a comprehensive knowledge about groundwater recharge sources and their contribution to adjacent aquifers. Several previous studies have used groundwater fluctuation and seasonal piezometric mounds to analyze recharge processes in mountain-front recharge areas (Shanafield and Cook, 2014; Bresciani et al., 2018). However, although hydraulic head data record the groundwater recharge events, the discrimination of different sources of recharge generally requires the use of environmental tracers. Commonly used tracers include stable isotopes and major ions (Liu and Yamanaka 2012; Zhu et al., 2018). The main advantage of using stable isotopes to analyze the mountain front recharge is that the signature of local rainfall on the plain are likely to significantly vary from the signature of rainfall in the mountains due to rainout effects (Clark and Fritz, 1997; Scanlon et al., 2002; Lambs, 2004; Kalbus et al., 2006). Similarly, for major ions, since changes in recharge rates and flow pathways can result in significant differences in the composition of the major ions, the latter could provide insights into mixing between different groundwater recharge sources (Liu and Yamanaka, 2012).

II.2. Mountain-block recharge

Mountain-block recharge (MBR) is the subsurface inflow of groundwater from the mountain-block to adjacent basin-fill aquifer (Wilson and Guan, 2004). It is important to mention that MBR refers only to groundwater that exits the montane watershed and enters the basin aquifer and not to water that recharge, discharge or used within the same watershed (Markovich et al., 2019). MBR can also be divided into two types, diffuse and focused MBR (Wilson and Guan, 2004). Focused MBR occurs through discrete permeable geologic features in the mountain block, such as steeply dipping fault zones or high-permeability sedimentary rock units that strike at a high angle to the mountain front, and through the unconsolidated sediment below streams in the watershed mouths.

This type of recharge is very difficult to characterize owing to several reasons. The main reason is the complexity of geological and hydrological settings in the mountain-block and the

mountain-front, often due to the presence of fault zones that can either enhance subsurface flow or act as barriers to this flow (Liu and Yamanaka, 2012). The second is the lack of direct hydraulic data from these areas with complex topography (Manning and Solomon, 2005). These factors have made the use of environmental isotopes an adequate tool for mountain-block recharge investigation (Manning and Solomon, 2005). Wilson and Guan (2004), Manning and Solomon (2005) and Markovich et al (2019) have reviewed the broad aspects of MBR and the studies that attempted to characterize and quantify this type of recharge.

II.3. Stream losses within ephemeral and intermittent streams in semiarid areas

In addition to the large perennial rivers (e.g. Nile, Niger, Chari …), streamflow losses in ephemeral and intermittent stream channels during episodic high flow events represent, often, a major component of groundwater recharge in arid and semi-arid zones (Dahan et al., 2008; Shanafield and Cook, 2014). For both types of non-perennial streamflow, their analysis and quantification continue to be a challenging from both a logistical and analysis perspectives. Dynamic and complex infiltration process, most notably flood events themselves are unpredictable, create scour and damage to equipment and their transient nature is vexing during analysis (Schwartz, 2016). Previous studies have reviewed various infiltration and recharge assessment methods and their applicability (Kalbus, 2006; Scanlon et al., 2002; Shanafield and Cook, 2014). Intermittent stream, characterized by spatially isolated reaches with streamflow along the entire channel and flowing through an extended portion of the year, are significantly less examined than ephemeral streams, and estimates of groundwater recharge is potentially even more challenging than ephemeral streamflow patterns. With ephemeral streams, total flow below the mountain-front provides a potential recharge value; however, with intermittent stream, there may be no flow at the mountain-front while reaches below have streamflow contributing to recharge. Ephemeral streams are normally dry for most of the year and flows only during and shortly after precipitation events; therefore, their recharge is scarce and episodic. Intermittent streams flow during winter and spring likely inducing larger recharge amounts.

III. Research questions and objectives

The present PhD project aims is to analyze various aspects of groundwater recharge in the mountain front of the High-Atlas of Marrakech, within the Tensift basin (Central Morocco). It has three main objectives:

- to determine groundwater recharge sources using the stable isotopes and groundwater level measurements.
- to study the hydrochemical evolution of groundwater and the processes controlling its quality for human use.
- Analyze the streamflow losses beneath an intermittent Atlasic wadi using heat as a tracer combined with sediment water content data.

IV. Thesis structure

The scientific development of this PhD research is made of five chapters:

- Chapter 2: this chapter presents the study area, which consists of 2 sub-basins: Ourika and Rheraya. A broad overview is given presenting the regional geology, hydrogeology, hydrology, climate, land use and land cover.
- Chapter 3: this chapter reports the study of the groundwater recharge sources in the mountain front of the Ourika wadi. Stable isotopes were used in this study and supported by major ions and water table data.
- Chapter 4: this chapter addresses the hydrochemical characteristics of groundwater in the mountain front of the Ourika wadi. The mechanisms responsible of shaping the hydrochemistry were determined, as well as the suitability to irrigation and domestic uses.
- Chapter 5: in this chapter we used streambed temperature and streambed water content to investigate stream losses from Rheraya wadi to the alluvial aquifer during a one-year study period. Modeling and analytical methods were used to interpret the datasets and to pull-out interesting findings on intermittent streams.
- Chapter 6: This chapter presents the general conclusions of the study, the perspectives and recommendations for future research in the area.

Chapter 2: Study area

I. Introduction

The Tensift basin is one of the largest hydraulic basins in Morocco, located in the central part of the country (Figure 2-1). It is bounded to the south by the High-Atlas mountain range and hosts the Haouz plain (Figure 2-2), one of the largest plains in Morocco. The High-Atlas contains many watersheds drained by intermittent and ephemeral wadis crossing the Haouz plain and discharges in the Tensift wadi to the North (Figure 2-1). These wadis transfer important volumes of water from the high elevations to the basin floor (Jarlan et al., 2015). This study was carried out around the Ourika and Rheraya wadis draining the Ourika and Rheraya watersheds located in central Haouz.

II. Presentation of the central Haouz area

II.1. Localization and geomorphology

The Haouz plain can be divided into three parts, the eastern Haouz, central Haouz and western Haouz (Figure 2-2). Central Haouz refers to the part of the Tensift basin located between R'dat and N'fis wadis and bounded to the north by Tensift wadi and to the south by the High-Atlas mountain range (Figure 2-2). The altitude in the Tensift basin ranges from 400 to 4160 m.

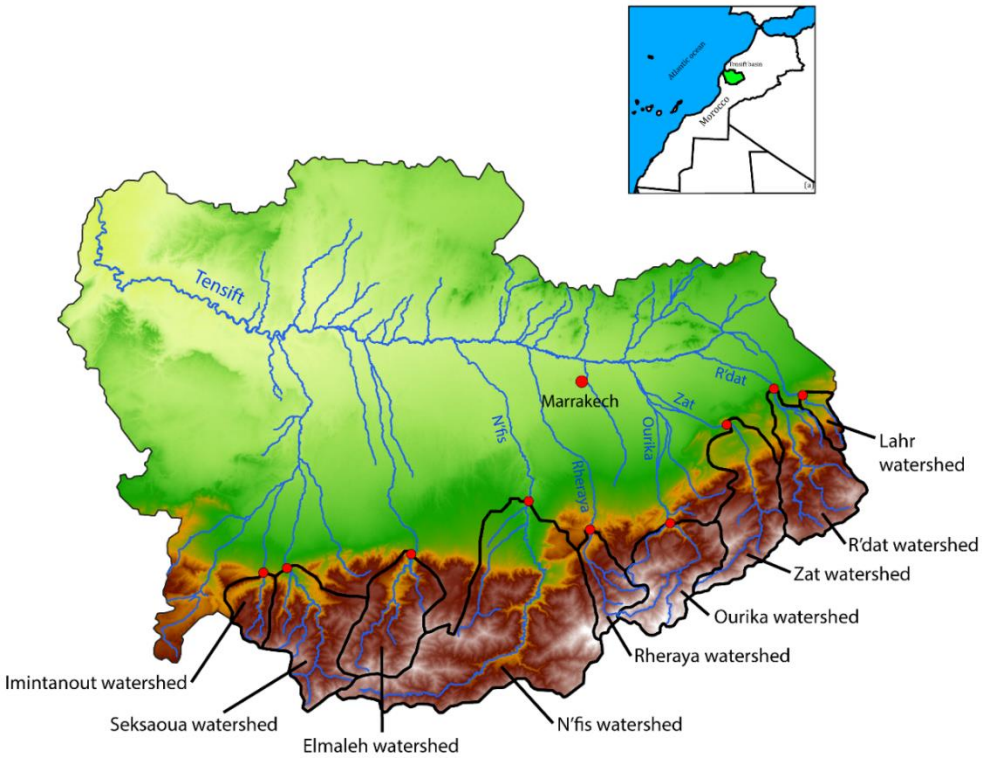

Figure 2- 1 : Localizations of the Tensift basin and its atlasic watersheds.

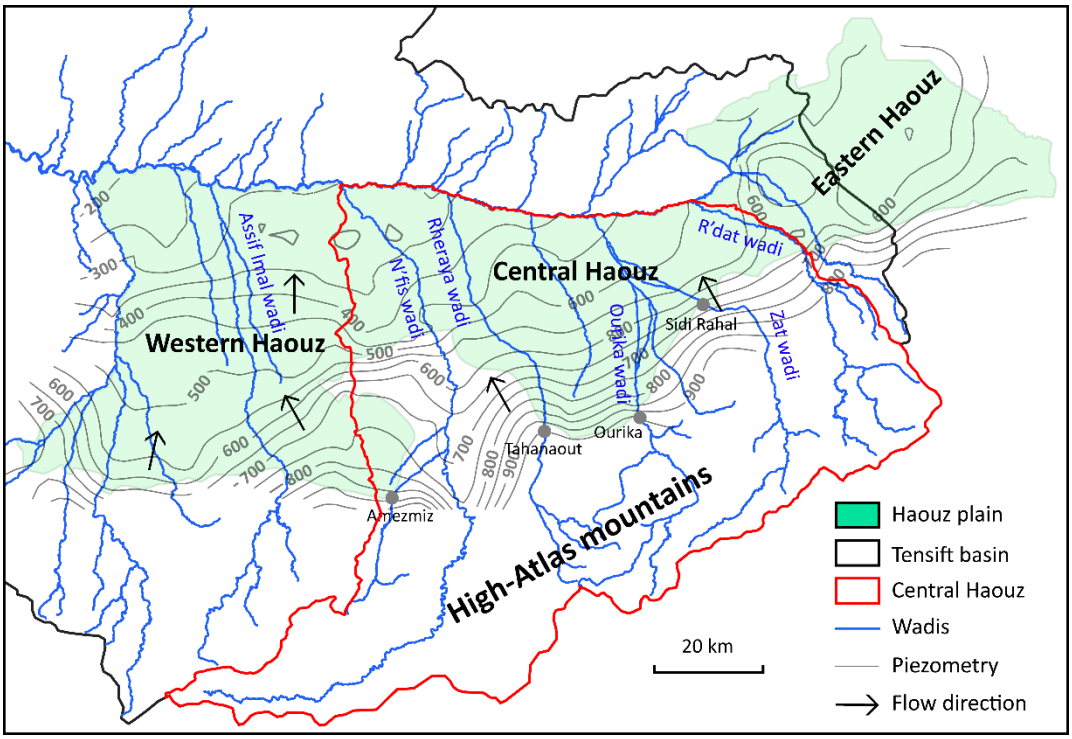

Figure 2- 2: Location of the Haouz plain (piezometric map from Boukhari et al, 2014).

The Tensift wadi drains the Tensift basin from the east to the west and discharges in the Atlantic Ocean. It is primarily fed by its southern tributaries draining the watersheds of the northern flank of the High-Atlas mountain range (nine watersheds). Four of them form the central Haouz part (Zat, Ourika, Rheraya and N'fis watersheds).

Ourika watershed is one of the sub-basins of the Tensift basin. It is located in the High-Atlas of Marrakech in central Haouz, approximately 30 km to the south of Marrakech city (Figure 2-1), centered at 31°10 N, 7°40 W. The mountain watershed covers an area of 579 Km^2 with the altitude ranging from 974 m at the outlet in Aghbalou to 4001 m at Jbel Tarourt. It has a slightly elongated morphology and characterized by strong slopes and relatively impermeable and compact lands covering almost half of the total area of the basin (El Fels et al., 2018).

Rheraya watershed is an Atlasic sub-basin of Tensift basin (Figure 2-1). It is located in the northern flank of the High-Atlas adjacent to Ourika wadi, and 40 km south of Marrakech city. The watershed covers an area of 225 km^2, almost half of the area of the Ourika watershed. The altitude in the Rheraya ranges from 1030 to 4160 m culminating at mount Toubkal, the highest summit in North Africa. The slopes are very strong in the upper part of the watershed (Hajhouji et al., 2018).

II.2. Climate and hydrology

The regional climate in the central Haouz is semiarid with a high spatial and temporal heterogeneity. In the plain, the semiarid climate is characterized by low and heterogenous rainfall, with episodic drought periods (Fniguire et al., 2017). The mean annual precipitation in Marrakech weather station in the period between 1962 and 2015 is 184 mm/year (Hajhouji et al., 2018).

Temperature in Ourika basin varies from -7.2 °C to 48.2 °C with an annual average of 27.8 °C depending on the altitude (Figure 2-3). The hottest months are July and August and the coldest months are December and January. The annual precipitation in the Aghbalou station is 527 mm/year (Figure 2-3) but can exceed 700 mm/year in the headwater catchment (Saidi et al., 2010). An important part of precipitation in headwater catchments of the central High-Atlas fall in form of snow. The watershed is drained by Ourika wadi, one of the important Atlasic wadis in term of flow. The Aghbalou gaging station located at 974 m monitors Ourika wadi. The mean flow of the wadi is 4.9 m^3/s. The analysis of Ourika wadi flow reveals two annual peaks following rainfall trends (Figure 2-4). The first peak of November is due to the raining in the area, and the first peak, which is the highest, is in April with conjugal effect of rain and snowmelt (Bouimouass et al., 2020).

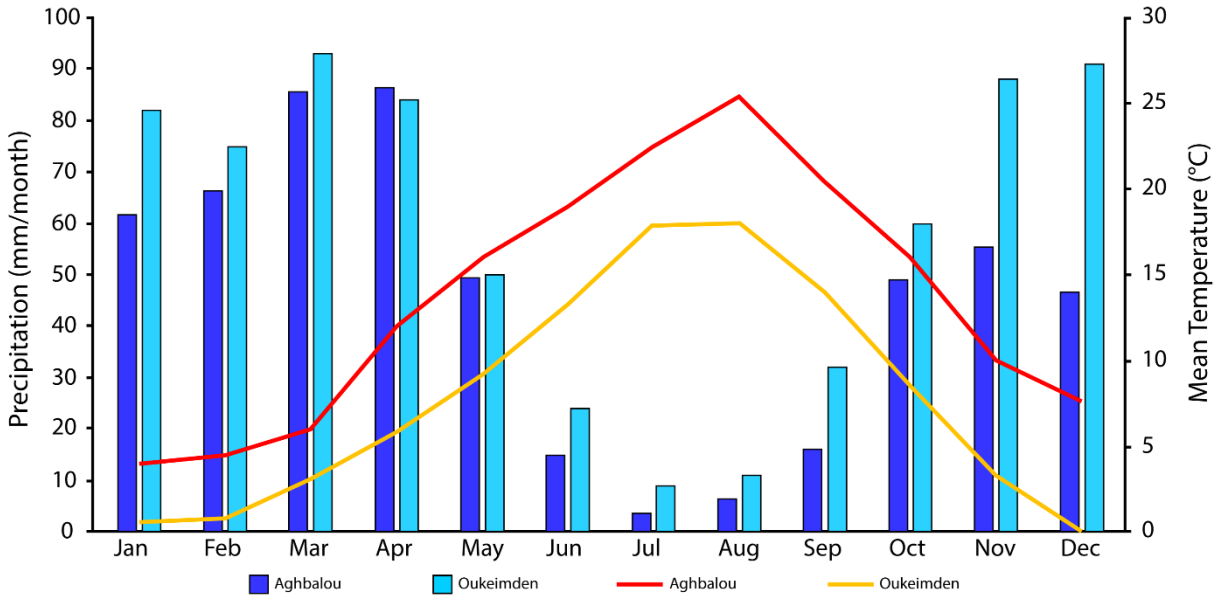

Figure 2- 3 : Interannual means of precipitation and temperature in Aghbalou and Oukeimden stations located in Ourika Watershed.

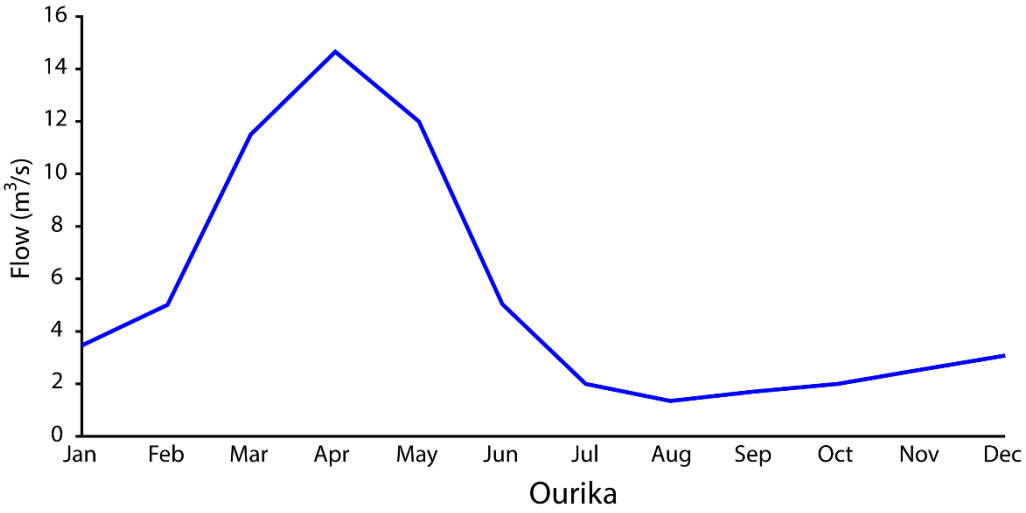

Figure 2- 4: Interannual means of Ourika wadi streamflow at Aghbalou Gage station.

Mean annual rainfall in Tahanaout station is 356 mm/year and increases with altitude (Hajhouji et al. 2018) (Figure 2-5). The Rheraya wadi, monitored by the Tahanaout station at 1030 m, drains Rheraya watershed. The mean annual streamflow at Tahanaout station is 1.15 m^3/s. The peak flow occurs in April (Figure 2-6) due to rain-on-snow events due to the rise of temperature (Zkhiri et al., 2017). Numerous studies have been carried out to assess snow resources in the High-Atlas within the frame of the SUDMED project (Chehbouni et al., 2008) and the LMI TREMA (Jarlan et al., 2015). These studies showed that snow contributes with an important fraction, ranging from 30 to 50%, to the annual flow of the Atlasic wadis (Boudhar et al., 2009; Marchane et al., 2015; Baba et al., 2018).

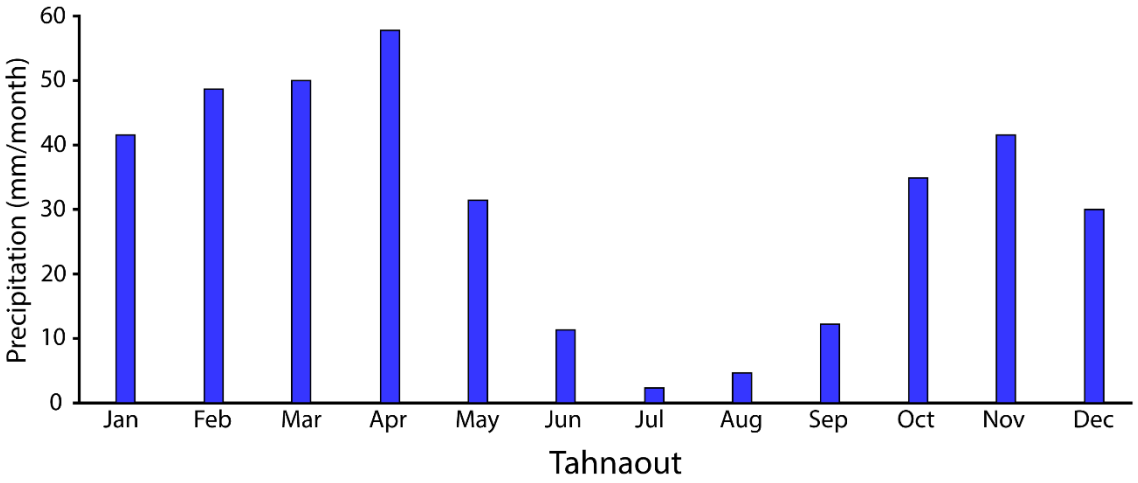

Figure 2- 5: Interannual means of precipitations in Tahanaout gage station (Rheraya watershed).

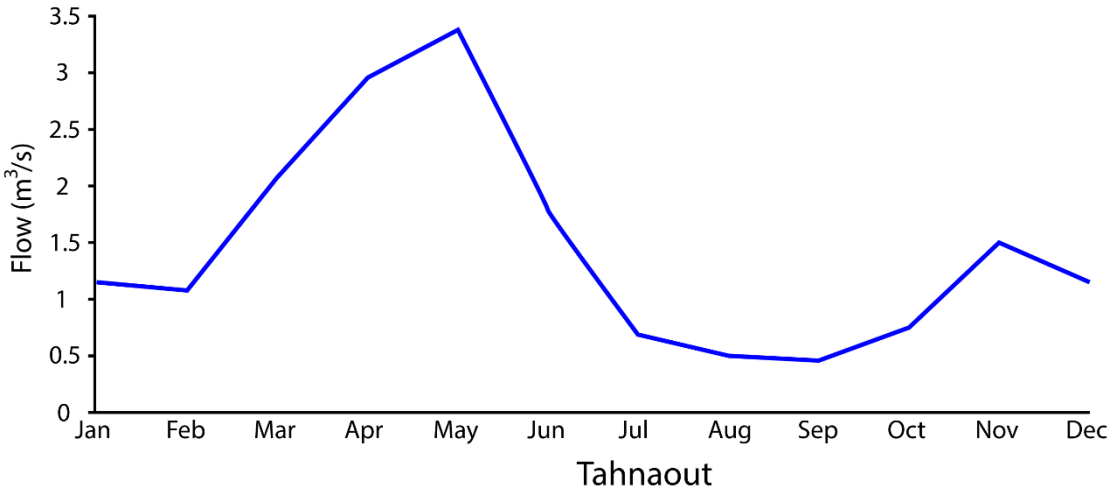

Figure 2- 6: Interannual means of Rheraya wadi streamflow at Tahanaout gage station.

II.3. Regional geology

The Haouz basin is a sedimentary basin with a tectonic origin. The basin is filled during the Neogene and Quaternary by detrital deposits issued from the erosion of the High-Atlas. The complex geology of the Haouz and the High-Atlas is summarized following the geological timescale (Figure 2-7):

- **The Precambrian:** It forms the axial zone of the High-Atlas of Marrakech (HAM). The Precambrian, highly metamorphosed, is formed of crystalline rocks such as granodiorite, amphibolite, shale, quartzite and granite (Michard, 1975).
- **The Paleozoic:** The Primary formations is widespread in the HAM. Pre-Hercynian formations (between the Cambrian and the Carboniferous) are formed of sandstone, clay, shale and limestone. The Visean is deformed and metamorphosed by the Hercynian orogenesis (Proust, 1961).
- **The Mesozoic:** The Permo-Triassic of the HAM is formed of a thick series, exceeding 1000 m, of clay and evaporates covered often by 200 m of doleritic basalts (Biron, 1982). The Jurassic outcrop in the lower part of the mountain is formed of conglomerate (15 to 30 m), siltstone (10 to 20 m) and sandstone with conglomeratic channels (80 to 100 m). The Cretaceous in the HAM is formed by the Albian, Cenomanian, Cenomano-Turonian and the Senonian. It is formed essentially of limestone, dolomitic limestone and clay.
- **The Cenozoic:** The Eocene is present in the bordure of the High-Atlas, and outcrops in some places especially in the Ourika and Zat watersheds. It is formed of limestone and

dolomite in alternation with marls and sandstone. During the Mio-Pliocene, a very intense tectonic compression occurred giving birth to the actual High-Atlas chain (Proust, 1961; Biron, 1982). Furthermore, the newly elevated chain is being dismantled and the sediments have accumulated in the adjacent depressions (such as Haouz basin). The Haouz depression began to be filled with detrital deposits transported by the Atlasic wadis (Sinan, 2006).

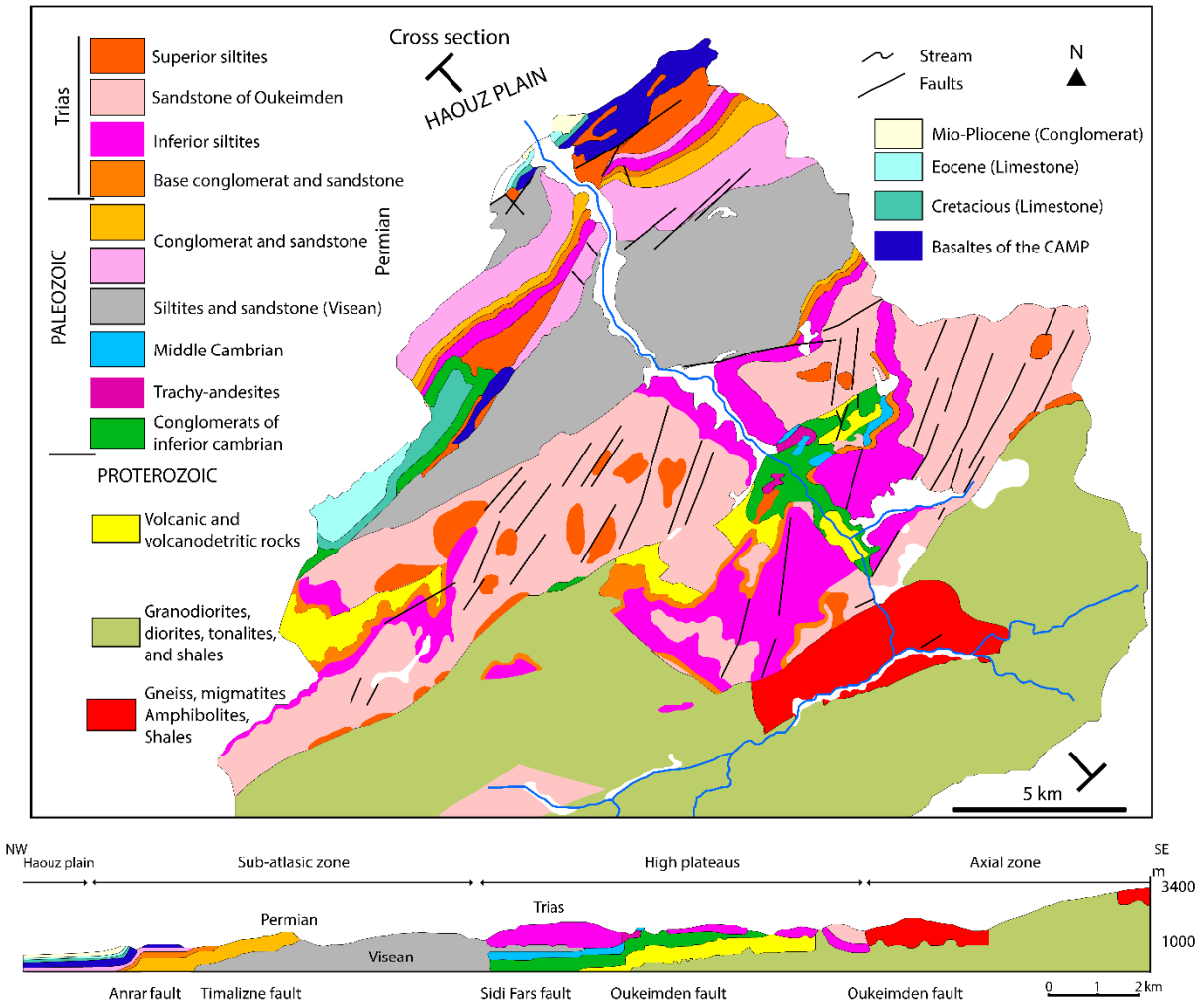

Figure 2- 7: Geology of the High-Atlas of Marrakech (Ourika basin, Ouanaimi , 2011)

III. Hydrogeology

The Haouz plain (6200 km^2) hosts the large phreatic aquifer of Haouz (Figure 2-2) and some confined aquifers encompassed within the limestones of the Eocene, Cenomano-Turonian and Jurassic deposits underlying the alluvial aquifer (Moukhchane, 1993; Sinan, 2000). In the central Haouz, the confined Cenomano-Turonian and Eocene aquifers cover an area between 160 and 170 km^2 in the southern border of the plain, adjacent to the High-Atlas (Moukhchane,

1983). These aquifers are recharged by precipitations and streamflow in the mountain-front where they outcrop to the surface along the border of the High-Atlas between Amezmiz and Ait Ourir (Sinan et al., 2000).

The alluvial Haouz aquifer is considered the most important source of groundwater in the whole Tensift basin. This unconfined aquifer is limited from the bottom by the marly Miocene and, in some areas, by clayey Triassic and Paleozoic shales constituting the substratum of the aquifer. It is formed by Quaternary alluvium with high vertical and lateral heterogeneity. Vertically, the aquifer can be schematized as a series of layers of lenticular structures of clay and marls in alternation with others of coarser elements. Laterally, many structures of deposits can be found in the Haouz aquifer such as paleo-channels, paleo-reliefs, and scree cones (Sinan, 2000).

The aquifer is highly heterogeneous (Sinan and Razack, 2006). Measured transmissivity varies between 5 10^{-5} m^2/s and 9 10^{-2} m^2/s with a mean of 6.7 10^{-3} m^2/s. Groundwater flows from the south to the north (Figure 2-2). The aquifer is believed to be primarily recharged by flood water infiltration within wadi channels and irrigation, irrigation returns, inflow from the underlying confined aquifer (Abourida, 2007), and direct infiltration from rainfall (Sinan, 2000).

IV. Water resources

There is no natural perennial surface water in the Haouz, hence, the majority of water demands for irrigation and drinking water supplies in the central Haouz relies on groundwater of the alluvial aquifer. More than 24000 pumping wells (inventory carried out between 2003 and 2006) consistently pump water from the Haouz aquifer (Le Page et al. 2012).

In order to support groundwater resources, an artificial canal (Rocade canal) was built in the 70s to transport water 120 km away from Moulay Youssef dam in the Lakhdar wadi to irrigate the agricultural perimeters and to provide the City of Marrakech (2 million inhabitants) with 90% of its domestic and drinking water demands. The Lala Takerkoust dam was constructed in 1937 in the N'fis wadi (central Haouz), with a capacity of 70 million m^3, to provide water for irrigation in the N'fis irrigated perimeter, for mining activities in the Guemassa mine and to provide Marrakech with drinking water in cases of need.

In the mountain front, local inhabitants have taken advantage of floods and snowmelt-driven runoff for irrigation purposes by developing a large network of gravity-fed surface

irrigation channels (locally named Seguias) that divert the runoff (Figure 2-8). To avoid conflicts over water, a regulated irrigation system was established, inspired from traditional water rights. This irrigation system is widespread in Morocco, but particularly within the south and north piedmont areas of the High-Atlas Mountains. Each major channel, managed by users' associations, irrigates a given area ranging from hundreds to thousands of hectares. The secondary channels have their own delegates who distribute water between farmers. The duration of irrigation deliveries to a single farmer initially depended on the land area. Upstream channels have priority to access water and are fed greater volumes than downstream channels. The channels located upstream also have access to the streamflow during low discharge periods in summer and autumn or during extended dry periods. Where, the downstream channels are supplied only during floods and high spring flow. Consequently, crops in the downstream areas rely on groundwater irrigation during the dry periods.

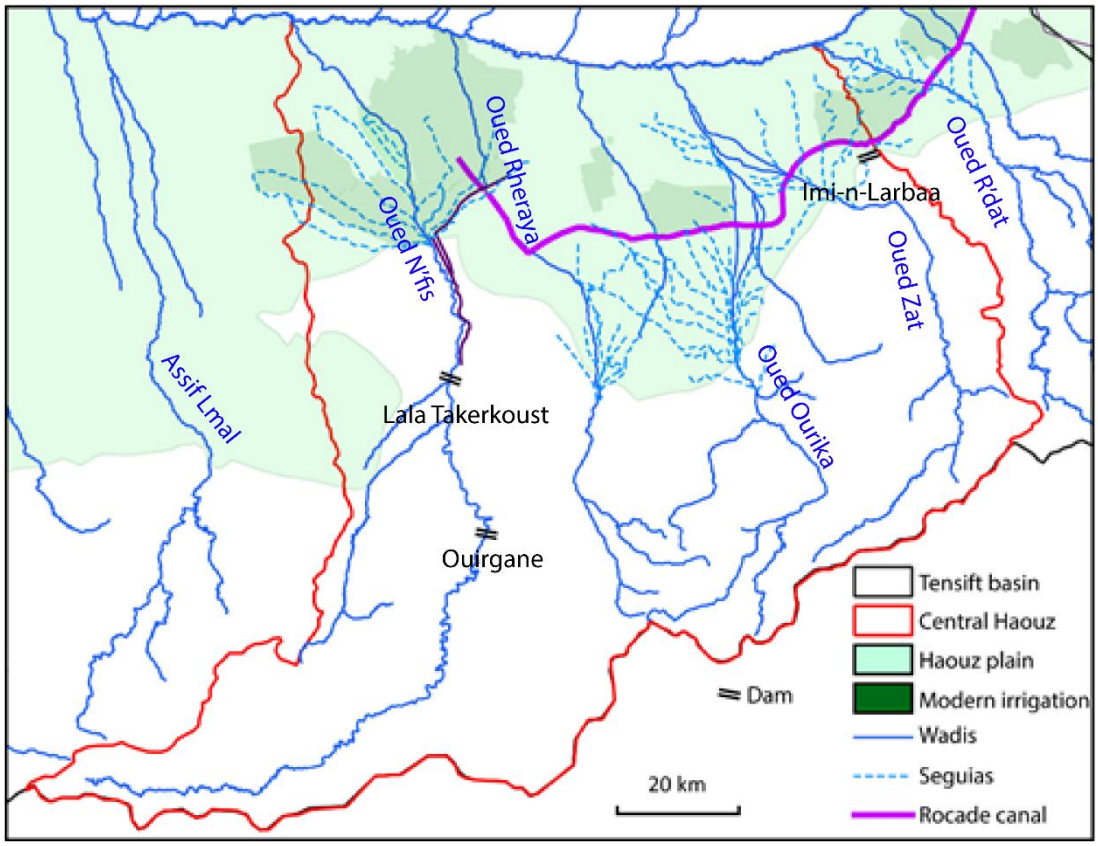

Figure 2- 8: Water resources in the central Haouz

Worldwide, a shifting from snow to rain in the total precipitation of snow-dependent basins is occurring due to climate change (Berghuis et al., 2014). Snow cover reduction and increase in temperature will reduce streamflow volumes and will be shifted from irrigation months in late spring and early summer (Malek et al., 2020). The agricultural activities in the Haouz plain

relies significantly on snowmelt water, however, spring streamflow decrease during the last two decades has forced the farmers to shift from seasonal agricultural practices (vegetables) to annual crops (cereals) relaying mainly on rain water and trees relying on groundwater pumping. At the other hand, groundwater has been taking all the pressure due to the population growth, which caused a severe withdrawal (Bouimouass et al., 2020).

Chapter 3: Groundwater recharge sources in the mountain-front of the High-Atlas: case study of the Ourika watershed

Paper published in *Hydrological Processes*

Bouimouass, H., Fakir, Y., Tweed, S., & Leblanc, M. (2020). Groundwater recharge sources in semiarid irrigated mountain fronts. *Hydrological Processes*, *34*(7), 1598-16

Received: 11 September 2019 | Accepted: 13 December 2019
DOI: 10.1002/hyp.13685

Check for updates

RESEARCH ARTICLE

WILEY

Groundwater recharge sources in semiarid irrigated mountain fronts

Houssne Bouimouass[1] | Younes Fakir[1,2] | Sarah Tweed[3] | Marc Leblanc[4]

I. Introduction

As mentioned in chapter 1, the main sources of recharge in semi(arid) mountain-fronts are focused infiltration from streambeds and subsurface inflow from the mountain block. Despite the importance of mountain front recharge for semi(arid) groundwater resources, there remain significant challenges in distinguishing those different sources and their specific contribution (Bresciani et al., 2018). This is particularly the case in irrigation areas, where the groundwater recharge may also include inflow from irrigation leakage (herein referred to as irrigation recharge IR) that is often a redistribution of both local- (pumping from alluvial aquifers) and mountain- (floods and streamflow generated from rainfall or snowmelt) derived water.

Previous studies have used groundwater fluctuation and seasonal piezometric mounds to analyze recharge processes in mountain-front recharge areas (Shanafield and Cook, 2014; Bresciani et al., 2018). However, although hydraulic head data record the groundwater recharge events, the discrimination of different sources of recharge generally requires the use of environmental tracers. Commonly used tracers include stable isotopes and major ions (Liu and Yamanaka 2012; Zhu et al., 2018). The main advantage of using stable isotopes to analyze the mountain front recharge is that the signature of local rainfall on the plain are likely to significantly vary from the signature of rainfall in the mountains due to rainout effects (Clark and Fritz, 1997; Scanlon et al., 2002; Lambs, 2004; Kalbus et al., 2006). Similarly, for major ions, since changes in recharge rates and flow pathways can result in significant differences in the composition of the major ions, the latter could provide insights into mixing between different groundwater recharge sources (Liu et al., 2020).

The objective of this chapter is the use of water table fluctuation data and stable isotopes to determine the sources contributing to groundwater recharge in the mountain-front of the High-Atlas. Seasonal variations of piezometric levels and isotopic composition of meteoric water, surface water and groundwater in the Ourika watershed and its mountain-front area, as well as historical piezometric data and streamflow diversion for irrigation will be analyzed and discussed.

II. Field measurements, sampling and analytical methods

A total of 91 samples were collected from rainfall (Rn), snow (Sn), streamflow (St), irrigation channels (Ir), private wells (W) and springs (Sp) (locations shown in Figure 3-1). Rain, snow and streamflow were sampled in the mountain, at different elevations. A flood event was sampled in the piedmont in March 2018; Three samples were collected during the recession

from the main stream (Ourika) and its tributaries (Igerifrouan and Elmaleh). In addition, 11 rain samples collected in 2014 (unpublished data) in the plain, the mountain-front and the High-Atlas were used to characterize the spatial variation in stable isotopes of precipitation.

Streamflow was sampled during 07 sampling campaigns between September 2017 and March 2018 on a monthly basis (except for October 2017). Irrigation water was collected from a concrete irrigation channel (Ir1) and an earthern irrigation channel (Ir2). Groundwater was collected during four field campaigns (1-5 September 2017, 10-15 November 2017, 25-30 December 2017 and 25-30 March 2018) covering dry and wet seasons. The samples were taken from two springs in the high mountain (n=11), one spring and three wells from the hillslope, and 27 private irrigation wells (n=56) from the alluvial aquifer in the mountain front area and further downstream. The wells are generally shallow, open hand-dug wells used mostly for irrigation with immersed permanent pumps. The results of all samples are presented in Table 1 (Appendix).

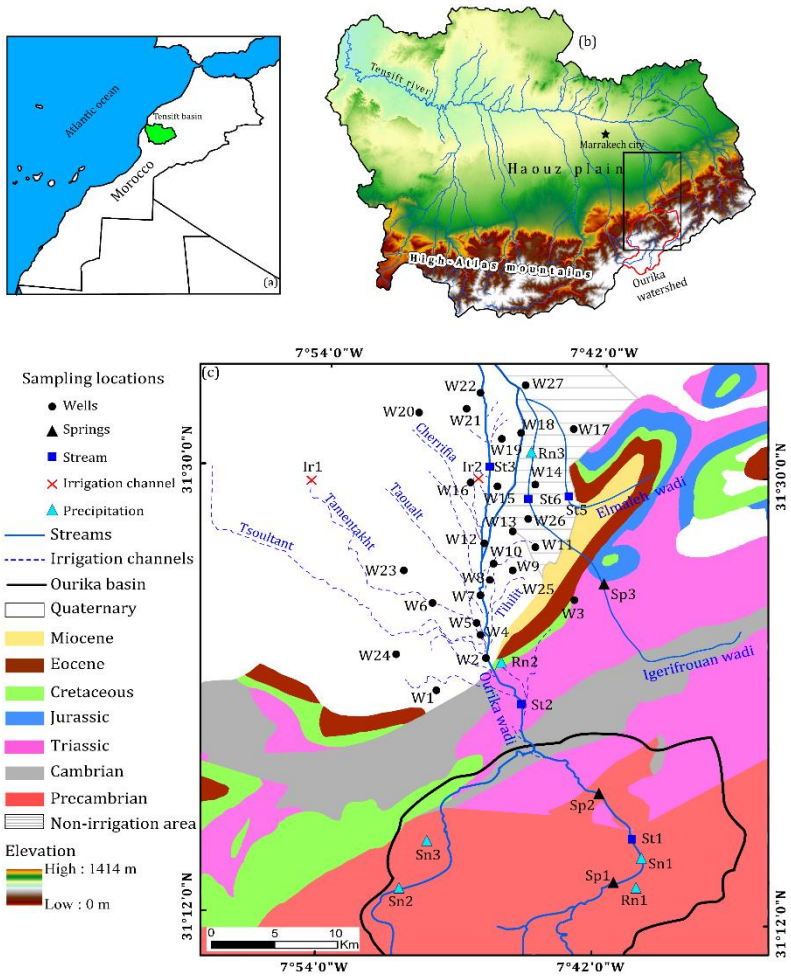

Figure 3- 1: Maps showing (a) the location of Tensift basin in Morocco, (b) the localization of the study area in the Tensift basin, and (c) the localization and types of the sampling points in the Ourika basin.

The groundwater samples were collected during or immediately after pumping. The physical parameters (temperature, pH, electrical conductivity) were measured in the field. Water was sampled for cations (filtered at 0.45 µm and acidified with HNO_3), anions and stable isotopes, and was analyzed at the Laboratory of Hydrogeology of the University of Avignon. The alkalinity was measured using a HACH digital titrator, and stable isotopes were analyzed using a Picarro Analyser L 2130-I. For the stable isotopes, the error was ±0.1‰ for $\delta^{18}O$ and ±1‰ $\delta^{2}H$.

Groundwater hydraulic heads were measured twice in September 2017 and March 2018 in a large network of 55 wells. The static level measurements were performed in stable wells or at least 2 days after pumping. The objective was to characterize and draw groundwater elevation and fluctuation maps.

The volumes diverted for irrigation were provided by the ORMVAH (Office Régional de Mise en Valeur Agricole du Haouz) and the multi-year groundwater level records by the ABHT (Agence de Bassin Hydraulique du Tensift).

III. Results

III.1. Irrigation diversion impacting streamflow

During low streamflow, upstream channels divert almost the totality of the streamflow leaving a dry streambed. It is only during high streamflow and floods that there are surface water volumes in excess of mountain front irrigation diversions, and therefore streamflow resources for the downstream irrigation areas. The channels named Tassoultant and Taoualt in the mountain-front divert a monthly mean volume of 1326986 m^3 (14.4% of the diverted volume) and 557286 m^3 (6.1% of the diverted volume) respectively, whilst the Cherrifia located further downstream only diverts a monthly mean volume of 45228 m^3 (0.5% of the diverted volume) (Figure 3-2). On average the whole irrigation network annually diverts more than 65% of the streamflow volumes (Figure 3-3).

In addition to the spatial variation of diverted streamflow, there is also a seasonal variation. The diverted volumes exhibit two peaks; one in November coinciding with rainfall floods, and one in April (the highest peak) coinciding with snowmelt floods. However, the peak in April

has decreased during the last decade attesting of a possible reduction in snowmelt contribution to streamflow.

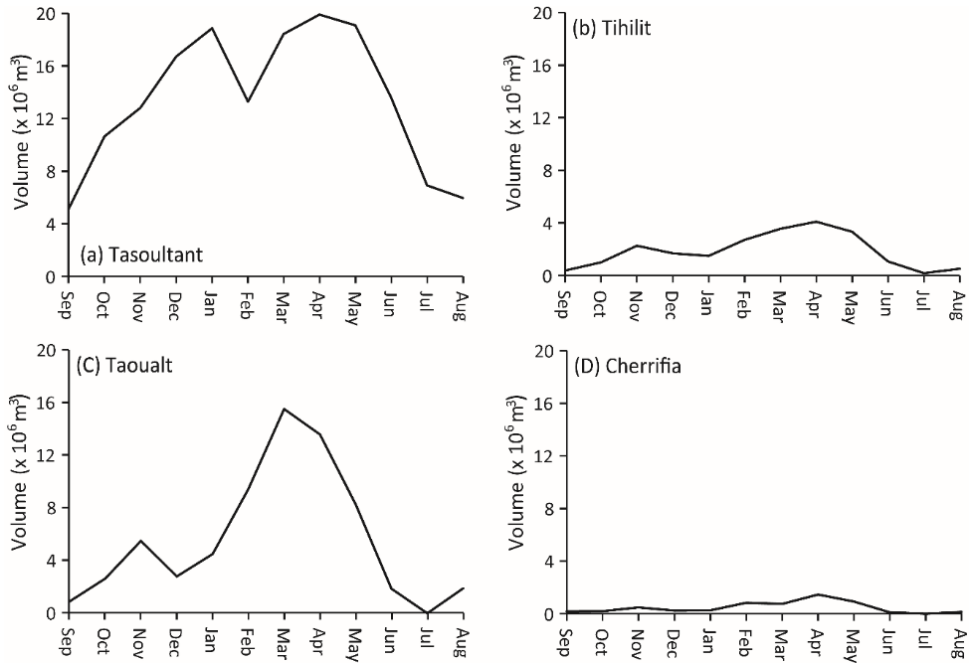

Figure 3-2: Monthly mean (2001–2016) volumes of water diverted by the major irrigation channels in the study area (locations shown in Figure 3.1). The channels Tasoultant (a), Taoualt (b) are located in the mountain front and divert water to the irrigation area on the left side of Ourika stream. The Tihilit (c) is also located in the same area as the channels Tasoultant and Taoualt but divert water to the right side of the Ourika stream. The Cherrifia (d) is located downstream.

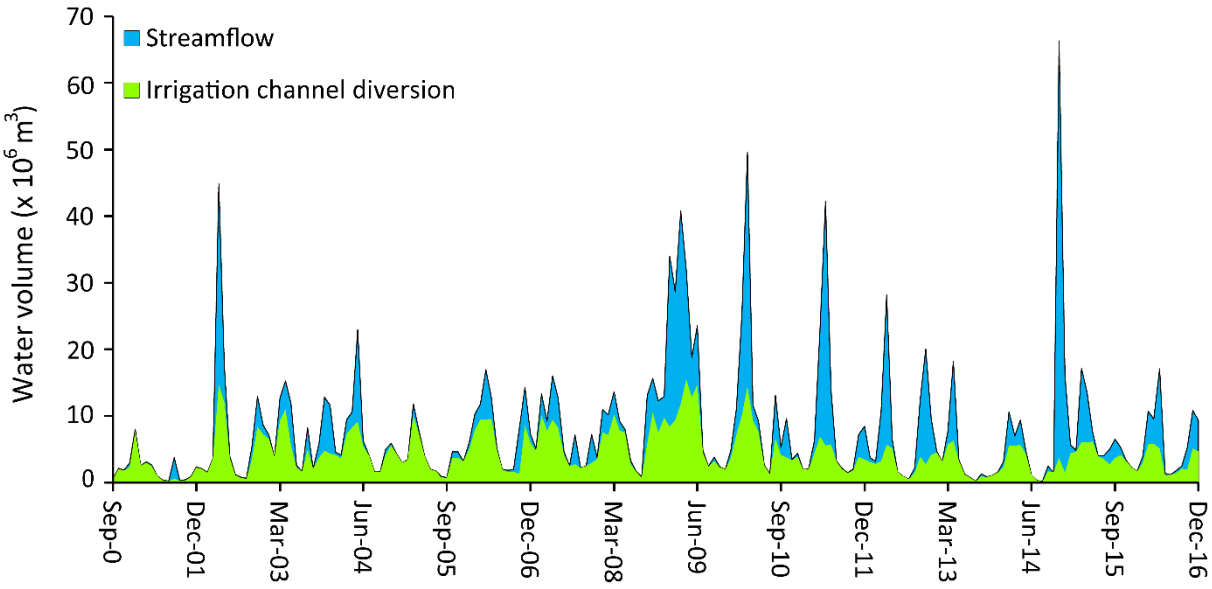

Figure 3-3: Time series (2000–2016) showing monthly Ourika runoff volumes measured at Aghbalou gauge station and the diverted volumes to the irrigation channels.

III.2. Groundwater flow and fluctuation

The piezometric maps of September 2017 (dry season) and March 2018 (wet season) indicate groundwater flowing from the south to the north, that is from the High-Atlas mountain front towards the Haouz plain (Figure 3-4a). From September 2017 to March 2018, the water table rose by 3.5 m upstream to 0.5 m downstream (Figure 3-4b). This attests for a variable seasonal groundwater recharge over the study site. The region with the highest water table fluctuations between the wet and dry season is located in the mountain front area, and extends west from the Ourika stream. As presented previously in the text, the upstream western irrigation area receives relatively high volumes of streamflow during the wet seasons and it is prioritized during the dry seasons. Therefore, within the mountain front region the irrigation leakage has generated more groundwater recharge compared with recharge via the streambed.

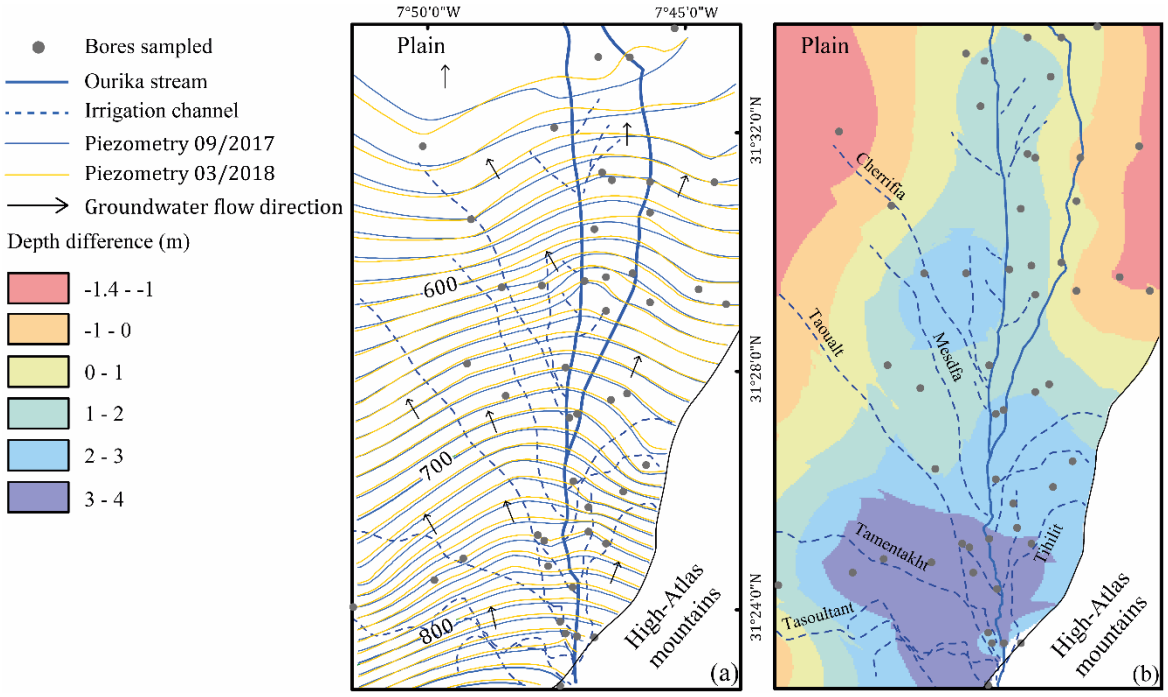

Figure 3-4: Maps showing (a) the piezometric contours for both the dry season (September 2017) and the wet season (March 2018; contour values shown are in mASL) and (b) the calculated difference in depth to water between the dry season and the wet season.

III.3. Stable isotopes

The precipitation samples in the High-Atlas, the mountain-front and the plain show a wide variation of stable isotope values in space and time. The values range from -18.1‰ to -3.4‰ for $\delta^{18}O$, and from -126 to -19 ‰ for ^{2}H (Appendix 1). The rain in the plain has higher stables isotopes values (-9.2 to -3.4 ‰ for ^{18}O and -47 to -19 ‰ for ^{2}H) compared with rain in the mountain front (-12.4 to -5.5 ‰ for ^{18}O and -111 to -31 ‰ for ^{2}H), and with rain and snow in

the High-Atlas (-18.1 to -8.2 ‰ for ^{18}O and -126 to -51 ‰ for ^{2}H). The altitude effect (Clark and Fritz, 1997) results in the rainfall stable isotope values decreasing with altitude (Figure 3-5a). The precipitation samples are scattered along the local meteoric water line (LMWL) previously established for the High-Atlas by Ouda and Marah (2014; unpublished data), and the global meteoric water line (GMWL; Craig, 1961).

All of the streamflow samples fall along the meteoric water lines, with values from -9.3‰ to -7.5‰, and from -60 to -48 ‰ respectively for ^{18}O and ^{2}H (Figure 3-7b). Their stable isotope values are temporally variable, with higher values during the dry season (mean ^{18}O values of -7.8 and -7.4 ‰ for St1 and St2, respectively) than the wet season (mean ^{18}O values of -8.9 and -8.2 ‰ for St1 and St2, respectively (Figure 3-5b). The lowest recorded values correspond to the flood water sampled in the Ourika stream in March 2018, with -9.3 ‰ for ^{18}O and -60 ‰ for ^{2}H. These low isotope values correspond to the high-altitude origins of precipitation feeding the flood waters. The two samples (St5 and St6) collected during the same flood event from the two tributaries, Igerifrouan and Elmaleh, have higher stable isotopes values (-8.1 to -6.9 ‰, and from -49 to -41 ‰ respectively for ^{18}O and ^{2}H; Appendix 1), indicating greater contribution from lower altitude rainfall in these streams. Stable isotope samples collected from the irrigation channels (Ir1 and Ir2) in February and March 2018 are similar to those of the Ourika streamflow.

Within the mountain block, the ^{18}O and ^{2}H values for groundwater (Sp1 and Sp2) are -8.6 ‰ to -5.9 ‰ and -54 to -36 ‰ respectively, which are similar to those of the streamflow (Figure 3-8b). Sp1 and Sp2 show an increase in stable isotope values from high to low altitude, which reflects a spring system fed by shallow or perched groundwater that is locally recharged. Springs also show a slight decrease in stable isotope values from the dry to the wet season (Figure 3-6c).

Within the hillslope, the spring Sp3 and the wells W1, W3 and W11 have the highest stable isotopes values (mean ^{18}O and ^{2}H are -5.4 ‰ and -32 ‰ respectively; Figure 3-7b, 3-8d) among all the water samples collected in this study. These waters are likely to have originated from the local recharge of rain on the plain.

Within the mountain-front and downstream areas, stable isotope values of groundwater plot along the meteoric water lines (Figure 3-5b). The $\delta^{18}O$ and $\delta^{2}H$ vary between -8.4 to -6 ‰, and – 54 to -35 ‰ respectively (corresponding average values of -7.6 and -49 ‰). The groundwater stable isotopes values are lower in the irrigation area (mean $\delta^{18}O$ and $\delta^{2}H$: -7.9 and -51‰

respectively) than in the non-irrigation area (mean $\delta^{18}O$ and $\delta^{2}H$: -6.4 and -38 ‰ respectively) (Figure 3-5b). These 02 groundwater clusters are herein referred to as Group 1 and Group 2 respectively.

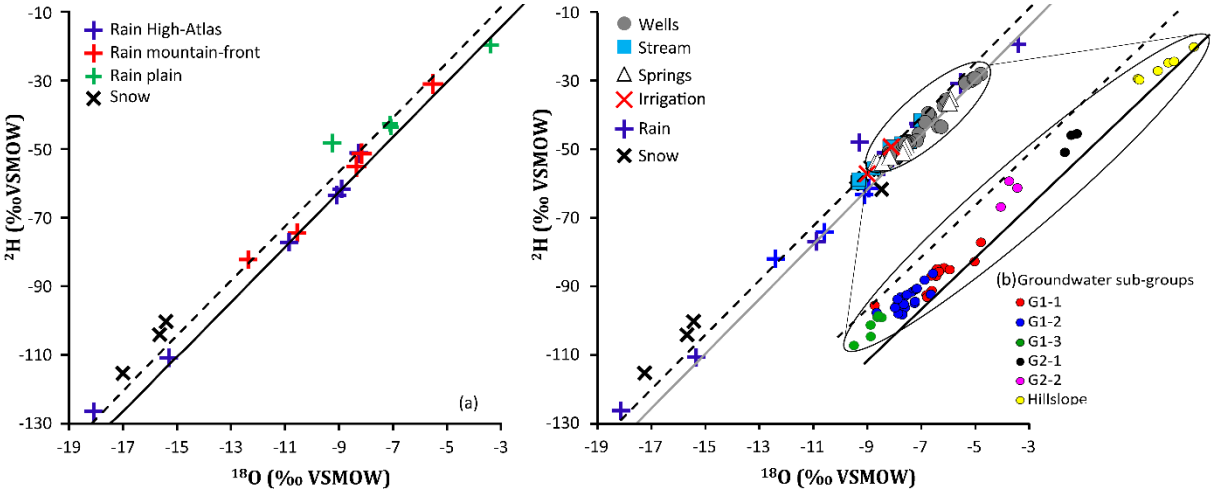

Figure 3-5: Plots of δ18O versus δ 2H for (a) rain and snow samples and (b) all the collected samples including groundwater, streamflow, and precipitation. The global meteoric water line is represented by the solid black line and the local meteoric water line is represented by the dashed black line.

The Group 1 (41 samples), characterizing the irrigation area (Figure 3-6a), have stable isotope values similar to the streamflow and the irrigation water. A decrease in stable isotope values is observed from the mountain-front towards the plain (Figure 3-6f), which is contrary to an altitude effect. Therefore, the Group 1 is divided into 03 sub-groups: G1-1 from the upstream irrigation area, G1-2 close to the Ourika stream, and G1-3 in the downstream irrigation area. The G1-1 (W2, W6, W9, W13, W23, W25) is the most enriched, its isotopic signature is similar to the Ourika stream during the dry period, and it is the unique group that shows decreases in stable isotopes from the dry to the wet season (Figure 3-6f). The G1-2 (W4, W5, W7, W8, W10, W12, W15, W16, W18, W19, W20) is relatively depleted. The G1-3 (W21 and W22) has the most depleted isotopic content (Figure 3-6f) among all the sampled wells; its isotopic signature is similar to the flood of March 2018 and to the high-altitude springs. This decreasing trend in groundwater stable isotope values from upstream to downstream of the mountain front can be explained by the effects of the irrigation system. The upstream irrigation area (G1-1) receives streamflow diverted by irrigation channels during both the low-flow period (high stable isotopes values in the dry season) and the high-flow period (low stable isotopes values in the wet season). However, the downstream irrigation area (G1-3) only receives flood waters and high spring-flow which have relatively low stable isotope values.

The Group 2 (06 samples) is sampled from the non-irrigated area in the upper belt of the mountain front (Figure 3-8a). Group 02 has $\delta^{18}O$ and $\delta^{2}H$ values higher than Group 1 and close to those of the hillslope groundwater (Figure 3-5b). There is also spatial variation in stable isotope values resulting in 02 sub-groups: G2-1 close to the mountain (low irrigation by groundwater) and G2-2 close to the streams. The G2-1 (W17 and W24) is more enriched than the G2-2 (W14 and W27) (Figure 3-6e). These differences in isotopes signatures could be explained by the fact that the Group 2 represents groundwater that is slightly or not influenced by the seasonal recharge by the streamflow. Its recharge could originate from subsurface inflow from the mountain block and/or recharge by infiltration of local low altitude rainfall.

IV. Discussion

IV.1. Hydraulic heads and stable isotopes as combined tools

By coupling groundwater fluctuation measurements and stable isotope values the extent of recharge areas and types of recharge processes are assessed. Within the mountain front close to the stream and beneath the irrigated crops, stable isotope values of groundwater are similar to streamflow (Figure 3-7). This indicates that groundwater is mainly recharged by the streamflow infiltrated through the streambed and the irrigation area. The irrigation recharge is characterized by a net variation of stable isotopes from the dry to the wet season while the stream recharge is characterized by a low and more steady content of stable isotope values. The groundwater elevation map delineates the spatial variation of the recharge. It shows that an important seasonal recharge has occurred and was higher and more extended in the irrigation area than along the streambed. Further downstream, the groundwater elevation map shows that recharge is lower, which corresponds with areas where the groundwater exhibits the lowest isotopes values. Therefore, the downstream irrigation area is recharged predominantly by low occurrence wet season flood water.

Within the non-irrigation area, the groundwater has limited recharge according to the hydraulic head fluctuations. The groundwater has relatively high stable isotope values, similar to groundwater sampled in the hillslope of the mountain block (Figure 3-7). The low groundwater fluctuations coupled with high stable isotope values suggest that there is lateral subsurface inflow from the mountain block to the mountain front, with minimal local recharge from low altitude precipitation.

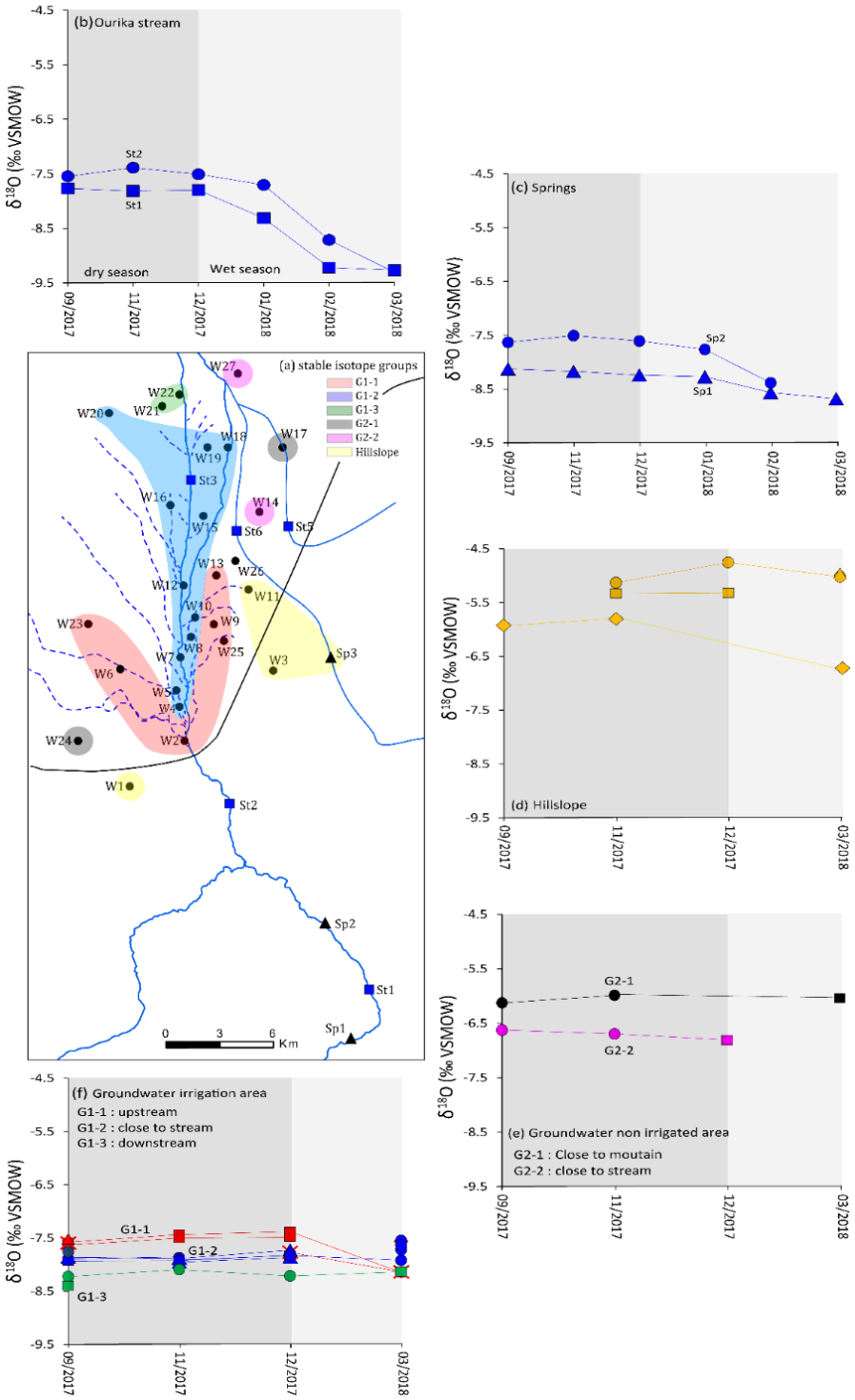

Figure 3-6: The location of the subgroups in the study area based on stable isotope values, and the temporal variations of δ18O in the (b) Ourika streamflow, (c) high mountain springs, (d) groundwater from the hillslope, (e) groundwater from the irrigated area (group 1), and (f) groundwater from the non-irrigated area (group G2).

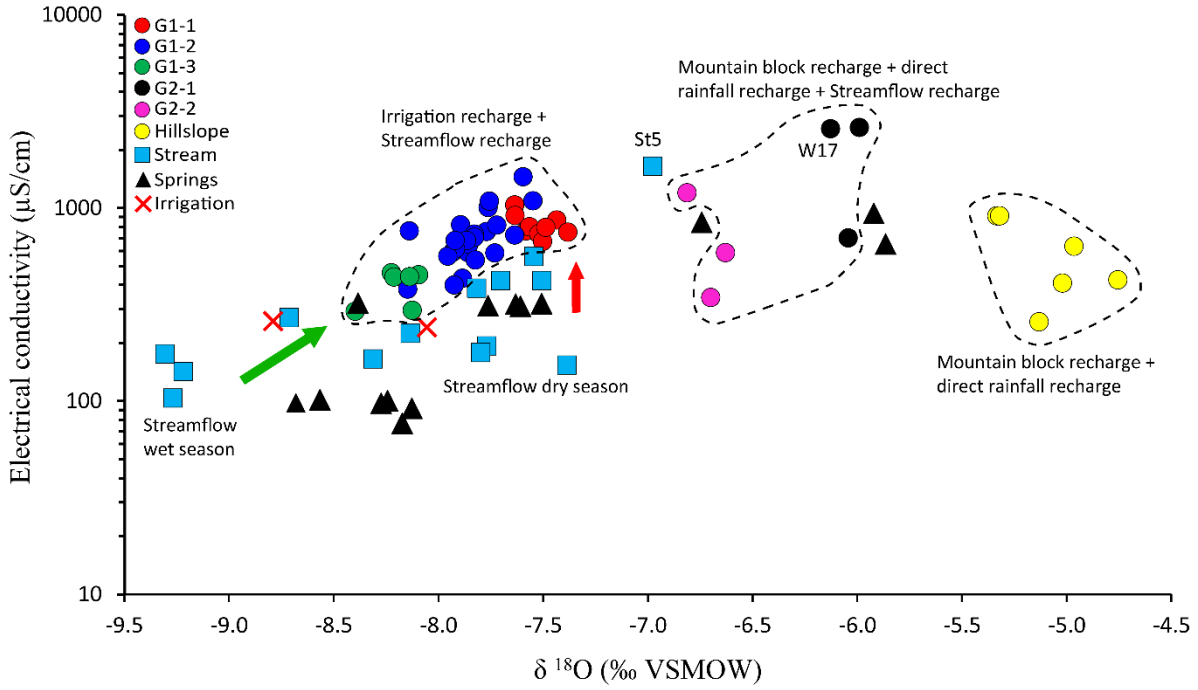

Figure 3-7: Differentiation of recharge components according to ^{18}O and electrical conductivity. Green arrow refers to the contribution from streamflow during wet season and red arrow to the contribution from streamflow during dry season.

IV.2. Impact of irrigation on the groundwater recharge and availability

Previous studies have highlighted the effect of irrigation water leakage on groundwater recharge (Willis et al., 1997; Wang et al., 2008; Qin et al., 2011; Ochoa et al., 2012; Meredith and Blais, 2019). The present study investigates the effects of a traditional irrigation system which has influenced the groundwater recharge in a semi-arid mountain front zone. The system relies on diverting an intermittent streamflow, thus generating extended recharge.

The upstream area of the mountain front receives the most recharge due to the high amount of streamflow diversion for irrigation throughout the year. The upstream irrigation area on the western side of the streamflow receives more diverted water and thus records higher recharge than the eastern side. Furthermore, because of irrigation priority, the downstream part of the mountain front is only irrigated during floods leading to a lower recharge. Therefore, irrigation practices are key to the renewal of groundwater resources in this mountain front area.

Traditional irrigation systems are often central to maintaining community stability in arid and semiarid rural piedmont areas (Fernald et al., 2012; Fernald et al., 2015; Turner et al., 2016). In our study region, the severe groundwater depletion observed in the plain is clearly attenuated in the piedmont thanks to the recharge via irrigation (Figure 3-8). Worldwide depletions in

groundwater resources have been observed in many regions where irrigation practices are primarily dependent on groundwater resources. Conversely, where irrigation is primarily surface water-based the groundwater resources are replenished (Taylor et al., 2009). An omnipresent issue is that the downstream residents may be deprived of the water resource used for irrigation (Cody, 2018; Kendy and Bredehoeft, 2006). Similar to the downstream irrigation region in this study, which receives limited stream water for irrigation. The issues associated with shared water resources in irrigation areas is expected to escalate with predicted declines in streamflow due to climate change (Gleick, 2003; Wheeler and Von Braun, 2013; Hajhouji et al., 2018), alongside the severe depletions in groundwater resources (Aeschbach-Hertig and Gleeson, 2012; Fakir et al., 2015), and the drive to increase agricultural production. Such combined pressures are central to serious conflicts over water resources between upstream and downstream users.

IV.3. Groundwater recharge sources in the mountain front

As arid and semi-arid basins receive low annual rainfall volumes, groundwater recharge often occurs indirectly via ephemeral or intermittent streamflow infiltration through streambeds and through subsurface inflow from adjacent mountains (Blasch and Bryson, 2007; Aji et al., 2008; Kao et al., 2012; Guo et al., 2015; Bresciani et al., 2018). Chowdhury et al. (2008) reported that the infiltration through streambeds along the mountain fronts is the primary recharge source to the Presidio-Redford Bolson and Rio Grande alluvial aquifers. Aji et al. (2008) have stated that the primary groundwater recharge source of the North China Plain is the subsurface inflow from mountainous areas transferred to lowland areas via the piedmont alluvial fans. These two natural recharge sources can be limited by various conditions. Stream losses can be limited by rapid runoff, clogging layers at the surface of channel beds and evaporation (Chowdhury et al., 2008; Schwartz, 2016). They are also dependent on streamflow volumes, streamflow duration (Dahan et al., 2009) and sediment characteristics (hydraulic conductivity and specific yield) (Sorman and Andulrazzak, 1993). For example, the deposition of clay sediments on the streambed surface after flood events, as has been observed in this study area, forms a thin confining layer that reduces the permeability of the streambed surface. Subsurface inflow from the mountain block can be limited by faults which can act as a barrier to groundwater flow (Wilson and Guan, 2004; Chowdhury et al., 2008; Liu and Yamanaka, 2012) or by low hydrodynamic characteristics of bedrock aquifers (Bresciani et al., 2018; Markovich et al., 2019).

In addition, these natural hydrological systems can be modified by anthropogenic activities, which may lead to the introduction of other sources of recharge such as irrigation. Ochoa et al. (2012) found that irrigation percolation and canal seepage contribute to groundwater recharge in shallow aquifers. Fernald et al. (2015) have shown how human-adapted irrigation systems sustained groundwater via seepage from irrigation ditches and fields. They also found a strong relationship between groundwater recharge in the basin floor and snowmelt runoff used for irrigation. Diverted streamflow to the paddocks may result in recharge due to over-irrigation (Ochoa et al., 2012; Fernald et al., 2015), and focused recharge may also occur along the earth irrigation channels during transport (Ochoa et al., 2012; Rotiroti et al., 2019). This irrigation recharge depends on soil properties, irrigation practices such as water volumes and duration (Kruse et al., 1990; Bethune et al., 2008; Ochoa et al., 2009), and root water extraction patterns and the water table depth (Bethune, 2004; Ochoa et al., 2012).

In the mountain front area of this study, three groundwater recharge processes are identified (Figure 3-9). (1) Recharge by irrigation water leakage (irrigation recharge). The recharge area is expansive thanks to the irrigation channels that divert the intermittent streamflow kilometers away from the streambed to the irrigated crops. (2) Focused recharge by streamflow along the streambed (stream recharge). This contributes to groundwater recharge within the mountain front especially during the snowmelt periods and the high floods. However, it is significantly reduced by the high streamflow diversion for irrigation in the upstream area. (3) Probable recharge by subsurface inflow from the mountain block and/or by infiltration of local rainfall, which is suspected where the streamflow and irrigation recharge influence is low. These two types of recharge are generally difficult to discriminate. Indeed, a recent review by Markovich et al. (2019) showed that the conclusions about mountain block recharge from studies using stable isotopes remain highly speculative since stable isotope values allow the identification of precipitation elevation source but not the location where this water was infiltrated.

V. Conclusion

In high elevation mountain areas, although there are natural recharge processes from streamflow losses and mountain block subsurface inflows, this study highlights that irrigation practices can result in the dominant recharge process for groundwater. This study presents the case of a semiarid irrigated mountain front area. The combined use of stable isotope values with fluctuations in hydraulic head data showed that there are three sources of groundwater recharge with various impacts: (1) irrigation recharge by diverted streamflow; (2) stream recharge; and

(3) probable subsurface inflow from the mountain block or/and local rainfall infiltration. The recharge from irrigation leakage was revealed as the main source of the observed seasonal groundwater rise. Indeed, because of the irrigation needs and the water resources scarcity, the majority of the mountain streamflow is diverted to irrigation, thereby reducing the potential of in-stream recharge and increasing the irrigation recharge beneath the agricultural lands. The mountain block and/or local rainfall recharge was suspected outside the zone of influence of the streamflow recharge. This was characterized by the highest stable isotope values.

The results from this study are important; particularly in highlighting that irrigation can deeply modify both the recharge processes and the water balance in the mountain front areas. Groundwater resources in such areas become reliant on the irrigation practices as an important source of recharge, and this anthropogenic modification of the hydrological cycle should be assessed and taken into consideration within both local and regional integrated water management strategies.

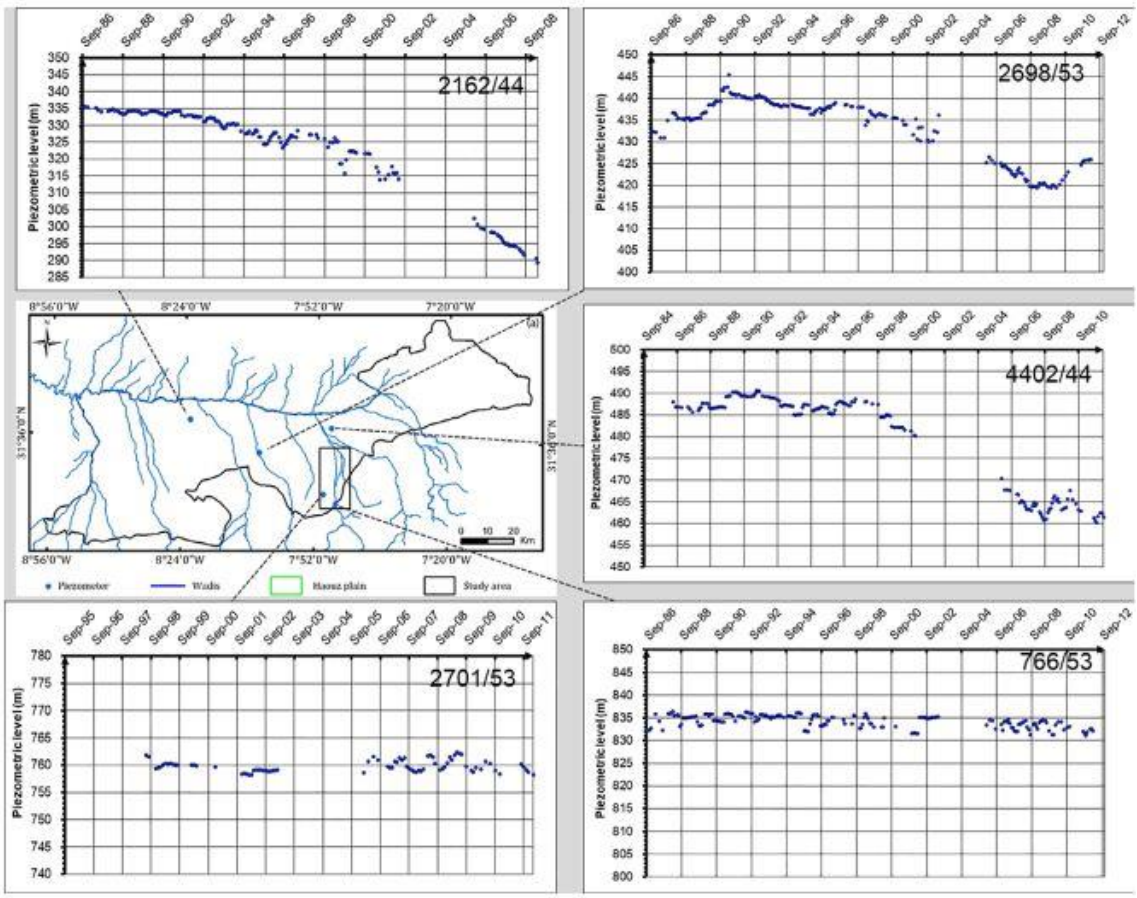

Figure 3-8: Groundwater elevation records over decades showing the difference in groundwater evolution between the mountain front area and the plain (the black rectangle indicates the study area). A severe groundwater depletion has been observed in the plain.

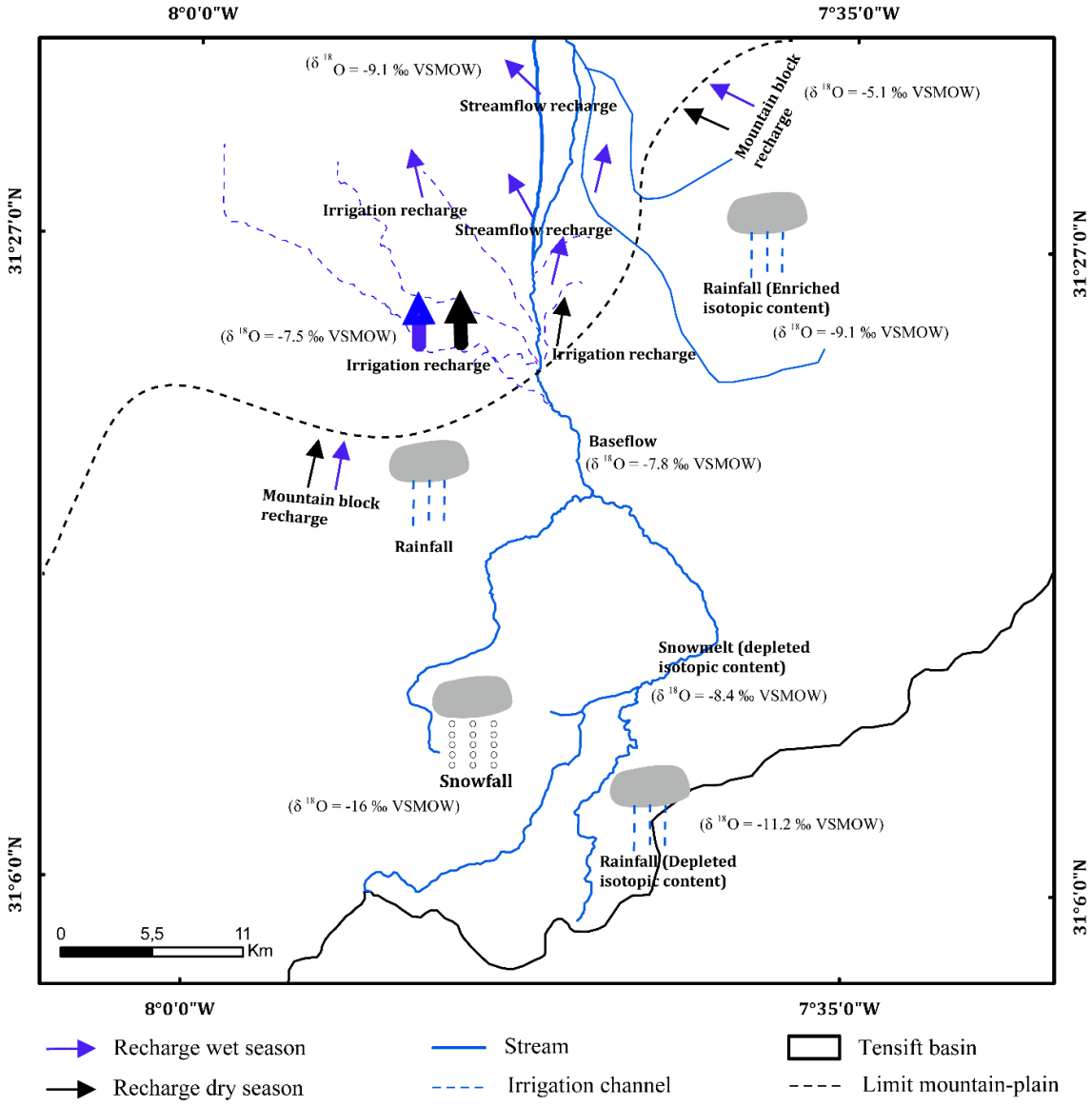

Figure 3-9: A conceptual model of groundwater recharge sources in the study area. Irrigation recharge is designated by IR, Ourika stream losses by SFR and lateral inflow from the mountain block by MBR. The size of the arrow refers to the contribution of the recharge sources to groundwater.

Chapter 4: Impacts of traditional irrigation practices on groundwater quality, Morocco.

I. Introduction

In many regions worldwide, agricultural practices are a major polluter of groundwater resources. Due to increasing food demand, irrigated agricultural systems are rapidly expanding and evolving, and have been found to significantly alter both the groundwater quantity and quality (Johansson et al., 2009). Many case studies, ranging from small to regional scales, have demonstrated the negative impact of irrigation on groundwater quality (Pérez-Sirvent et al., 2003; Feng et al., 2005; Duncan et al., 2008; Zhang et al., 2012; Haj-Amor et al., 2017). In particular, a number of studies have highlighted the degradation of groundwater quality during the transition from rainfed to irrigated agriculture in semi-arid regions (Hu et al., 2019; Merchán et al., 2015a; 2020).

Groundwater degradation in irrigated areas can result from multiple causes, including the use of agricultural contaminants, the use of degraded waters to irrigate, the transfer of contaminants from the unsaturated zone, or changes in the water budget resulting in the mobilization or evapo-concentration of contaminants. For example, where the surface water used to irrigate is of poor quality, irrigation results in the distribution of contaminants. Therefore, the contaminants that were previously restricted to rivers are, via irrigation, dispersed across catchments. This is observed in agricultural regions located down-gradient from cities that are either heavily populated, have high runoff events, and/or have poor infrastructure to treat wastewater from domestic and industrial zones before flowing into the connecting rivers (Li et al, 2016., Panda et al., 2018; Liu et al., 2020). Irrigation with diverted surface waters can also result in groundwater mounds within the irrigation zone. This rise in the water table can result in the mobilization of contaminants, more rapid transfers of contaminants and an increase in the evaporative effects on the concentrations of contaminants in the shallow groundwater (Scanlon et al., 2007) especially under semi-arid climates.

In addition, in semi-arid zones the salinization of groundwater resources can result from multiple natural processes such as the dissolution of evaporites that have accumulated in the unsaturated zone, and high evapotranspiration of both soil water and shallow groundwater (e.g. Tweed et al., 2011). Groundwater recharge by surface water irrigation in those regions can therefore potentially act to increase or reduce the salinity of groundwater (Stigter et al., 2006; Rotiroti et al., 2019; Jia et al., 2020) depending on the quality of irrigation water.

Many studies regarding the impact of irrigation on groundwater quality have considered the modern irrigation systems, such as drip irrigation and cross-regional transfers (Chen and

He, 2003; Jia et al., 2020). In comparison, fewer research has focused on traditional irrigation systems such as the ancestral streamflow diversion by irrigation channels called Seguias (Bouimouass et al., 2020) or Acequia (Fernald et al., 2015; Turner et al., 2016). In semi-arid zones where the irrigated areas are adjacent to a mountain range, high elevation streamflow from rainfall and snowmelt is a substantial source of those systems.

As is the case for the whole of North Africa, Morocco is characterized by an arid to semi-arid climate with high inter-annual variability and several periods of below average precipitation (Jarlan et al., 2016). Piedmont areas along the High-Atlas in Morocco benefit from a milder climate and from streamflow generated at high altitudes (Toubkal peak at 4165m) by rainfall and snowmelt. Since hundreds of years, they host traditional agriculture, consisting of a subsidence production system composed mainly of olive trees and wheat. This traditional agriculture has been secularly irrigated by a large network of gravity-fed surface irrigation earth channels (locally named Seguias) that divert the streamflow. This hydro-agro-system is similar to the so-called spate irrigated systems, which are particularly found in areas where mountain catchments border lowlands, in the Middle East, North Africa, West Asia, East Africa and parts of Latin America (Van Steenbergen et al., 2011). This type of traditional irrigation used to expand from the piedmont in south to the plain in north. During the last century after the French colonization, it began to retreat from the plain in favor of modernized agriculture, as it is the case for most of the plains around the world (Scanlon et al., 2007) with resultant impacts on groundwater quality and quantity (Hu et al., 2019). Nowadays, the traditional irrigation is extended over the piedmont area.

The present study investigates a piedmont area located in a semi-arid catchment of the Ourika stream, which is one of the main streams flowing from the High-Atlas Mountains of Morocco. The area preserves a traditional agriculture where local small-scale farms use organic fertilizers for growing wheat and olives trees, irrigated by diverting the streamflow of the High-Atlas mountains using Seguias. The study investigates the hydrochemistry of the water as it evolves from the high elevation mountains to the piedmont. It also identifies the effects of the traditional irrigation practices on the groundwater chemical quality, including the impacts on salinity, nitrate and major ion concentrations. At the end, we discuss whether the current state of the traditional irrigation is still close to sustainable agricultural practices and what kinds of threats it faces.

II. Material and methods

II.1. Sampling and laboratory analyses

In this study major ions data is used. The details of the sampling procedure and the data are presented in chapter 3 where a part of this data was used to determine the groundwater recharge sources, whilst in this study the objective is to use this data to focus on hydrochemical processes and water quality assessment. The sampling points are presented in figure 4-1.

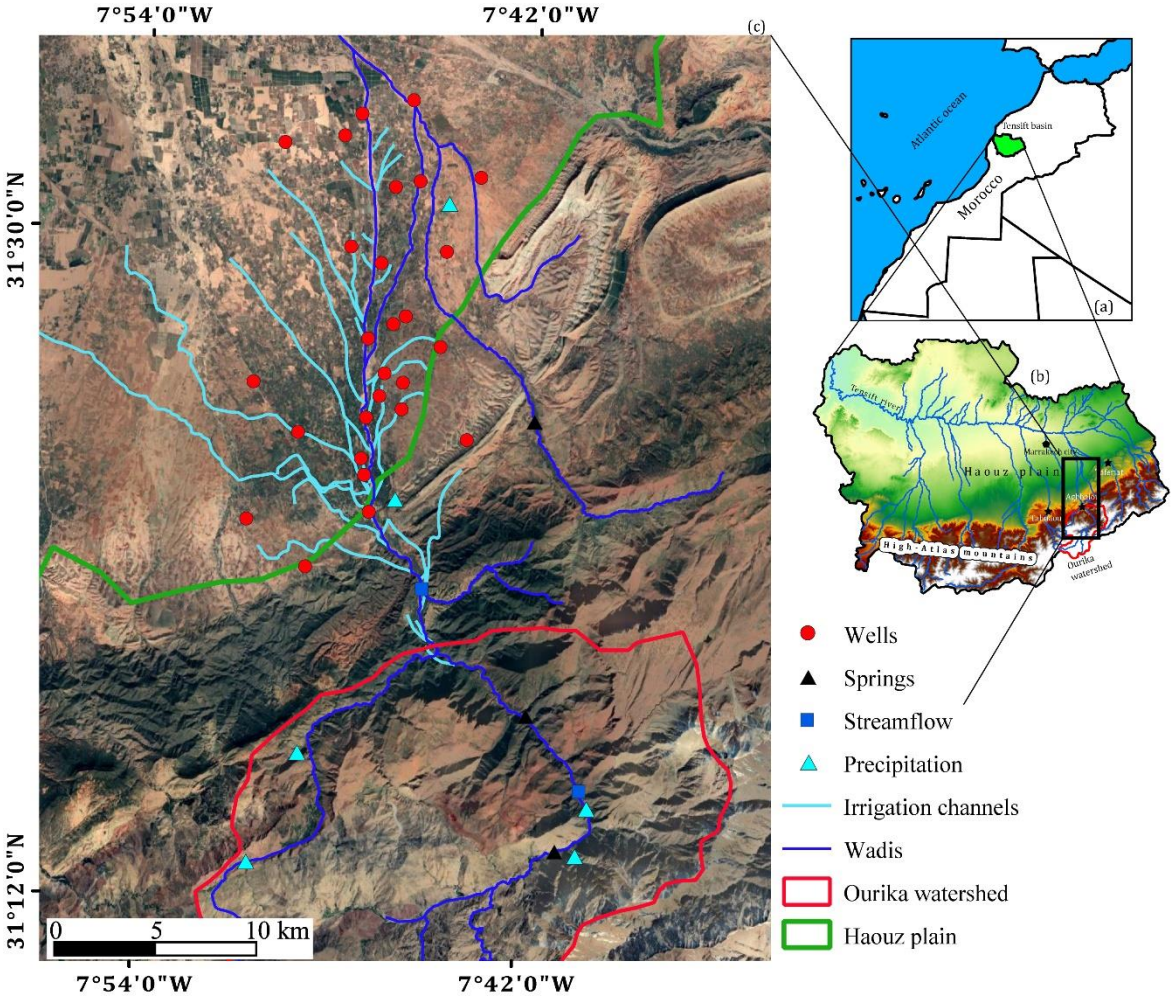

Figure 4-1 : Localization of the study area and sampling points.

II.2. Data analysis

The hydrochemical data were analyzed using boxplots, Piper diagram, scatterplots, ionic ratios, chloro-akaline indices, and saturation indices. By studying the relationships between the major elements, the distribution of the element's concentrations in the scatterplots, their correlations and ratios, it is possible to determine the chemical features of water and identify the involved geochemical processes (Kim et al., 2002; Bennettes et al., 2006; Alcalà and

Custodio, 2008; Li et al., 2016; Marghade et al., 2019; Celestino et al., 2019; Zhang et al., 2020).

The chloro-akaline indices (CAI-I and CAI-II) introduced by Schoeller (1965) are widely used as indicators of ion exchange occurring in aquifers (Li et al., 2013; Talib et al., 2019). The indices, expressed by the equations 1 and 2, are negative when the cation exchange occurs, meaning that Na^+ is released from the medium in exchange with Ca^{2+} and Mg^{2+} in water. However, positive indices mean that Na^+ is adsorbed in the medium simultaneously with the release of Ca^{2+} and Mg^{2+}, known as reverse ion exchange.

$$\mathrm{CAI-I} = \frac{Cl^- - (Na^+ + K^+)}{Cl^-} \qquad (1)$$

$$\mathrm{CAI-II} = \frac{Cl^- - (Na^+ + K^+)}{HCO_3^- + SO_4^{2-} + CO_3^{2-} + NO_3^-} \qquad (2)$$

Saturation indices (SI) indicate whether a water sample is oversaturated or undersaturated with respect to a mineral. This provides an indication of the potential for minerals to be dissolved or precipitated in the solution. Saturation indices were calculated in this study using PHREECQ software (Parkhurst and Appelo, 1999) based on the following equation (3):

$$SI = \log(IAP/K) \qquad (3)$$

where IAP is the ion activity product of the mineral, and K is the equilibrium constant of the mineral. The SI value is negative when the mineral may be dissolved, positive when it may be precipitated, and zero when the water and mineral are at chemical equilibrium.

II.3. Water suitability for domestic use and irrigation

Water quality index is widely used tool to assess the suitability of groundwater for drinking supplies (Talib et al., 2019). Drinking water could be a serious health risk if its quality is deteriorated (Zhang et al, 2020). The WQI relies on the concentrations and the weight coefficient of the chemical elements. The coefficients are based on the impact of each element on the human health (Xiao et al., 2019). The WQI is calculated according to the following equation:

$$WQI = \sum[W_i \times \left(\frac{C_i}{S_i}\right) \times 100] \qquad (4)$$

Where C_i is the concentration of each parameter, S_i is the corresponding standard WHO values (WHO, 2017) and W_i is the relative weight of each parameter computed following the equation:

$$W_i = \frac{w_i}{\sum_{i=1}^{n} w_i} \qquad (5)$$

Where w_i is the weight of each parameter and n is the number of parameters. Table 1 shows the relative S_i and W_i for each parameter (Talib et al., 2019).

Nitrates (NO_3^-) are also analyzed as an indicator of groundwater contamination by leaching of (mineral and organic) fertilizers or septic waste, and as they are important for health concerns (WHO, 2011).

Similarly, to drinking water, there are several indices used to assess the suitability of groundwater and surface water for irrigation (Talib et al., 2019). The commonly used indices are the sodium adsorption ratio (SAR), residual sodium carbonates (RSC), sodium percentage (% Na) and Kelly's ratio (KR) (Vincy et al., 2015). These indices are computed using the following equations:

$$SAR = \frac{Na^+}{\sqrt{(Ca^{2+} + Mg^{2+})/2}} \qquad (6)$$

$$RSC = (CO_3^- + HCO_3^-) - (Ca^{2+} + Mg^{2+}) \qquad (7)$$

$$\%Na = [\frac{(Na^+ + K^+)}{(Na^+ + K^+ + Ca^{2+} + Mg^{2+})} \times 100 \qquad (8)$$

$$KR = \frac{Na^+}{Ca^{2+} + Mg^{2+}} \qquad (9)$$

Table 4-1: WQI index.

Parameter	S_i (mg/l)	Weight	Relative weight
TDS	1000	5	0.13
Cl^-	250	5	0.13
SO_4^{2-}	250	5	0.13
F^-	1	5	0.13
NO_3	50	5	0.13
Na^+	200	4	0.10
Mg^{2+}	150	3	0.08
Ca^{2+}	200	3	0.08
K^+	12	2	0.05
HCO_3^-	250	1	0.03
		$\sum W_i = 38$	$\sum W_i = 1$

III. Results

III.1. Hydrochemical properties from the mountain to the piedmont

The electrical conductivity (EC) is very low for mountain streamflow (average = 273 μS/cm), increases slightly for mountain springs (average = 328 μS/cm), and more substantially for piedmont groundwater (average = 807 μS/cm) (Table 2) that is generally fresh: only 14 groundwater samples exceed 1000 μS/cm, and two of them exceed 2000 μS/cm (sampled from the well W17). The groundwater EC is lower for the irrigation area (mean = 727 μS/cm and max = 1094 μS/cm) than the non-irrigation area (mean = 994 and max = 2620 μS/cm; Table 4-2). From the dry (September to November) to the wet season (January to March), the EC decreased in streamflow from 324 μS/cm to 244 μS/cm in average, and in the groundwater beneath the irrigation area from 841 μS/cm to 692 μS/cm. The pH is higher in the mountain stream water (an average of 7.94 and a maximum of 9.1) than in piedmont groundwater (an average of 7.58 and a maximum of 8.37).

The major ion concentration is similar in streamflow and springs, but undergoes a sensible increase in the piedmont groundwater (Table 4-2, Figure 4-2), which is enriched particularly of carbonates (Ca^{2+}, Mg^{2+}, HCO_3^-). The irrigation area mostly has lower major ion concentrations compared with groundwater from the non-irrigated area (Figure 4-2); the largest differences are observed for Na and Cl, whose mean values increase by 46 and 44 % respectively in the non-irrigated area.

Table 4-2: Statistics of the field parameters and major ions.

Hydrochemical variables (mg/l)	Mountain streamflow (n=11)			Mountain springs (n=14)			Irrigation area (n=39)			Non-irrigation area (n=16)			WHO (2017)
	Min	Max	Mean	Min	Max	Mean	Min	Max	Mean	Min	Max	Mean	
pH	6.64	9.05	7.94	7	9.1	7.72	7.00	8.2	7.5	7.0	8.4	7.8	6.5-8.5
EC	104.0	563.0	273.1	77.0	943.0	328.2	293.0	1945.0	726.7	258.0	2620.0	994	
TDS	79.0	423.0	194.5	54.0	705.0	241.3	216.0	1130.0	491.2	198.0	1615.0	655.3	500
Na^+	3.3	24.7	11.7	2.6	55.4	15.39	18.1	257.7	53.6	10.2	425.5	100.0	200
K^+	0.5	2.1	1.2	0.3	3.6	1.42	0.6	1.4	3.0	0.2	2.9	1.1	200
Mg^{2+}	3.0	9.5	7.2	1.9	21.5	7.5	6.6	16.6	30.5	7.8	46.9	25.4	NA
Ca^{2+}	11.5	69.7	29.5	7.4	38.4	21.49	30.5	129. 9	64.4	27.0	111.4	59.3	200
Cl^-	3.2	32.2	14.8	2.4	79.9	19.53	17.4	462.8	93.4	7.8	719.3	167.4	250
$SO4^-_2$	6.9	27.1	16.3	5.6	70.4	23.03	11.0	91.5	29.1	2.5	149.8	39.9	200
HCO^-_3	49	256.0	110.5	27.0	371.0	132	112.2	370.9	222.8	131.8	398.9	247.3	NA
$NO3^-$	0.5	8.1	3.2	1.9	7.1	3.8	1.2	22.5	10.1	2.4	22.1	10.1	50

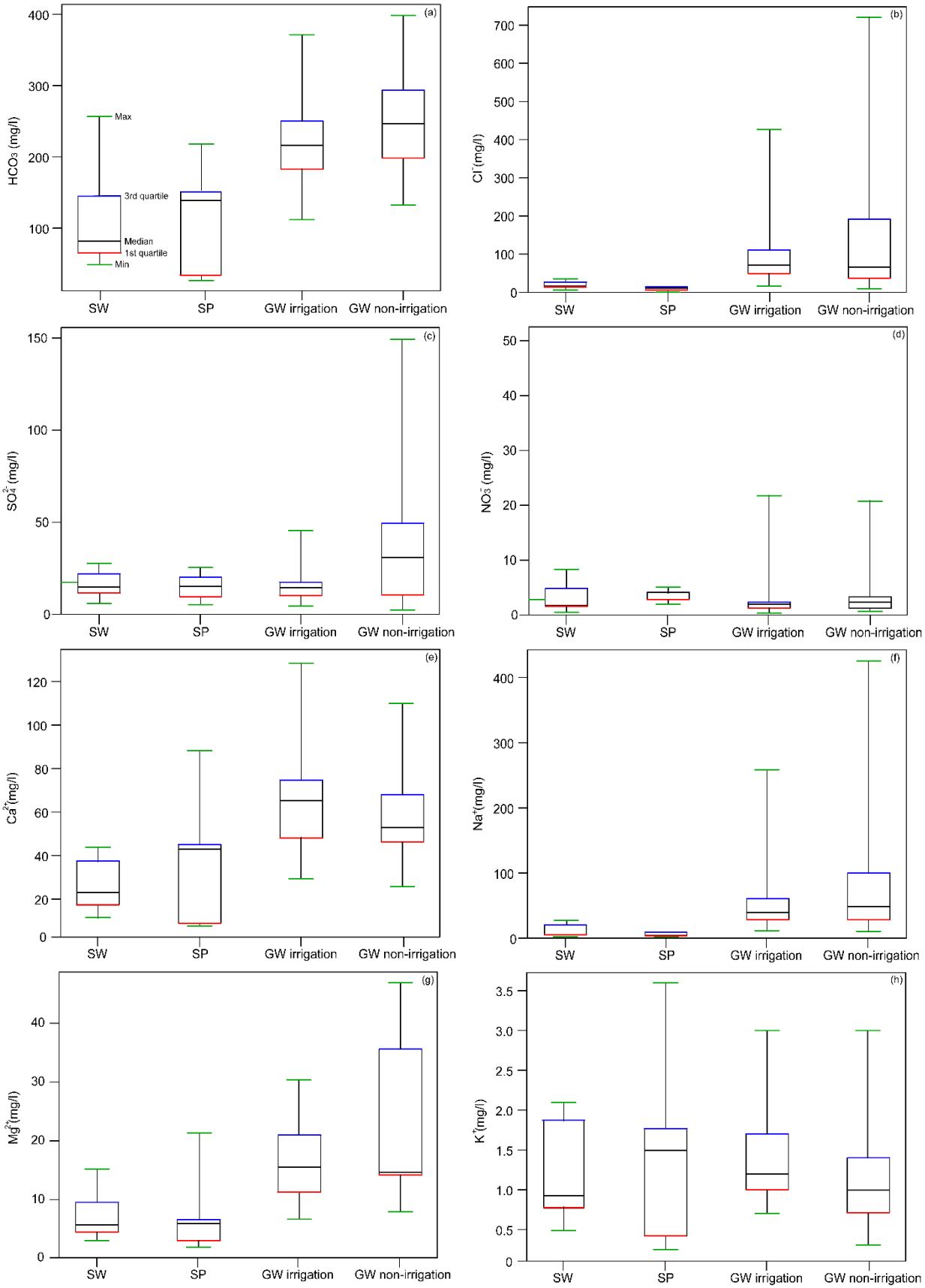

Figure 4- 2: Boxplots of the major ions in groundwater (GW), spring (SP) and surface water (SW).

On the Piper diagram (Figure 4-3), the hydrochemical facies of the streamflow is of Ca-HCO_3 type similar to that of atmospheric precipitation (rain and snow). Compared to precipitation, a slight enrichment of Na^+, Mg^{2+} and SO_4^{-2} is observed. The majority of the groundwater in the piedmont also has a Ca-HCO_3 facies (Figure 4-3). It shows in addition two secondary facies (Figure 4-4), Ca-Mg-Cl and Na-Cl related to specific enrichment in Cl-, Na^+, and Mg^{2+}. Indeed, 7 wells located close to the Ourika wadi exhibit Ca-Mg-Cl facies. 3 wells in the non-irrigated area, W17, W19 and W27, have Na-Cl facies; they are close to a tributary, Elmaleh wadi (Elmaleh in Arabic means the salty), which drains the low-altitude halite-rich terrains. .

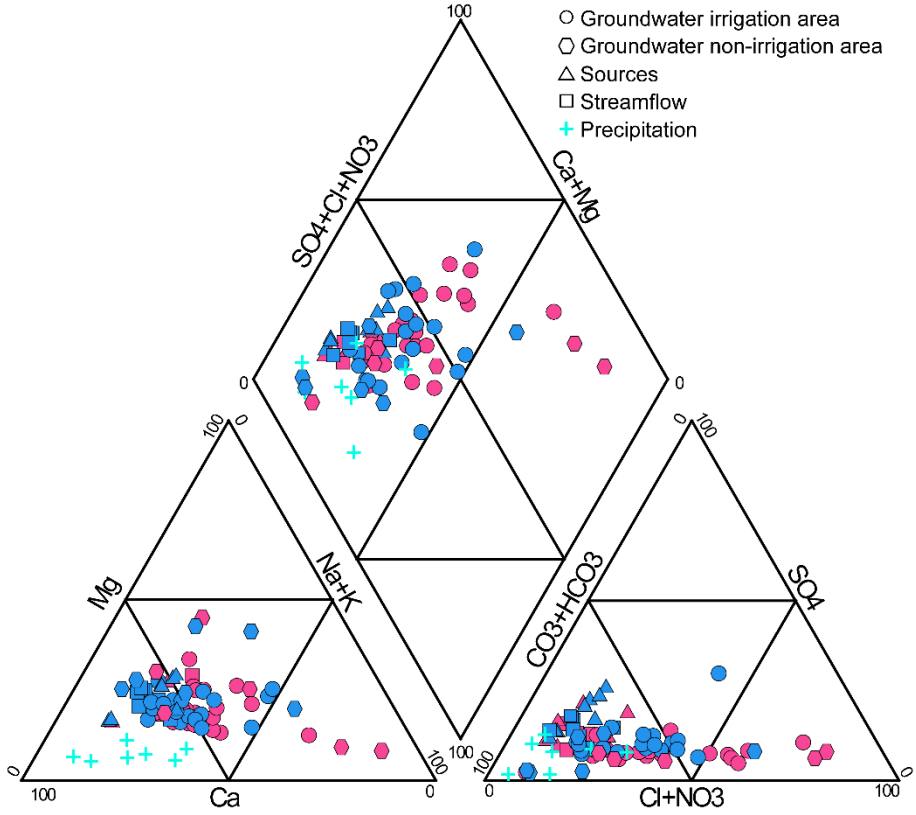

Figure 4- 3: Piper diagram. Pink color refers to dry season and blue color refers to wet season.

III.2. Origins of ions in mountains water and groundwater

The natural chemical composition of water is potentially influenced by atmospheric precipitation, evaporation, transpiration, evaporite dissolution and rock weathering. In mountain waters Ca^{2+}, HCO_3^-, Na^+, Mg^{2+}, SO_4^{2-} ions are likely sourced firstly from precipitation and secondly from the weathering of silicate minerals in the crystalline rocks of the High-Atlas massif. The piedmont groundwater samples show similar facies with mountain water, however

their relatively higher concentrations of Na^+, Cl^-, and in a lesser proportion of Ca^{2+}, Mg^{2+} and HCO_3^- suggest additional sources of mineralization.

On the Na^+/Cl^- versus Cl^- scatter diagram (Figure 4-5), samples with Na/Cl ratios close to 1 with increasing Cl^- concentrations indicate either halite dissolution, evaporation or transpiration is the major process increasing Na^+ and Cl^- concentrations. The groundwater samples from the non-irrigated area exhibit little changes in the Na^+/Cl^- ratio with high Cl^- concentrations (> 10 meq/L). A previous study by Bouimouass et al. (2020) using the stable isotope values of groundwater for the same samples, showed no evidence of evaporation effects. Therefore, high Na^+ and Cl^- concentrations in groundwater are driven by Triassic halite dissolution. For Cl^- concentrations lower than 10 meq/L, there are greater variations in the Na/Cl ratio that indicates either contributions from rock weathering reactions (Na/Cl > 1) or ion exchange effects (Na/Cl < 1). Based on the Na/Cl ratio, the piedmont groundwater is divided into two groups (Figure 4-6). The sodium enriched group n° 1 (where Na/Cl > 1), which is similar to the mountain streamflow Na/Cl ratios, is mostly located in the irrigation area (Figure 8). The sodium depleted group n° 2 (where Na/Cl < 1) is predominantly composed of samples located along the Ourika wadi.

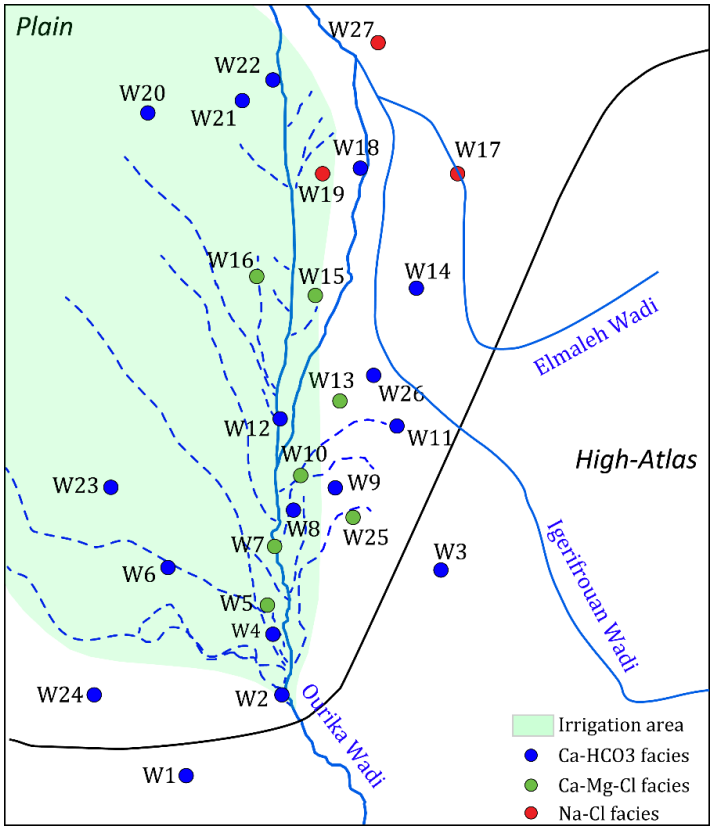

Figure 4- 4: Map of groundwater facies distribution. The extent of the area irrigated by surface water is colored blue. Data represent the average/dry season/wet season value from sites where multiple samples were analyzed.

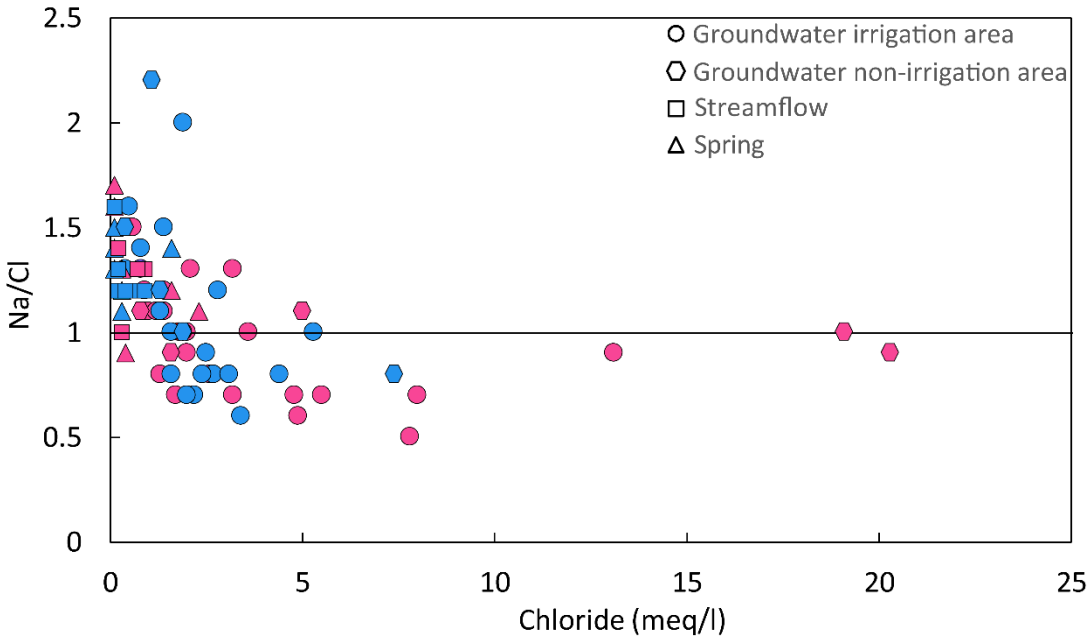

Figure 4- 5: Plot of Na/Cl ratio versus Cl. Red color refers to dry season and blue color refers to wet season.

For group n° 1 (Na/Cl > 1) representing the irrigation area, the enrichment of Na could be due to weathering by the streamflow in the mountains of the Na-silicate such as albite and plagioclase (equations 10 and 11) (Gao et al., 2020) since Na-silicates are largely present in the High-Atlas as granodiorite and granite.

$$2NaAlSi_3O_8\ (Albite) + 9H_2O + 2H_2CO_3 = Al_2Si_2O_5(OH)_4 + 2Na^+ + 2HCO_3^- + 4H_4SiO_4 \qquad (10)$$

$$(Na_{0.82}Ca_{0.18})Al_{1.18}Si_{2.82}O_8(Plagioclase) + 1.18CO2 + 1.77H_2O = 0.82Na^+ + 0.18Ca^{2+} + 1.18HCO_3^- + 0.59Al_2Si_2O_5(OH)_4 + 1.64SiO_2 \qquad (11)$$

In the HCO_3^- versus Na^+ plot (Figure 7a), water samples falling along the 1:1 and 1.18:0.82 lines indicate albite and plagioclase weathering might increase HCO_3^- and Na^+ in water (Kim et al., 2002; Zhang et al., 2020). All streamflow and mountain groundwater lie along and above the line 1.18:0.82 indicating contribution from weathering of albite and plagioclase to Na^{2+} and HCO_3^- in these waters. The majority of the piedmont groundwater samples lie on or between the two lines (Figure 7a) implying that weathering of albite and plagioclase is responsible for amounts of Na^+ and HCO_3^-. The groundwater samples contaminated by salts plot far to the right of the 1:1 line. The additional sources of HCO_3^- ion could originate from various sources including calcite dissolution (equation 12), and Ca-silicates weathering such as anorthite (equation 13), pyroxene (equation 14) and amphibole (equation 15) (Zhang et al., 2020). Based on chemical reactions 12, 13, 14 and 15, samples falling along the lines 1:1, 2:1, 1.7:1, 7:2 in

figure 7b are due to the dissolution of carbonates such as calcite and dolomite, and the weathering of Ca-silicates such as anorthite, pyroxene and amphibole, respectively. All mountains streamflow and springs samples, and most of the piedmont groundwater samples fall between the lines 1:1 and 1.7:1 (Figure 7b) indicating that the dissolution of calcite and some Ca-silicates such as pyroxene contributes to HCO_3^- concentrations in these waters.

$$CaCO_3 + CO_2 + H_2O = Ca^{2+} + 2HCO_3^- \quad (12)$$

$$2CaAl_2Si_2O_8(\text{Anorthite}) + 4CO_2 + 6H_2O = 2Al_2Si_2O_5(OH)_4 + Ca^{2+} + 4HCO_3^- \quad (13)$$

$$CaMg_{0.7}Fe_{0.3}Si_2O_6(\text{Pyroxene}) + 3.4CO_2 + 2.3H_2O = Ca^{2+} + 0.7Mg^{2+} + 2SiO_2 + 3.4HCO_3^- + 0.3H^+ + 0.3Fe(OH)_3 \quad (14)$$

$$Ca_2Mg_5Si_8O_{22}(OH)_2(\text{Ampibole}) + 14CO_2 + 22H_2O = 2Ca^{2+} + 5Mg^{2+} + 14HCO_3^- + 8H_4SiO_4 \quad (15)$$

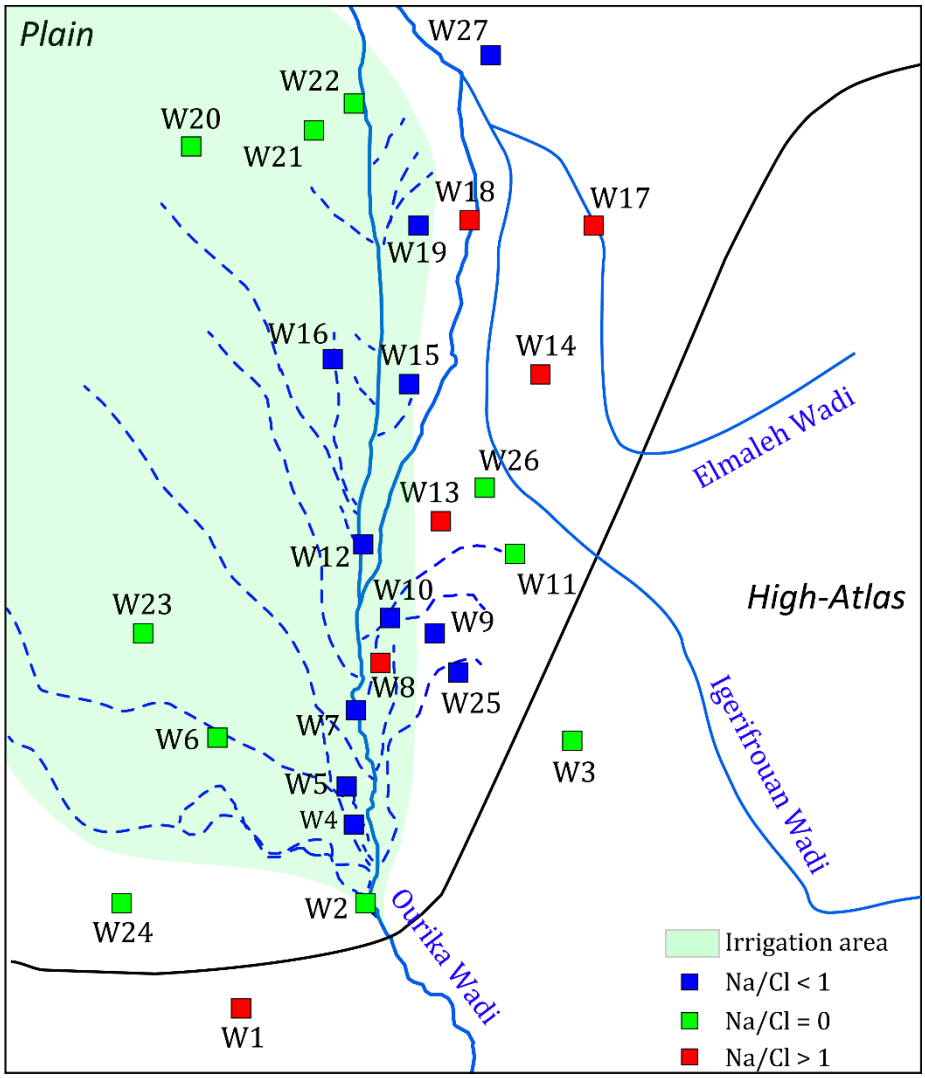

Figure 4- 6: Map of Na/Cl rations distribution. Data represents the average/dry season/wet season value from sites where multiple samples were analyzed.

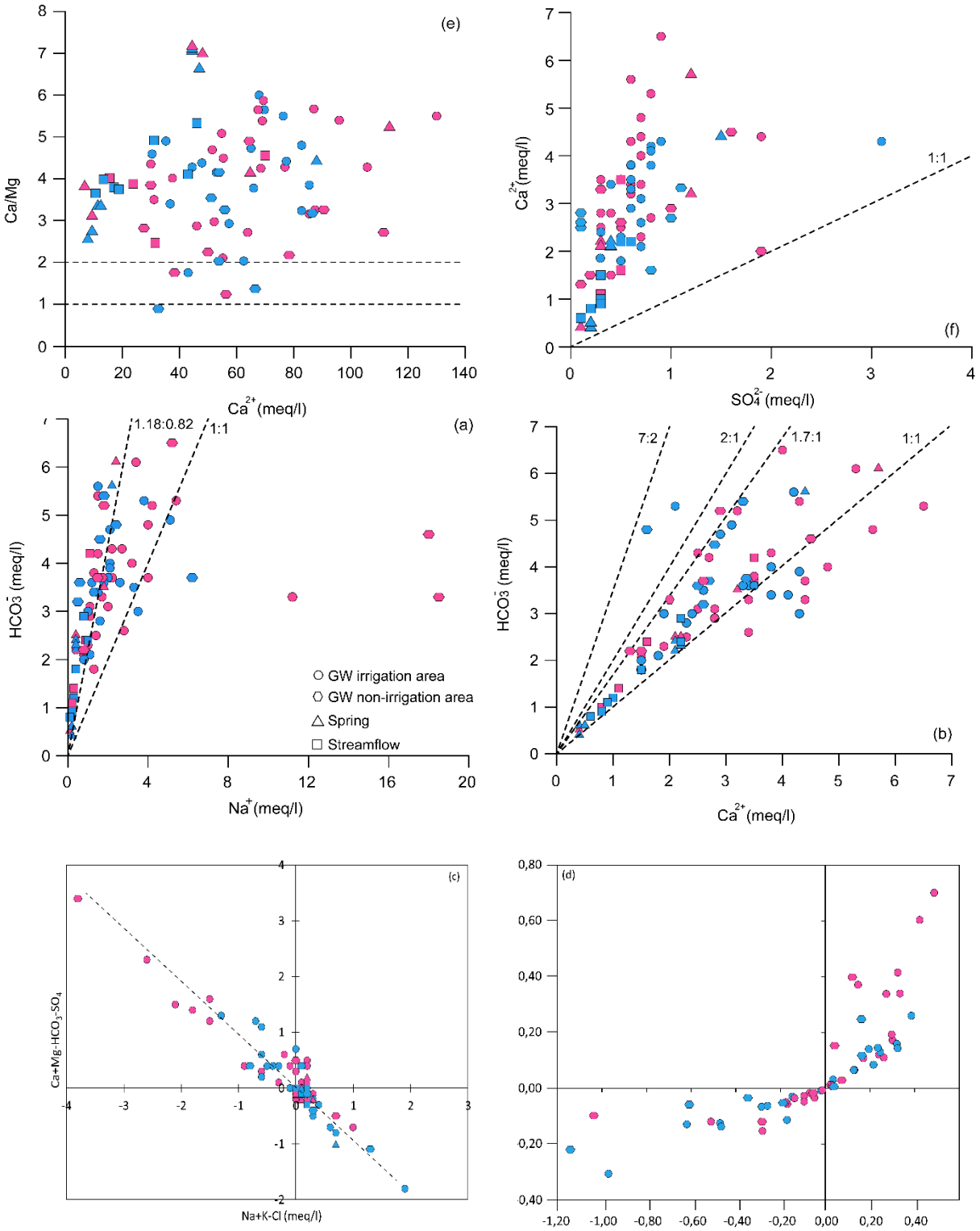

Figure 4- 7: *Scatter plots of ions. Red color refers to dry season and blue color refers to wet season. Symbols with cross refer to wells located in the non-irrigation area.*

For group n° 2 (where Na/Cl < 1) representing the piedmont groundwater along the wadi, the ion exchange processes and anthropogenic sources of Cl^- (Celestino et al., 2012) could be responsible of Na depletion or Cl^- enrichment. The plot of $Na^+ + K^+ - Cl^-$ versus $Ca^{2+} + Mg^{2+} - SO_4 - HCO_3^-$ (Figure 7b) shows a linear relationship with a slope of -0.83, close to -1, indicating the occurrence of ion exchange (Yang et al., 2016). Piedmont groundwater samples are almost equally distributed between positive and negative CAI-1 and CAI-2 values (Figure 7c) (25 samples with positive values, 23 with negative values and 04 with CAI-I and CAI-II equal to 0). This indicates that both base cation exchange (positive CAI-1 and CAI-2 values) and reverse ion exchange (negative CAI-1 and CAI-2) potentially occur. Along the wadi (group 2), the base cation exchange dominates implying depletion of Na^+ in groundwater. Reverse ion exchange characterizes groundwater beneath the irrigation area (Group 1), it induces a release of Na^+ of the aquifer matrix in groundwater and adsorption of Ca^{2+} and Mg^{2+} (Carol et al., 2012; Zaidi et al., 2015).

Ca^{2+} in water could also be due to gypsum dissolution, alongside SO_4, as indicated by the equation 17. A Ca^{2+}/SO_4^{2-} ratio around 1 indicates that these ions are derived from gypsum dissolution. The majority of samples (Figure 9f) are plot to the left of the 1:1 line indicating an excess of Ca^{2+} over SO_4^{2-} ; the Gypsum would be responsible of low amounts of Ca^{2+} and Mg^{2+}.

$$CaSO_4 \text{ (Gypsum)} = Ca^{2+} + SO_4^{2-} \qquad (17)$$

Saturation indices (SI) of piedmont groundwater were calculated by PHREECQ software (Parkhurst and Appelo, 1999). According to SI values (Figure 8a and 8b), groundwater is under-saturation with respect to halite and gypsum, indicating that these minerals have the potential to be dissolved. The SI values of calcite ranged from -0.95 to 0.89 with a mean of 0.04, and for dolomite the SI ranged from -2.31 to 1.61 with a mean of -0.16. These results indicate that in groundwater with respect to calcite and dolomite evolves from undersaturation to oversaturation (Figures 8c and 8d) depending on the season. The groundwater at most sites is saturated with respect to both of these minerals during the low-water season (November-December). In comparison, groundwater is mostly undersaturated with respect to both of these minerals during months that represent the peak of irrigation (March) and the end of irrigation (September), corresponding to the recharge season (Bouimouass et al., 2020).

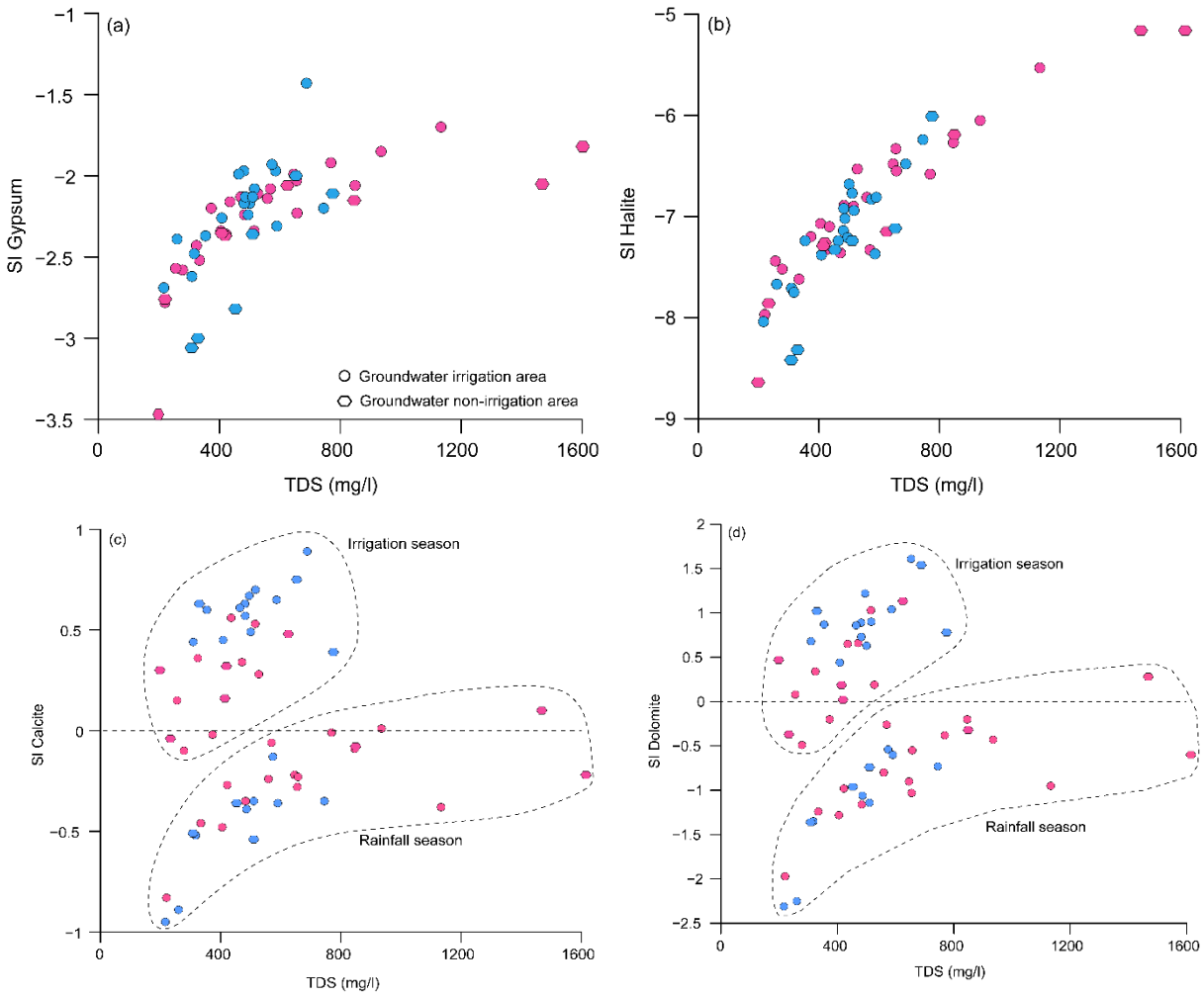

Figure 4- 8: *Saturation indices versus TDS in piedmont groundwater.*

III.3. Origins of nitrate

Nitrate (NO^-_3) are an important plant nutrient and are naturally present in the environment as a part of nitrogen cycle, but often in very low concentration less than 10 mg/l (Hill, 1996). The multiple natural origins of nitrates are related to evaporative enrichment of dry and wet deposition, biogenic sources through bacterial activity in soil, or to a geogenic origin (Stadler et al., 2008).

Nitrate concentrations are low in the streamflow (average = 3.2 mg/l, and a max of 8.2 mg/L) and springs (average = 3.8 mg/l, and a max of 7.15 mg/L), and in piedmont groundwater, the nitrate concentrations are higher (10 mg/l in average). In the irrigation area, additional source of NO^-_3 might originate from plants degradation and mineral, organic fertilizers or animal and domestic sewage (Stadler et al, 2008). Furthermore, nitrates increase slightly from the dry season (average = 8.4 mg/l) to the wet season (average = 12 mg/l). This is explained by

an accumulation of NO^-_3 in the soil during the dry period and its leaching from the soil by rainfall and irrigation returns that are more important during the wet period.

III.4. Quality of drinking and irrigation water

Domestic water needs in the study area are supplied by groundwater. The municipal wells exist only in the agglomerations with thousands of people. Small agglomerations with tens to hundreds of inhabitants use community-managed wells and some inhabitants still use their own wells to meet their domestic needs. Water from these wells is usually used without further treatment but occasional chlorination, which constitutes a potential health risk if the quality of this water is or becomes unsuitable for human use. Groundwater is also used for irrigation in the study area. In the irrigated area, groundwater is used during summer and autumn months when streamflow is absent. In the non-irrigated area, rain-fed agriculture is dominant but some farmers use groundwater to irrigate olive fields.

pH ranges from 7.0 to 8.4 with a mean of 7.6 indicating that water is within the range for drinking standards (6.5-8.5) defined by the WHO. The overall quality of groundwater can be assessed by the water quality index (WQI) (Talib et al., 2019, Sadat-Noori et al., 2014). WQI values are classified into five categories (calculated using the parameters …): excellent (<50), good (>50), poor (>100), very poor (>200) and water unsuitable for drinking (>300). The WQI values range from 3 to 95 with a mean of 24. According to this classification, all groundwater and surface water are "excellent" for drinking purposes. Only the 03 samples of the non-irrigated area and contaminated by salts are close to the "poor "quality category. Although groundwater is of good quality from a mineral perception, additional biological analyses are needed to fully assess the adequacy of groundwater to human use.

The nitrates in mountains streamflow (average of 3.18 mg/L) and springs (average of 3.8 mg/L) are very low and meets all the standard of good quality water. In piedmont groundwater, nitrates (average of 10.1 mg/L) are also very low regarding the WHO standards fixed at 50 mg/L (WHO, 2017).

The suitability of groundwater for irrigation is assessed through the Wilcox diagram (Figure 11) and various irrigation water quality indices, such as SAR, RSC, %Na and KR (Table. 3). As a conclusion, most of the water is suitable for irrigation. Those few presenting unsuitable characteristics due the Na^+ content correspond to the samples collected from the well W17, which is characterized by high Na^+ and Cl^- concentrations and located outside of the irrigated

area. Compared to the others wells in the study area, the well W17 is influenced by the dissolution evaporates.

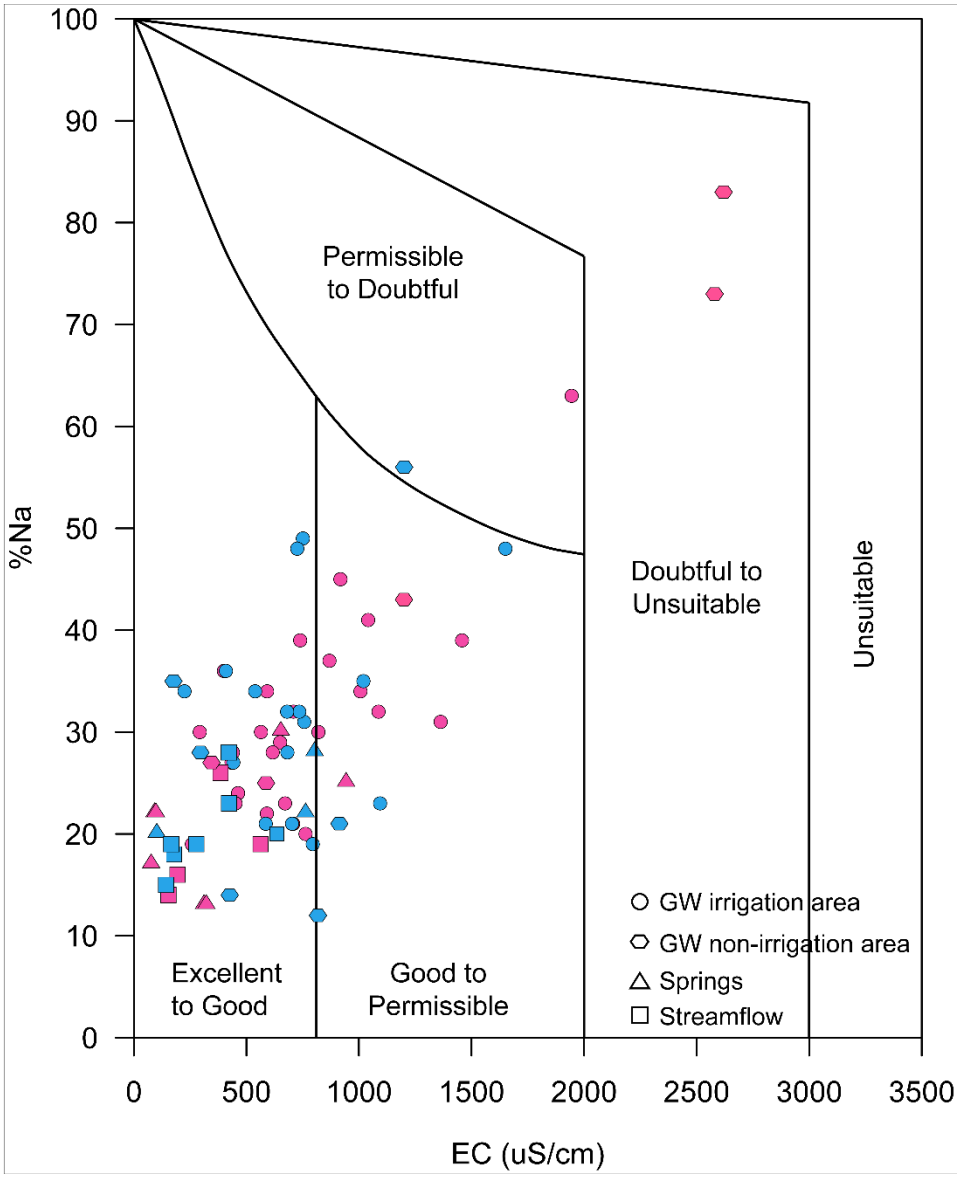

Figure 4- 9: *Wilcox diagram. Red color refers to dry season and blue color refers to wet season.*

Table 3: Statistics of the irrigation water quality indices in the study area.

Indices	Groundwater			Surface water			Permissible limit	Unsuitable samples
	Min	Max	Mean	Min	Max	Mean		
SAR	0.2	13.4	1.6	0.2	0.8	0.5	≤ 18	-
RSC	-4.0	1.1	-0.8	-0.5	-0.1	-0.3	≤ 2.5	-
%Na	12	83	30	14.3	27.5	19.6	≤ 60	3
KR	0.1	4.9	0.5	0.1	0.3	0.2	≤ 1	3

IV. Discussion

IV.1. Hydrochemical processes from the mountain to the piedmont

In the high-atlas mountains, the streamflow and springs are supplied by rainfall and snowmelt, and flow through large outcrops of silicates rocks formed of Precambrian Granodiorite and Gneiss containing plagioclase, amphibole and micaschist, as well as Visean and Triassic siltite and sandstone rocks. They have a Ca-HCO_3 facies similar to that of atmospheric precipitation, and a slight enrichment in Na^+, Mg^{2+} and SO_4^-. The Na-silicates weathering is the main source of Na^+ and HCO_3^- in mountain surface water and groundwater as indicated by their simultaneous evolvement and their strong correlation (R^2 = 0.82 in springs and R^2= 0.84 in surface water), but with lesser contribution to piedmont groundwater (R^2= 0.32). The Ca-silicate weathering contributes to the loading of Ca and Mg. The pyroxene, amphiboles and calcic feldspar are common minerals in basic rocks and are easily weatherable (Jacks, 1973; Bartarya, 1993; Rajmohan and Elango, 2004), therefore their weathering constitutes an important mechanism that controls the mineralization in the Mountains. The presence of SO_4^{2-} might be due to sulfate mineral dissolution such as gypsum.

In the piedmont, groundwater displays in majority a fresh water (average = 713 µS/cm), with a dominant Ca-HCO_3 facies similar to the streamflow. This similarity results from the alluvial aquifer in the piedmont to be exclusively recharged by streamflow mainly as irrigation returns and in-stream losses (Bouimouass et al., 2020). Therefore, piedmont groundwater primarily inherits the hydrochemical characteristics of the high-altitude mountain water. When evolving in the piedmont and compared to streamflow, groundwater acquires a higher total mineralization and exhibits two secondary facies, Ca-Mg-Cl and Na-Cl.

The general higher ions content of the groundwater in the piedmont compared to the recharging streamflow could be explained by evaporation effect as the climate is (semi)arid or by longer residence time in the alluvial aquifer favoring the water-rock interactions. Evaporation is considered the most important process of salinization in the areas where water table is shallow (<5 m) (Deverel and Gallanthine, 1989) and the potential evapotranspiration is high (Yechieli and Wood, 2002). In the study area, even though the potential evapotranspiration is high up to 5 mm/day in average (Elfarkh et al, 2020), evaporation effects in piedmont groundwater were not detected using stable isotopes (Bouimouass et al., 2020). This could be explained by a rapid infiltration of irrigation water, by a renewal of groundwater related to seasonal recharge by fresh mountain streamflow, and by a deep unsaturated zone as the

groundwater depths are higher during the summer months (Bouimouass et al., 2020). Concerning the groundwater residence time in the piedmont, while the mountain water was always found undersaturated of carbonates, an oversaturation of carbonates in piedmont groundwater was found during the dry season, possibility resulting from longer residence time.

The secondary Na-Cl facies in piedmont groundwater was observed in the right side of the wadi; it is due to halite dissolution from Triassic deposits. The Ca-Mg-Cl facies was observed near the wadi, along with the Na^+ depletion; this was explained by cation exchange inducing Na^+ adsorption and, Ca^{2+} and Mg^{2+} release in groundwater.

Beneath the irrigated area, reverse ion exchange was related to Na^+ enrichment; it seems that the irrigation return recharge brings Ca^{2+} and Mg^{2+} that are adsorbed by clay minerals while Na+ is released in groundwater. The occurrence of this process might be explained by the dynamic of the seasonal recharge by diverted streamflow from the Ourika wadi. Traditional irrigation by flooding relatively large lands with streamflow, induces more interaction between surface water and sediment matrix during infiltration.

IV.2. Impact of the traditional irrigation on the groundwater quality

Piedmont groundwater is generally considered highly vulnerable to anthropogenic pollution due to shallow water table depths, dense populations and agriculture activities. Indeed, when agricultural activities and urban areas are present in the piedmont, anthropogenic processes such as leaching of chemical fertilizers and wastewater infiltration significantly affect the quality of groundwater (Li et al., 2016). In in semi-arid climates, irrigation piedmont groundwater is also threatened by salinization from evaporation or from recycling of irrigation water that dissolves more saline matter from the soils (Nativ and Smith, 1987; Chourasia and Tellem, 1992; Elango and Ramachandran, 1991; Hamilton and Helsel, 1995; Fisher and Mulican, 1997; Tweed et al., 2011, Sun et al., 2016; Mirzavand et al., 2020),

In our piedmont, the agriculture still relies mainly on the use of organic fertilizers (e.g. animal residues) rather than chemical fertilizers. In addition, the irrigation area has the prime location of being at the foot of a major mountain range that is lowly populated and cultivated, and where streamflow is supplied by rainfall and snowmelt generally from winter to early summer. The diverted streamflow by a network of irrigation channels managed by community-driven systems is of low mineralization and of excellent chemical quality (EC = 273 µS/cm, and NO_3 = 3.2 mg/L), and such features constitute favorable factors of groundwater quality since the streamflow is the main groundwater recharge source. The piedmont groundwater

beneath the irrigated area is characterized by low mineralization, and excellent to good chemical quality regarding both drinking and irrigation uses. The substantial induced recharge from irrigation return flow leads to seasonal groundwater renewal, and counterbalances effects of salinization mechanisms that often characterize irrigated arid zones. From the dry to the wet season, the piedmont groundwater salinity beneath the irrigated area deceases in average from 588 mg/l to 480 mg/l, attesting of a dilution due to new recharge. Almost all the ions showed a dilution from the dry to the wet season. The effects of recharge on groundwater quality were highlighted in other works. Rotiroti et al. (2019) studied the effect of traditional irrigation by surface water from the Oglio river in the Po plain, Italy. They stated that irrigation could be very beneficial to the groundwater quality as it has a tampon effect on pollutants. Fernald et al. (2015) highlighted that groundwater water quality enhancement is one of the benefits of recharge from traditionally diverted surface water by irrigation channels (Acequias) in the semiarid southern USA.

However, in our study the nitrates showed a slight increase from the dry to the wet season, from an average of 8.4 mg/l to 12 mg/l. This increase is explained by the leaching of nitrates by the irrigation returns. The process of nitrates leaching from soils is well known and constitutes the main process of nitrates pollution (Green et al., 2018).

IV.3. Piedmont traditional irrigation and sustainability

Mountains are water towers for the adjacent lowland basins because they receive more precipitation due to the orographic effect, and the accumulation of snow and ice contribute to runoff during hot and dry seasons (Immerzeel et al., 2020). Mountain streamflow sustains the downstream areas (Viviroli et al., 2007; Immerzeel et al., 2010) and a recent study (Viviroli et al., 2020) showed that almost 1.5 billion people will depend on water contributions from mountain areas by the mid-twenty-first century. However, mountains are highly sensitive to climate and anthropogenic changes (Viviroli et al., 2011, Hock et al., 2019; Immerzeel et al., 2020). With the worldwide snow decrease observed in the last decades (Berghuijs et al., 2014; Malek et al., 2020; Immerzeel et al., 2020) and forecasted under climate change (Marchane et al., 2015; Baba et al., 2018; Hajhouji et al., 2020; Immerzeel et al., 2020; Viviroli et al., 2020), lower amounts of streamflow would reach piedmont systems. Therefore, surface water irrigation and induced groundwater recharge in piedmonts would be reduced and the related groundwater renewal processes affected. In addition, due to the growing anthropogenic activities piedmont groundwater is threatened by pollution.

The results in this study highlight a system where the irrigation practices have not, to date, adversely impacted groundwater resource quality. The irrigation practices have not significantly adversely altered processes controlling the major ion composition, nor significant transfers of nitrogen-based fertilizers to the shallow groundwater. Thus, the traditional irrigation practices in this mountain piedmont, which have been in place for hundreds of years, are considered a low impact practice in terms of groundwater resource quality and even an enhancing factor of quality.

However, the presence of nitrates currently at low levels is an indicator of anthropogenic pollution threats to the groundwater resources. The pollution threats are linked to the increase of population producing more waste water, and to the development of intensive agriculture using high amount of water and mineral fertilizers as it is currently the case in the neighboring anthropized plain. Within the plain, the intensive modern agriculture has severe impacts on groundwater quantity decreasing by 1 to 3 m/year (Fakir et al., 2015; Le Page et al., 2021), the groundwater nitrates that are increasing (Boukhari et al., 2015), and the soils salinity as well (Sefiani et al., 2019).

Traditional irrigation piedmonts irrigated by high mountains clean freshwater are one of the rare long lasting human exploited systems that are likely to remain clean or lowly polluted. Such systems represent a strong connection between water and users to ensure sustainability and drought survival, and constitute a main driver of socio-economic activities for centuries. A key success of survival of such ancestral system is the sense of mutualism between the users. This mutualism defined by Gunda et al. (2018) as the feeling of collective well-being including social identity, pride of place, and maintenance of historical traditions. For those piedmonts, the current traditional agricultural practices should be maintained and enhanced in order to preserve their groundwater resources sustainability and the one of the adjacent downstream plains, since piedmonts are generally favorable recharge zones in (semi)arid basins (Wilson and Guan, 2004; Liu and Yamanaka, 2012). The traditional agriculture could be improved by introducing organic agriculture (FAO, 2013) that could increase the financial incomes of farmers, better optimize irrigation water and increase its value.

V. Conclusion

In piedmonts where traditional irrigation and groundwater recharge are supplied by clean and snow mountains streamflow, the hydrochemistry of groundwater could be controlled on the one hand by the chemical characteristics of the streamflow acquired in the mountains, and on

the other hand by local hydrochemical processes that occur specifically during infiltration and recharge. Over the mountains where crystalline rocks largely outcrop, silicates weathering is the principal source of water mineralization. In the piedmont, the local hydrochemical processes consist mainly of carbonates dissolution, cation exchange and reverse ion exchange favored by a large flooding of irrigation water. The piedmont groundwater quality benefits from substantial seasonal recharge. The groundwater recharge counterbalances the potential effects of salinization mechanisms common in irrigated areas of (semi)arid zones, such as evaporation and leaching of saline soils.

Since hundreds of years of exploitation, the hydrological processes, the irrigation practices and the use by local farmers of organic fertilization have preserved the traditional hydro-agro-systems that still closer to sustainable agricultural systems. However, they are threated in last decades by population growth, climate change effects, and by the invasion of intensive modern agricultural practices overexploiting the water resources and using more mineral fertilizers. Protection measures should be taken in the framework of adaptive strategies to sustainable management and to water heritage.

Chapter 5: Seasonality in intermittent streamflow losses beneath a semiarid wadi

Paper submitted to *Water Resources Research* (in revision)

Preprint available at ESSOAR : https://doi.org/10.1002/essoar.10503827.1

I. Introduction

Recharge from streamflow infiltration is the seepage of water through the stream channel, banks and flood plain. Infiltrated streamflow water is a potential recharge of groundwater; but it may not reach the aquifer and return to the atmosphere by evapotranspiration (Healy, 2010). The infiltration rates depend on the type of channel material and its associated hydraulic properties, channel geometry, wetted area, and depth of groundwater. The magnitude and direction of flux depends on the following physical factors (Besbes et al., 1978; Shanafield and Cook, 2014):

- Streambed permeability and thickness;
- Permeability of aquifer;
- Geometry of the aquifer;
- Geometry of the streambed;
- Distribution of difference between stream and groundwater heads;

There is a number of studies that have concentrated on infiltration processes and water resources management issues related to focused groundwater recharge (Flint et al., 2000; Kulongoski and Izbicki, 2008; McCord et al., 1997, Schwartz, 2016). In a disconnected system, water table can be relatively deep, most of the infiltrated water can be lost in the unsaturated zone on its way to the aquifer system (Shanafield and Cook, 2014). However, the water table can be relatively shallow near the mountain front (Bouimouass et al., 2020), which can make recharge from streamflow and flood events important in this area.

For ephemeral streams, streamflow losses have been documented to represent a major component of alluvial aquifer recharge (Niswonger et al., 2008); however, for intermittent streams their spatial and temporal dynamics are inadequately documented (Cuthbert et al., 2016) and broad assessment continues to be challenging from both a logistical and analytical perspectives. Ephemeral streams water losses have been largely studied using temperature measurements and related analytical and numerical modeling methods (Constantz and Thomas, 1997; Ronan et al., 1998; Stonestrom and Constantz, 2003; Goodrich et al., 2004, Hoffmann et al., 2007; Kulongoski and Izbicki, 2008; Rau et al., 2017). Much lesser studies have used water content as a tracer of ephemeral stream losses (Dahan et al., 2007; Dahan et al., 2008; Schwartz, 2016). When analyzing their context, several other reasons might have contributed to the proliferation of research works on ephemeral streams. First, being normally dry for most of the year and flow as floods only during and shortly after precipitation events, ephemeral stream

channels are less challenging for deployment of equipment within the streambed before the arrival of a flood; flood events are unpredictable, create scour and damage to equipment. Second, in dry and desert area since floods are rare and have little seasonality, short monitoring and few measurements are generally sufficient to characterize the water losses and the recharge that is subsequently scarce and episodic. Third, since the ephemeral stream losses often occur in dry sediment under unsaturated conditions, their variation is not much influenced by pre-conditions of the sediment moisture; consequently, the infiltration and recharge behavior might present low seasonality. Finally, the early advances in flow modeling under variably saturated flow opened large perspectives of numerically quantifying ephemeral stream losses.

The difficulties in quantifying streamflow loss are greater with intermittent flow compared with spatially continuous ephemeral flows. Intermittent streams are generally more common in semi-arid regions bounded by mountains, where the climate is dry in summer and autumn, and wet in winter and spring. During dry seasons, intermittent streams are generally dry or flow after episodic storms; consequently, their recharge pattern might be similar to ephemeral streams, occurring in dry and unsaturated sediment (Reid and Dreiss, 1990). In wet seasons, intermittent streams are fed by rainfall or snowmelt, and may flow continuously or intermittently, thus, their stream losses and recharge pattern might be expected to range between the spatial pattern of perennial stream and ephemeral in addition to intermittent flow patterns. Furthermore, intermittent stream flow during longer periods than ephemeral streams, potentially creating greater streambed infiltration, streambed saturation and groundwater recharge.

For the present research, continuous streambed water content and streambed temperature were jointly monitored beneath a single intermittent stream channel, a wadi, in a semi-arid Mediterranean climate. The goal was to continuously monitor streambed parameter designed investigate infiltrations processes and estimate the stream losses for an intermittent reach over an entire water year as related to groundwater recharge beneath intermittent streams. A pair of primary streambed measurement tools were deployed: continuous vertical streambed sediment temperature profiling and continuous vertical sediment water content profiling. Using heat as a tracer via temperature profiling has been shown to estimate streambed fluxes, while vertical streambed water-content profiling provides crucial information on variations of hydraulic connection between the stream and the groundwater, with clear documentation of streamflow losses converted to groundwater recharge. Water content also allows to easily measure the velocity of the wetting front and infer infiltration fluxes; however, the method can only be used

when the streambed is initially unsaturated (Hoffmann et al., 2007; Dahan et al., 2008); once the sediment is fully saturated, it is no longer possible to calculate infiltration fluxes. Using temperature as a tracer of stream losses is more useful in estimating water fluxes in various moisture regimes. Indeed, heat continues to be widely used thanks to technological developments that made temperature acquisition devices rigid, easy to install and inexpensive (Anderson, 2005; Kalbus et al., 2006; Constantz, 2008; Shanafield and Cook, 2014), and to the development of various methods and models that use temperature data series (Anderson, 2005; Blasch et al., 2007; Kurylyk et al., 2019).

Discussed in detail in other sections below, after identifying the hydrological events (streamflow occurrence) at the experimental site based on the near surface sediment temperature and flow gauge data, analyzing the stream losses beneath the streambed were determined at a single vertical streambed profile to a depth of 5.5 m continuously over an entire 1-year period. The resulting records were used in a 1-dimensionl heat transport model to calculate the potential recharge rates. The specific goals of this study were: 1) describe the seasonal change in the sediment moisture and temperature according to the streamflow losses, 2) analyze the effect of the sediment moisture on the infiltration processes, 3) determine the seasonal variation of the subsequent potential groundwater recharge and 4) possibly investigate any impact of lateral mountain-front recharge on hydraulic connection beneath the channel. All four were able to be addressed to varying degrees during hydrologic events over one year for this single wadi.

II. Material and methods

II.1. Experimental site

The experimental site is located in the middle of the active channel of the Wadi Rheraya stream. The alluvial aquifer in the area is formed by alluvial fans and fluviatile deposits of Neogene and Quaternary age. It is recharged mainly by high-elevation meteoric water (Boukhari et al., 2015). Within Rheraya streambed (Figure 5-1), at the surface the alluvium is formed of rollers, sandy gravel, and boulders with different sizes. Clay layers are usually deposited by floods. At the onset of the experiment, the water table was at 5.5 m depth in the experimental site.

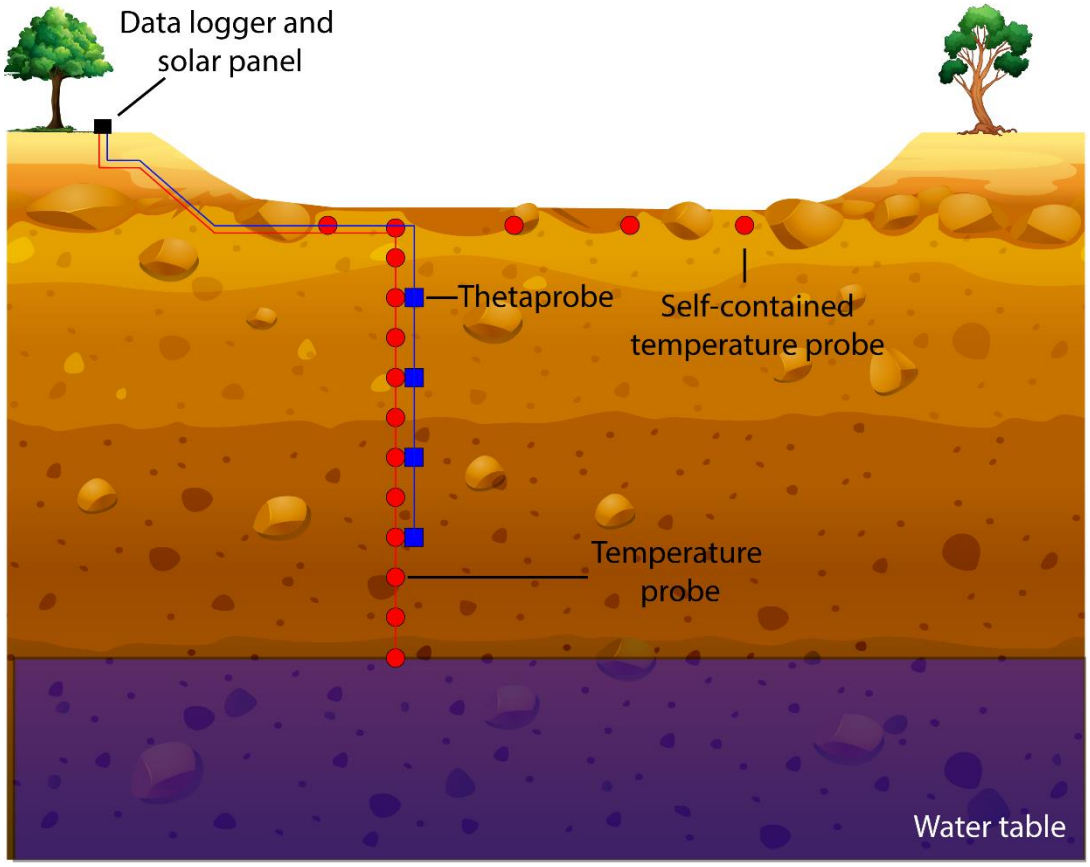

Figure 5-1: On left, photograph showing the Wadi Rheraya streambed, with in the background the foothills of the High-Atlas Mountains. On right, schematic cross-section of the instrumentation with the temperature probes (4 self-contained temperature probes at the top surface and 12 across.

II.2. Streamflow detection

Stream gauges are the standard method to monitor streamflow; however, gauging stations are expensive to install and maintain along streams, and these expensive are considerably high for ephemeral stream, with shifting gravel streambed that shift the streamflow rating curve and flashy flows that often damage gauges (Constantz and Thomas, 1997). The installation of a series of temperature probes at the near surface of streams was successfully used in different studies to detect the presence, extent and duration of streamflow (Blasch et al., 2000; Constantz et al., 2001; Blasch et al., 2004; Mendez, 2005; Moore, 2007; Stewart-Deaker et al., 2007; Stonestrom et al., 2007). As there is only For our Wadi Rheraya, a single gauging station located 8 km upstream of the experimental site, which is characterized by streamflow during the wet season and a dry channel during most of the dry season; thus, we used a temperature-based method to detect the presence of streamflow and its duration at the site. Four self-contained temperature sensors (Lascar Electronics) were installed at the surface of the sediment (at 0.20 cm depth) across the streambed (Figure 5-1). Each sensor recorded temperature every 30

minutes from 11/04/2013 to 11/21/2014. We used the moving standard deviation (MSD) method proposed by Blasch et al. (2004) to detect streamflow presence and duration. The advantage of the MSD over direct visual inspection of the temperature data is that the daily fluctuations in temperature data are minimized and the perturbations caused by streamflow are magnified and easier to discern. The method is based on calculating the moving standard deviation (MSD) of temperature in a specified time interval. A filter of 05 parameters is applied to the MSD in order to distinguish the events from atmospheric perturbations such as cold fronts. The parameters are the length of the MSD window, the reference time within the window, the threshold parameter, the minimum duration of a flow event and the minimum duration between two flow events. The effectiveness of this method was tested by Partington et al. (2020) and was found to be useful in identifying flow events.

II.3. Measurements of changes in temperature and sediment water content

Using heat as a tracer of streamflow infiltration continues to be widely used thanks to technological developments that made temperature acquisition devices rigid, easy to install and inexpensive (Anderson, 2005; Kalbus et al., 2006; Constantz 2008, Shanafield and Cook, 2014), and to the development of various methods and models that use temperature data series (Anderson, 2005; Blasch et al., 2007; Kurylyk et al., 2019). Water content allows to easily measure the velocity of the wetting front and infer infiltration fluxes (Dahan et al., 2008). Moreover, vertical streambed water-content profiling provides crucial information on variations of hydraulic connection between the stream and the groundwater.

Our experiment was designed to vertically monitor the downward movement of intermittent streamflow beneath the semi-arid Wadi Rheraya (Figure 5-1). The experiment profile was installed in the middle of the active channel that drains water even during periods of low flow. At the start of the experimentation, the water table was located at 5.5 m below the surface of the Wadi Rheraya streambed. Hence, to monitor the volumetric water content of the sediment, four Thetaprobes (Delta-T Devices) were installed at 1, 2, 3 and 4 m. To measure temperature, 12 temperature probes (Cambell Scientific) were placed every 0.5 m from the surface down to 5.5 m deep to record the sediment temperature. The probes were connected to a data logger (Cambell Scientific) placed on the right stream bank and powered by a solar panel. Data were recorded every 30 minutes. The measurement period was from November 04, 2013 to November 21, 2014. At the end of this period, a strong flood (60 m^3/s) caused serious damages to the set up.

II.4. Calculating vertical infiltration fluxes with 1-Dimensional model of heat transfer

Temperature data were used together with the physical, hydraulic, and thermal properties of the alluvium, to construct a 1-D model to simulate heat transfer beneath the Wadi Rheraya streambed. The computer program VS2DH (Healy and Ronan, 1996), pre- and post-processed by 1DTemPro (Koch et al., 2016), a finite difference-based model designed to solve heat transport problems in variably saturated media, was used to infer vertical water fluxes. A form of the advection-dispersion equation is used within VS2DH to describe heat and groundwater transport (Healy and Ronan, 1996):

$$[\theta C_w + (1-\emptyset)C_s]\frac{\partial T}{\partial t} = \nabla.\mathrm{K_T}(\theta)\nabla\mathrm{T} + \nabla.\theta\mathrm{C_w}\mathrm{D_h}\nabla\mathrm{T} - \nabla.\theta\mathrm{C_w}\mathrm{qT} + \mathrm{QC_w}\mathrm{T}' \quad (1)$$

The temporal change in sediment temperature at a given depth	Heat conduction (Fourier's law)	Heat dispersion	Heat advection (Darcy's law)	Heat source /sink

where t is time in s; Θ is the volumetric moisture content (dimensionless); ϕ is the sediment porosity (dimensionless); Cw is the volumetric heat capacity (density*specific heat) of water (J m^{-3} $°C^{-1}$); Cs is the volumetric heat capacity of bulk sediment (J m^{-3} $°C^{-1}$); T is temperature (°C); K_T is bulk thermal conductivity (W m^{-3} $°C^{-1}$); D_h is the thermomechanical dispersion tensor (m^2 s^{-1}); q is water velocity (m s^{-1}); Q is rate of water added per volume of porous medium from an external or internal source (s^{-1}); T' is temperature of fluid source (°C).

The main physical parameters were assessed at the site. Across the unsaturated zone of the experiment site, four sediment samples, of about 5 kg each, were taken at every m depth to characterize the sediment texture and infer the hydraulic conductivity. Particle-size distribution parameters were determined by sieve analysis (Landon et al., 2001). The hydraulic conductivity was estimated from the formula of Alyamani and Sen (1993) which is based on the slope and intercept of the grain-size distribution curve. This formula (equation 2) was tested by Landon et al. (2001) against other techniques and showed a good agreement.

$$K = 1300\,[I_0 + 0.025\,(d_{50} - d_{10})]^2 \quad (2)$$

The effective porosity of the sediments was estimated based on the water content measured by the probes installed at various depths, and is defined here as the difference between the quasi-saturated water content and the field capacity (Heppner et al., 2007), where quasi-saturation is nearly saturated with a small amount of air trapped in the pore space.

The thermal properties (sediment heat capacity, thermal conductivity, and dispersivity) of streambed sediments are almost independent of texture and vary only little between different

streambeds (Constantz and Stonestrom, 2003). These parameters generally vary from 1.1 10^6 to 2.9 10^6 J m^{-3} $°C^{-1}$ for sediment heat capacity, and from 0.2 to 2.2 W m^{-1} $°C^{-1}$ for thermal conductivity and 0.01 to 1 for dispersivity (Pahud, 2002; Niswonger and Prudic, 2003; Kulongoski and Izbicki, 2008).

The model domain is a column that extends vertically from the streambed surface to a depth of 5.5 m. The model domain was divided in five layers of specific thickness and physical characteristics. Twelve (12) observation points of temperature were centered horizontally in the vertical column. The domain was divided in 100 active cells spanning the distance between the uppermost and the deepest thermistor. The measured temperatures were used to initialize the model but afterwards the temperature of the uppermost thermistor was used as the boundary condition at the top of the domain, and temperature of the deepest thermistor as the boundary condition at the bottom of the domain. The active cells are surrounded by no-flow boundaries from the sides. The simulation period was 12 months and each time step was 30 minutes.

The model was calibrated based on a manual-trial and error method, which is considered appropriate for 1-Dimentional modelling (Niswonger and Prudic, 2003; Moore, 2007; Kulongoski and Izbicki, 2008). Model calibration in the context of using heat as a tracer usually requires the adjustment of hydraulic conductivity (K) or head difference (H) until the simulated temperature match the measured one. In our case study, we used the estimated K from grain-size distribution curve and adjusted H taking into account the maximum stream stage values of floods reported from the experiment site. Best fit of simulated temperature-depth profiles to observed ones was determined by minimizing the RMSE (Root Mean Square Error).

III. Results

III.1. Sediments characteristics

The grain size analysis of the sediment samples from various depths shows (Table 5-1) that the sediments are mostly composed of gravel (2000> μm) and coarse sand (250-2000 μm). Among the fine materials, clay (<2 μm) constitutes a relatively important fraction. Sediments from the first and the fifth meters have more coarse material while the second and the third meters have finer material. The estimated hydraulic conductivity values from grain size analysis vary from 6 10^{-5} to 4 10^{-4} m/s (Table -1). They are relatively low but are in good agreement with other reported for the area (Sinan and Razack, 2006). On the streambed surface floods generally deposit clay sediments that forms a thin layer with a thickness ranging from millimeters to several centimeters. This clogging layer is expected to reduce the hydraulic

conductivity of the very shallow sediments. In addition, the presence of boulders could further reduce the permeability of the sediment, by reducing the cross-sectional area of permeable streambed material.

Table 5-1. The results of grain size analysis of four samples taken from various depths in the experiment site and estimated hydraulic conductivity.

Depth (m)	Gravel (>2000 µm)	Coarse sand (250-2000 µm)	Fine sand (50-250 µm)	Silt (2-50 µm)	Clay (<2 µm)	Hydraulic conductivity (m/s)
1	58.3	27.4	5.1	0.5	8.7	$4\ 10^{-5}$
2	41.9	34.9	9.4	0.7	13.1	$6\ 10^{-5}$
3	32.7	41.1	11	1.1	13.3	$1\ 10^{-4}$
5	47.2	30.2	9.5	0.8	12.2	$4\ 10^{-4}$

The effective porosity of the sediment was deduced from the measured water content data. The results (Table 5-2) show that the effective porosity at 2 m and 3 m (0.18 % – 0.20 %) depth is lower than this at 1 m and 4 m (0.27 % – 0.30%).

Table 5-2: Calculation of the Effective Porosity in the Study Site Using Water Content.

Tethaprobe number	Depth (m)	Part of sediment represented (m)	Min of water content (%)	Max of water content (%)	Estimated effective porosity (%)
H1	1	0 - 1.5	0.13	0.43	0.30
H2	2	1.5 - 2.5	0.27	0.44	0.18
H3	3	2.5 - 3.5	0.26	0.46	0.20
H4	4	3.5 - 6.5	0.22	0.49	0.27

III.2. Detection of streamflow events

Wadis in general have unconsolidated gravel streambed surfaces with periodic flashing streamflows, resulting in challenging sites to maintain both streamflow rating curves and as well as stream gauges themselves; although streamflows are logged elsewhere, streamflow was

not directly monitored at the experimental site. Alternatively, the surface-streambed temperature is used to determine the effective occurrence of streamflow and flood events (Constantz et al., 2001; Blasch et al., 2004; Partington et al., 2020). Streambed temperature is normally influenced by seasonal and diurnal air temperature; for this study, minimum recorded temperature was 8.8 °C in January 2014 and the maximum was 34 °C in August 2014. Abrupt changes in streambed temperature are due to streamflow events or a change in atmospheric conditions (Constantz et al., 2001). Figure 5-2 presents a detailed inspection of a perturbation; after a decrease in the daily streambed-temperature fluctuation by 5 °C (Figure 5-2a) due to the decrease in air temperature by 8 °C (Figure 5-2b), the effect of the streamflow event of September 21st, 2014 is reflected by a perturbation (temperature drop) of sinusoidal shape of the daily streambed-temperature thermographs. The described perturbation is related to a rainfall event and to a flood recorded at the Tahanaout gauging station (Figure 5-2c). For this analysis, the start of the thermal anomaly is deemed the initiation of the event and the increase of diurnal variation of temperature is considered as the recession of the event (Constantz et al., 2001).

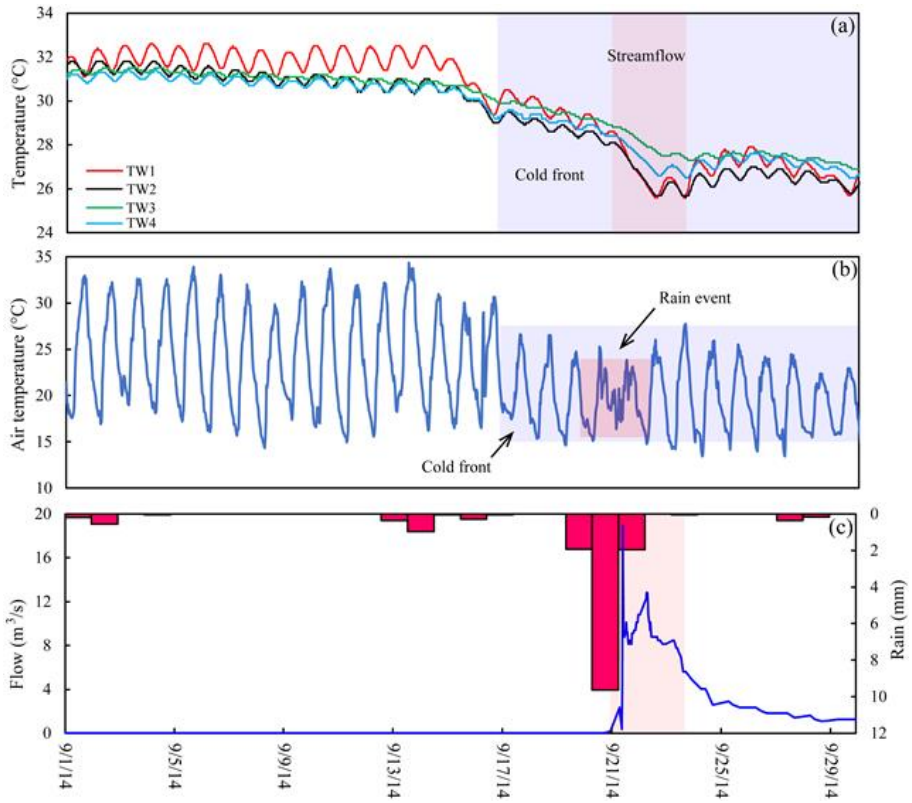

Figure 5-2: Procedure of detecting thermal anomalies based on near-surface temperature (a) and air temperature records (b). Their superposition to measured data of runoff or precipitation (c) allowed determining the type of the hydrological events that generated the perturbations.

Because of the uncertainty that can result from the direct inspection of the thermographs, we applied the MSD technique (Blasch et al., 2004) to further improve the identification of flow events. Figure 5-3 shows the MSD of the four temperature probes installed at 20 cm below the surface across the wadi during the period between 26/03/2014 and 06/04/2014. A window length of 6 hours with the time reference at the end of the window was used. The minimum time of the event was chosen to be 5.5 hours corresponding to the shortest flood detected in Tahanaout gage station (flood of 27/08/2014). Two flow events occurred in this period in 28/03/2014 and 02/04/2014 with peak flows of 8.1 m^3/s and 7.8 m^3/s, respectively, according to streamflow data recorded in Tahanaout gage station. In response to these events, a damp in MSD daily fluctuations is observed in all the probes but more obvious in TO1 located in the main active channel. The MSD was maintained above a value of 0.1 °C during the entire period of the event. Using temperature data at 20 cm, it was possible to detect high-flow events because standard deviation values during those events are often maintained above or around 0.1 °C which can also help estimate the duration of the event. However, even though the high-flow events are obvious and above 0.1 °C, standard deviation values varied a lot which make determining the threshold parameter difficult. This can be due to the depth of probes being too sensitives to the smallest atmospheric changes. To test this, we will use the MSD technique on the temperature data recorded by the probe installed at 0.5 m in the temperature profile. Figure 5-4 present the standard deviation results from January to May 2014. The filter of events detection was designed as follows:

- A window length of 06 hours was chosen with referenced time at the end of this window.
- Following Blasch et al. (2004), we used the maximum standard deviation value during the longest no flow period in the study period as the threshold parameter (0.04 °C).
- The minimum flow event duration was determined as 5.5 hours.
- The minimum duration between two flow events was determined as 20 hours.

Standard deviation fluctuations during the high-flow events were damped and remained often above the threshold parameter, however, some perturbations remained below this value. Overall, 22 perturbations were chosen to be potential flow events. These perturbations were compared to flow in the Tahanaout gage station and rain in the Rheraya catchment (Table 5-3). All the high-flow events (n=10) were successfully determined by the MSD technique and the used filter. 03 low-flow events were also determined but their standard deviations values were below the threshold parameter unlike the high-flow events. The other perturbations which not correspond to any flow events in the Rheraya catchment (n=7) corresponded well with rainfall

events. Consequently, temperature at 0.5m below the surface can successfully identify the presence of streamflow events but still can lead to misleading between perturbations due to low flow events and those due to local rainfall infiltration.

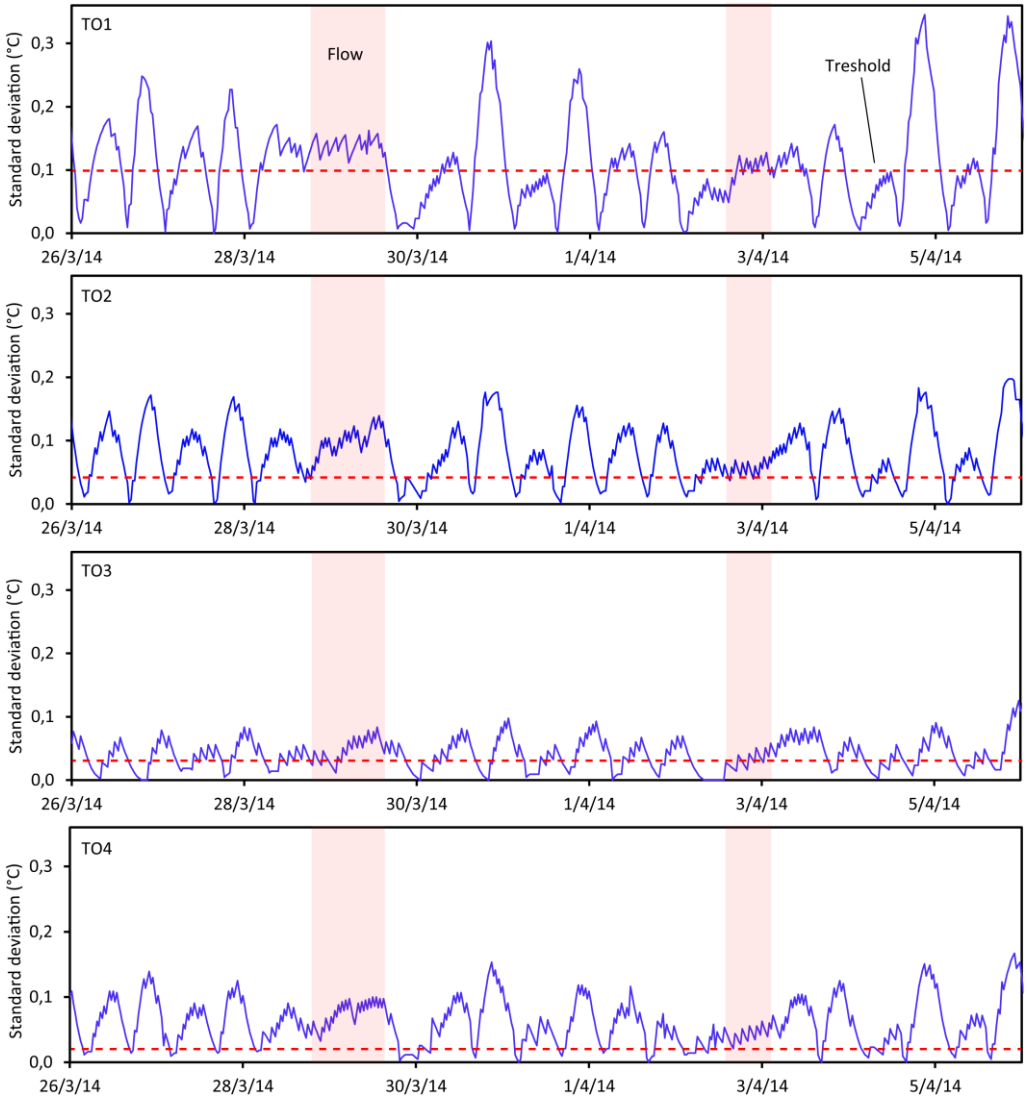

Figure 5- 3: MSD of temperature measured at the four probes installed across the wadi during the period between 26/03/2014 and 06/04/2014.

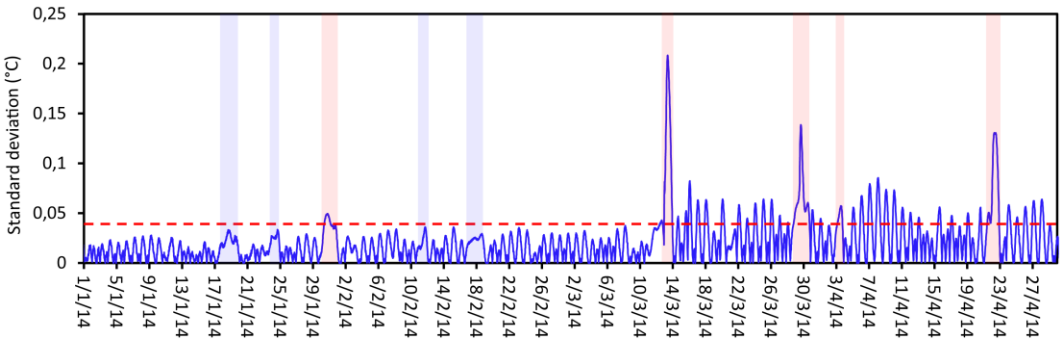

Figure 5- 4: Standard deviation of temperature at 0.5 meter, the dashed red line represents the threshold parameter.

Table 3-5: Type of the Detected Streamflow Losses Events and their Depth. The Rows in Bold Correspond to the Potential Recharge Events

Number	Date	Rain (mm)	Measured streamflow m^3/s	Type	Recorded depth of perturbation (m)
1	1/17/2014	10.8		Ungauged	0.5
2	1/22/2014	19.6	0.48	Normal flow	2
3	**1/29/2014**	**34.8**	**9.40**	**Flood**	**5.5**
4	**2/10/2014**	**14.5**	**0.24**	**Normal flow**	**3.5**
5	**2/16/2014**	**8.6**		**Ungauged**	**3.5**
6	**3/12/2014**	**45.0**	**44.80**	**Flood**	**5.5**
7	**3/28/2014**	**20.0**	**8.10**	**Flood**	**5.5**
8	**4/2/2014**	**17.6**	**7.76**	**Flood**	**2.5**
9	**4/21/2014**	**31.0**	**34.80**	**Flood**	**5.5**
10	5/2/2014	8.1	0.15	Normal flow	2
11	5/6/2014	1.2		Ungauged	2
12	**5/8/2014**	**15.0**	**0.15**	**Normal flow**	**2.5**
13	5/16/2014	0.8		Ungauged	2
14	6/6/2014	0.6		Ungauged	0.5
15	**8/27/2014**	**17.2**	**27.50**	**Flood**	**1.0**
16	8/30/2014	20.0	42.70	Flood	1.0
17	9/15/2014	0.4		Ungauged	1
18	**9/21/2014**	**25.0**	**19.00**	**Flood**	**4**
19	10/12/2014	0.2		Ungauged	0.5
20	**11/4/2014**	**28.6**	**24.00**	**Flood**	**5.5**
21	**11/9/2014**	**23.0**	**36.00**	**Flood**	**5.5**
22	**11/21/2014**	**1.6**	**60.00**	**Flood**	**5.5**

Over the year, every measured flood at the gauging station was detected at the site, with most of these detected events occurring in the wet period. In late August, the two floods in response to summer storms are examples of flashfloods, lasting no more than 6.5 hours. The largest flood (60 m^3/s) in November 21, 2014 caused massive damage to our experiment, marking the end of data acquisition, a common data-clipping problem in arroyos of the Western Hemisphere and Australia (Shanafield and Cook, 2014) along wadis in the Middle East.

III.3. Water content changes

As described earlier, to complement thermal analysis, Water content (WC) changes were monitored over 1 years' time, every 30 minutes, every 1m depth interval, 4 m beneath the streambed surface. The general evolution of WC could be divided in 2 moisture states of the sediment (Figure 5-5): (i) wet sediment state during 5 months (February 2014 to June 2014), the WC values increase progressively from the surface to the bottom of the sediment, and (ii) dry sediment state during 3 months (from July to September 2014).

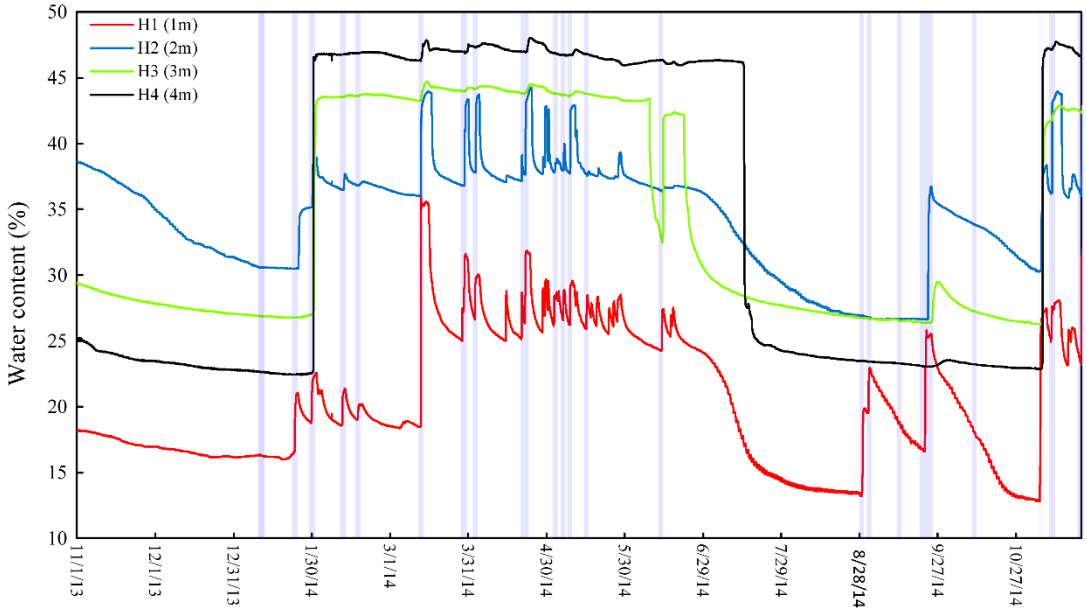

Figure 5- 5: Water content data measured at four depths (1 to 4 m), 1 m apart, beneath the Rheraya streambed. The bands represent the events that led to streamflow losses; the blue ones indicate potential recharge events.

During the wet season, the moisture state of the sediment appears to be caused by both streamflow losses and rising of capillary fringe above a rises water table, as described in detail as follows. Figure 5-6 presents the WC variation in the vadose zone before, during and after the first flood of January 29, 2014; however, WC probes show differing behaviors. WC at the probes 1 and 2 increased by the same magnitude (4%). At probe 3, first the WC increased to 36

% then after a short slowdown it increased to a maximum of 43.6%. Second, the highest rise in WC was observed at the probe 4 installed at 4 m depth, where WC increased to 46.5%. Notably the WC increased at 4 m (probe 4) before increasing at 3 m (probe 3), suggesting that the quasi-saturation at 4 m depth m was caused by the rise of the water table. The latter led to wetting conditions from the bottom that reached with a delay the probe 3 as well. In summary, the increase of WC at 1m and 2 m depth as well as the first increase at 3 m were due to streamflow losses, while the increase of WC at 4 m and the second increase at 3 m were due the rise of the water table.

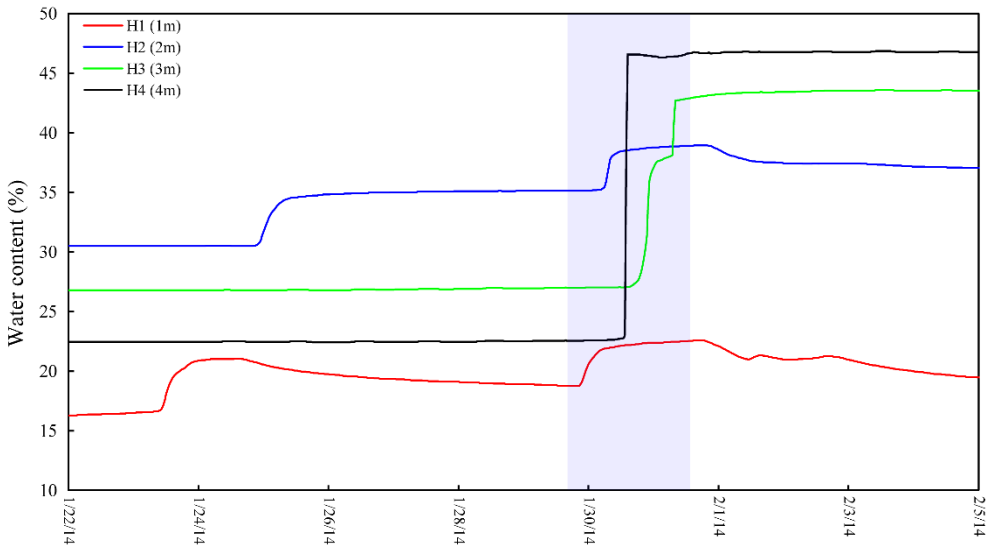

Figure 5- 6: Time series of the water content variation during the event of January 29, 2014. The water content at 4 m increased before the one at 3m, indicating the rise of the water table. At 3m, the first increase in WC could be due to water percolation from the surface and the second to the rise of the water table.

Furthermore, during the wet season the WC fluctuates significantly in the upper part of the sediment, while remaining stable at a quasi-saturation level at 3 m and 4 m depth. These characteristics indicate the temporally varying WC at the upper part of the sediment was induced by streamflow losses inducing sharp increases, while at depth higher WC values were maintained by the proximity to the groundwater. Alternatively, in early summer, a general decrease of water content in the sediment was observed (Figure 5-4). The decrease was abrupt at 3 m and 4 m depth marking the drop of the water table, while more progressive decreases at 1 m and 2 m depth indicates a normal drying of the sediment.

III.4. Streambed-sediments temperature changes

Typically, temperature at very shallow depths (0.25 m and 0.5 m) are influenced by both diurnal and seasonal variations, while the temperatures of the deepest probes show a dampened

seasonal variation (Figure 5-7). Overall, the general shape of the thermographs is sinusoidal with the lowest recorded temperatures in the winter and the highest temperatures in summer. From November 2013 to March 2014, temperature increases with depth. From April 2014, the temperature gradient shifted. Streamflow losses induced temperature declines more frequent during winter and spring than summer. The perturbations of temperature induced by the floods are more obvious. The magnitude of the temperature drop was up to 7 °C (floods of March 12, 2014 and November 4, 2014) at the upper temperature probes and up to 2 °C at the deeper probes (flood of November 4, 2014).

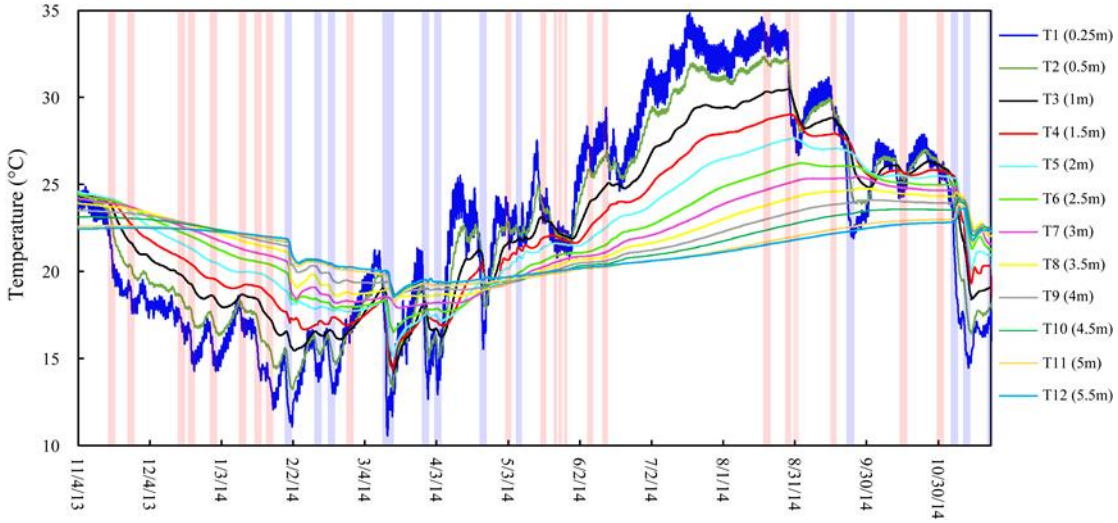

Figure 5- 7: Streambed temperature measured at 12 depths (up to 5.5 m), 0.5 m apart, beneath the Rheraya streambed. The bands represent the streamflow losses events; the blue ones indicate the potential recharge events.

During Summer (the dry period in July and August), the variation of temperature at the surface was important but rapidly damped with depth, resulting from insolation and absence of flow (Rau et al., 2017). The rare floods of late August induced a rapid change in the upper probes, though these rapid changes were not reflected in lower streambed sediments, indicating a lack of deeper percolation from these streamflow events.

The MSD technique was also applied to temperature from the sediment profile (Figure 5-8). The MSD will help track the evolvement of abrupt temperature changes due to flow events through the surface, thus, determine the depth in which water has reached. Figure 5-8 shows the MSD results for the probes installed at 0.5, 1, 3, 4 and 5 meters coupled with water content at 1, 2, 3 and 4 meters for the period between 01/01/2014 and 30/04/2014. In section 4.2, 9 temperature perturbations were detected in this period, 5 of them coincided with high-flow events, 02 with low-flow events and 02 were ungauged but coincided with rainfall in the study area. Only the high-flow events of 29/01/2014, 12/03/2014 and 28/03/2014 were detected at 05

meters. The two other high-flow events of April, 2014 were detected only at 0.5 and 1 meter even though they are flood events.

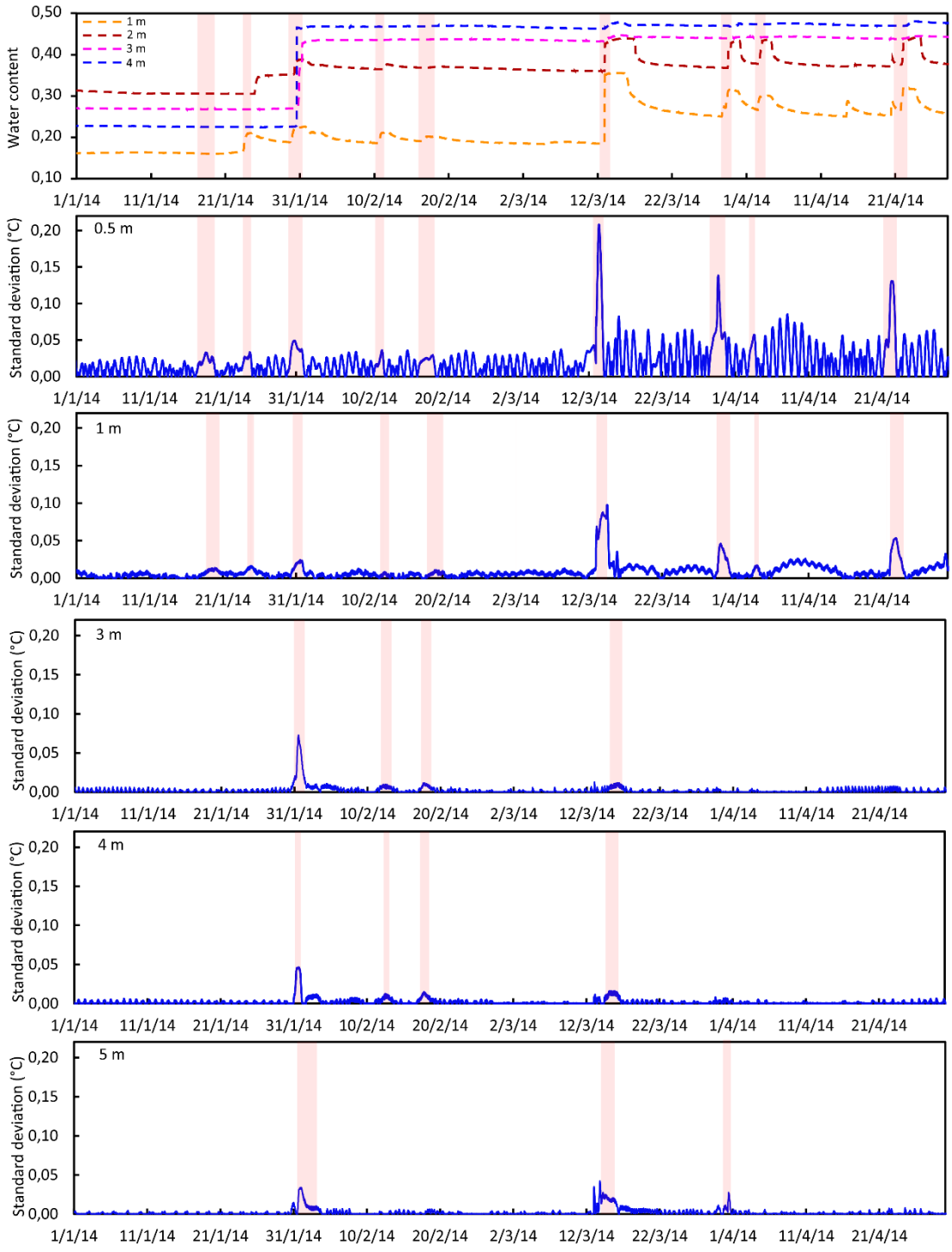

Figure 5- 8: Standard deviation of temperature data at multiple depths (0.5, 1, 3, 4 and 5 meters) coupled with water content data at multiple depths (1, 2, 3 and 4 meters).

The water content data shows that the event of 02/04/2014 induced an increase in water content at 1 and 2 meters and the event of 21/04/2014 induced an increase in water content at

1, 2, 3, 4 meters. This further confirm the advantage of coupling temperature and water content for identification of recharging events. The perturbations of 17/01/2014 (ungauged) and the low-flow event of 21/01/2014 were only detected at 0.5 and 1m. The perturbations of 10/02/2014 (low-flow event) and 16/02/2014 (ungauged) were detected at 0.5, 1, 3 and 4 meters. The two ungauged perturbations could be due to rain water infiltration, flow from a downstream effluent of Rheraya wadi or an irrigation dam release. The perturbations of February, 2014 persisted deeply compared to those of January, 2014 reached which were not detected at 3m, this can be due to the initial saturation sediment conditions before the events. Water content in early January, 2014 was at 0.16 at 1m, 0.31 at 2m and increased to 0.18 at 1m and 0.38 at 2m in early February, 2014. This is further confirmed by water content data showing that the ungauged perturbation of 17/01/2014 was not observed in water content at 1 meter and the low-flow event of 21/01/2014 was only observed in water content data at 1 and 2 meters.

III.5. Delineating potential recharging events

During the one year of monitoring of the sediment temperature and water content, 22 infiltration events were identified (Table 5-3). They correspond to 10 floods, 04 normal streamflow and 08 rainfall/ungauged reach flow. For 9 floods (out of 11), 2 normal streamflow and 1 ungauged event, almost all in the wet period, deep water percolation (beyond 2.5 m depth) was recorded (Table 3, Figure 5-4, Figure 5-6). Because the water table was maintained around 3 m depth during the wet period, these events are considered to have recharged the groundwater. The two flashfloods in the late August 2014 (N° 15, 16) despite their high flowrate only led to a temperature and moisture change at the surface while the water table fell to more than 4m, therefore they are not considered as generating deep percolation. As a conclusion, the potential recharge events are in general those floods that occurred in wet sediment conditions.

III.6. Numerical modeling of heat for recharging events

Using the elaborated VS2DH model, the recharge events were modeled by matching observed temperature to simulated one, until reaching the best fit between observed and simulated temperature (Figure 5-9). The RMSE for each event is listed in table 4. The RMSE values vary between 0.1 and 0.9 °C which seems very acceptable owing to various uncertainties related to this type of modeling. In our case, the main sources of uncertainty could be the scarce data on streamflow stage and by the assumptions related to the one-dimensional vertical model, which does not consider lateral flow derived from infiltration beyond the vertical model's domain (Rau et al, 2014).

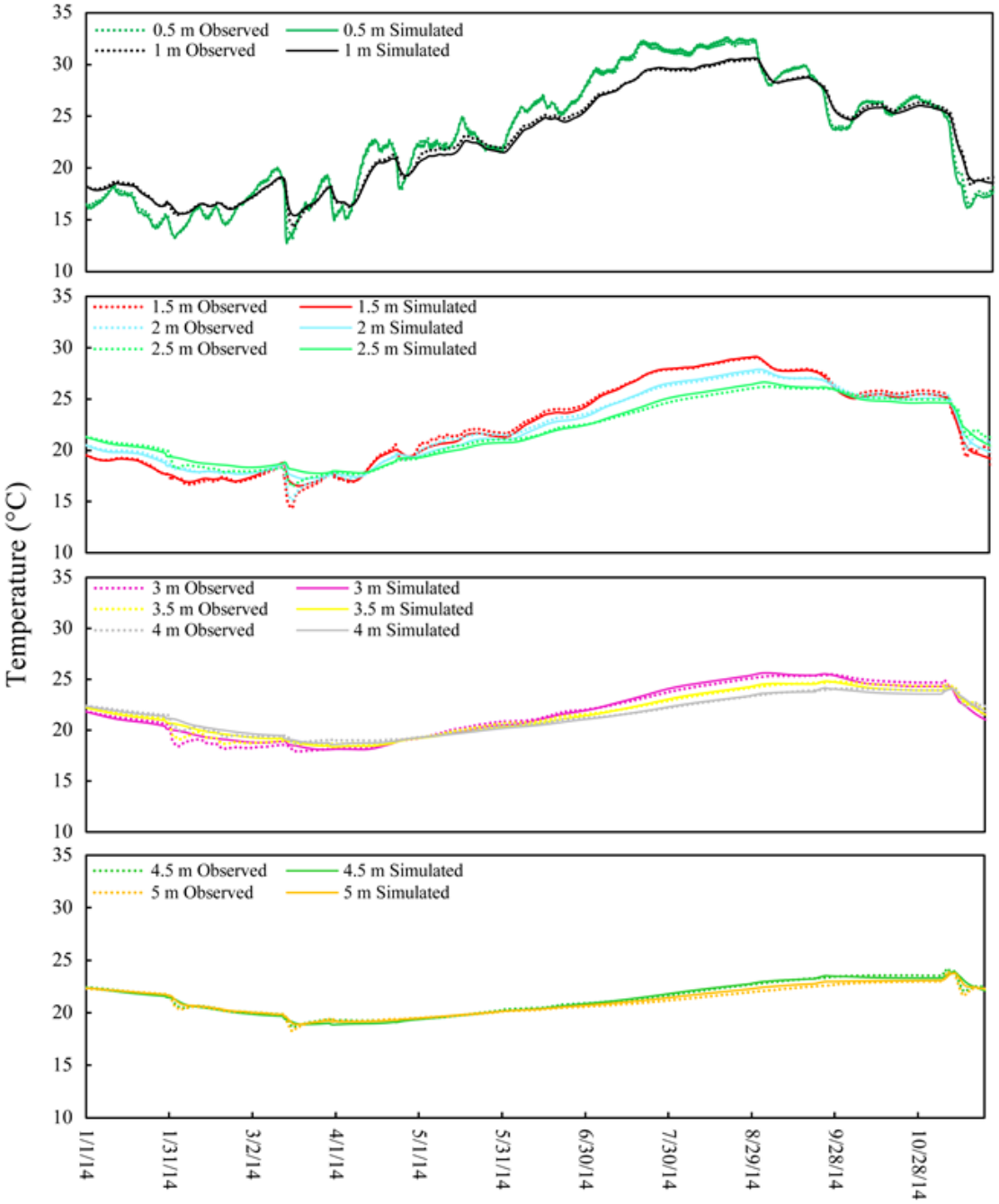

Figure 5- 9: Observed versus simulated temperature at different depths, for the whole study period.

The recharge fluxes that are calculated by VS2DH correspond to the vertical flowrate of water through the streambed per unit of streambed surface area ($m^3\ m^{-2}\ s^{-1}$). They vary between 0.03 and 4.65 mm/h with a mean of 1.7 mm/h. The highest flux of 4.7 mm/h corresponds to the large flood of November 21, 2014 while the lowest flux of 0.03 mm/h corresponds to the low streamflow event of February 16, 2014 (Table 5-4). The cumulative flux per event varied from 1 mm to 158 mm.

Table 5-4: Percolation fluxes calculated by VS2DH heat modeling.

Event number	Streamflow m3/s	Type	Start	End	Duration (h)	Fluxes (mm/h)			RMSE (°C)	Total flux (mm)
						Min	Max	Mean		
9	9.4	Flood	1/29/2014 20:30	1/31/2014 16:00	44	0.14	0.86	0.82	0.20	36
10	0.24	Normal flow	2/10/2014 7:00	11/2/2014 16:00	33.5	0.03	0.05	0.04	0.06	1
11	-	Ungauged	2/16/2014 01:00	2/18/2014 13:00	60.5	0.03	0.03	0.03	0.15	2
13	44.8	Flood	3/12/2014 23:00	3/14/2014 00:30	26	0.14	3.69	3.28	0.62	85
14	8.1	Flood	3/28/2014 21:00	3/30/2014 12:30	40	0.10	0.27	0.26	0.15	10
15	7.76	Flood	4/2/2014 13:00	3/4/2014 10:00	21.5	0.20	0.21	0.21	0.04	4
16	34.8	Flood	4/21/2014 19:30	4/22/2014 14:00	19	0.04	2.30	2.13	0.26	40
19	0.15	Normal flow	5/8/2014 22:30	5/10/2014 19:30	45.5	0.33	1.18	1.08	0.12	49
26	19	Flood	9/21/2014 10:00	9/22/2014 16:30	31	0.25	1.00	0.95	0.10	29
29	24	Flood	4/11/2014 23:30	6/11/2014 18:30	43.5	0.56	1.74	1.63	0.12	71
30	36	Flood	9/11/2014 17:30	12/11/2014 9:00	64	0.54	2.58	2.47	0.91	158
31	60	Flood	11/21/2014 08:00	11/21/2014 13:00	5.5	4.63	4.66	4.65	0.36	26

IV. Discussion

IV.1. Near surface temperature as a proxy to infer streamflow presence and duration

As described earlier, Wadi Rheraya is characterized by intermittent streamflow driven by rainfall storm and snowmelt (Hajhouji et al., 2018), and since the Tahanaout gaging station is located several kilometers upstream the experiment site, we used temperature to detect the presence and duration of streamflow. Analysis of the entire record, we determined that 22 thermal anomalies of the surface-streambed temperature were related to hydrological events. 10 events were related to gauged floods, 04 to gauged normal streamflow, and 08 to rainfall or ungauged flow from reaches located below the gauging station. Temperature records at the near surface streambed sediment have detected the occurrence of hydrological events, but were insufficient alone to detect the type of the hydrological events; in fact, we relied on runoff measurements even far from the study site was necessary to help distinguish between different types of events. However, we determined near surface temperature records were very useful to measure the duration of each detected event.

IV.2. Effects of the sediment moisture on the infiltration processes

A key finding for Wadi Rheraya is similar streamflow events generated varying streamflow losses, i.e., there was seasonality (seasonal variation) in streamflow losses for similar flows. This seasonality of streamflow versus streamflow-losses relation was shown to be based on the moisture state of the sediment. During the wet sediment period (from winter to early summer), floods generate deep infiltration. During the dry sediment period, even large high-flow rate events failed to generate deep infiltration, a pair of flood events during late August, despite their magnitude both events generated shallow infiltration (1 m deep). These results show that the correlated relationship between streamflow magnitude and infiltration rates and percolation depths is high influenced by streambed sediment moisture level, which is generally considerable higher during the wet season than the dry season when sediment can be extremely dry, greatly damping percolation depths. To estimate the role of sediment water content on the infiltration process, the maximum velocities of the advance of the wetting front during infiltration were calculated using the time of the first indication of a water content increase at a given probe. They show that the advance of the wetting front is significantly faster in wet sediment (from 19 cm/hour to 330 cm/hour) than in dry sediment (from 3 cm/hour to 9 cm/hour). Thus, streambed sediments may be orders of magnitude more favorable for deep percolation and recharge during winter flow event compared with a summer flow event. From a practical perspective, the importance of antecedent streambed moisture conditions in estimating groundwater recharge for given streamflow events should be appreciated by water resource managers and hydrologic models to avoid large misprediction of recharge.

IV.3. Seasonal variation of the potential groundwater recharge

During the year of monitoring, the analysis of combined streambed temperature profiles with streambed water-content profiles, lead to the following results. The interpreted result for the wadi is: 9 of 11 large streamflow (flood) events generated groundwater recharge, 1 of 4 baseflow (normal) streamflow events generated ground water recharge and 1 of 8 ungauged rainfall events generated groundwater recharge. For the events interpreted as groundwater recharge, all of them appeared from analysis of the profiles to generate deep percolation surpassing 2 m depth, and importantly, all of these recharging events occurred in the wet season. The vertical 1-dimentional modeling over the one-year experiment showed that among the total percolation estimated to 459 mm/year, approximately 90% occurred during the wet period. Therefore, almost the entire deep percolation occurred in winter and spring. It is mainly

generated by floods, while the normal flow related percolation was low. Those results highlighted a strong seasonality of groundwater recharge controlled by two factors: the importance of the hydrological events and the moisture conditions of the sediment. This variation contrasts with other previous studies. Dahan et al. (2008) studied a sequence of five individual floods during the rainy season 2006. They concluded that all floods produced very similar flux rates, which were explained by a flux-regulating mechanism at the top of the vadose zone that may be due to the sediment texture and/or structure "the alternation of layers acts as the regulator that limits infiltration rates and buffers the fluxes, even during the relatively high flood stage". Note, these calculated fluxes only represent the vertical percolation as a vertical 1-dimentional modeling was used. Therefore, the lateral recharge was not accounted for. As discussed below in detail, the lateral component groundwater flow toward and into the wadi appears to augment recharge, by raising the water table and thus increasing streambed sediments moisture content.

IV.4. Lateral recharge beneath the channel

For Wadi Rheraya, sediment water-content data indicates the first rise of groundwater was not caused by the vertical infiltration at the wadi experimental site, but rather by a lateral recharge that raised the groundwater elevation upwards through the streambed sediments. The water table beneath the wadi remained elevated during late winter, spring and early summer. During this period, the top streambed sediment was variably saturated, while near saturation conditions were maintained at the bottom of the sediments. The water table declined to lower elevations beneath the wadi during summer and autumn. This annual water table elevation change is consistent with regional groundwater variation in intermittent stream alluvial aquifers in mountain front areas under Mediterranean climate (Leduc et al., 2017; Bioumouass et al., 2020). In winter and spring, the water table increases due to high recharge from high flows fed by rainfall and snowmelt, and low discharge. In summer and autumn, the water table decreases due to low or absent groundwater recharge, and high groundwater discharge to satisfy moisture depletion down gradient or due to groundwater abstraction.

IV.5. The pattern of the intermittent streamflow losses

In summary, the depth and magnitude of the stream losses depend on the streamflow type and the moisture conditions of the sediment, factors that assign a seasonality to groundwater recharge. During winter and spring, the recharge is performed mainly by floods. The normal flow generally generates low and shallow infiltration; however, it plays a crucial role in

contributing to maintain wet conditions at the upper part of the sediment that enhance the percolation conditions. Indeed, high streambed moisture greatly enhances potential recharge due to higher hydraulic conductivities and less unsaturated pore volume to absorb event-generated percolation. During the dry period, the scarcity of the streamflow and the dry state of the sediment are much less favorable to recharge; even important flashfloods only generate low or no recharge. Therefore, analysis indicates the entire deep percolation occurred in winter and spring, with this pattern of percolation was responsible for the entire cumulative recharge. However, the vertical moisture pattern was more complex than simply saturated sediments during wet seasons streamflow events. The sediment moisture profiling indicated there was not a steady saturated hydraulic connection between the stream and the water table. The sediment above the water table evolved as a variably saturated flow system, and the temporal pattern of the groundwater recharge remained transient and dominated by separated recharging events. During the wet season, saturated-sediment conditions only occur during flood events, while during steady lower streamflow was insufficient to induce saturated conditions though still contributed to deep percolation. Finally, for this specific wadi, though not uncommon for wadis in agricultural basins, upstream surface-water diversions occurred for irrigation, leading to both lower downstream flows and lower streambed sediment moistures during the dry season would have occurred without diversions; thus, the lack of summer recharge in the study reach of the wadi, may partially be a result of these diversions (Bouimouass et al., 2020).

V. Conclusions

For wadis and other stream channels with intermittent streams in arid and semiarid basins, streamflow losses may be important sources of groundwater recharge; however, it is more challenging to directly measure recharge than simpler non-intermittent ephemeral streams. As a consequence, this study utilized a unique coupling of continuous monitoring of streambed sediment temperature profiles and sediment water-content profiles, for successful, indirect estimates of streambed deep percolation and recharge beneath Wadi Rheraya during an entire hydrological year. Streambed water content allowed monitoring of the moisture conditions of the sediment and to detect downward surface water infiltration and the movements of groundwater table. The streambed temperature records provided insightful information about the depth and the duration of the infiltration from streamflow. Furthermore, the vertical streambed water content profiles lead to parsing at the start of the wet season whether groundwater recharge was created by deep percolation or from lateral inflow beneath the wadi probably derived from a mountain-front recharge.

For Wadi Rheraya, non-recharging versus potentially recharging events were distinguished according to the stream water infiltration depth. The floods of winter and spring constituted the major source of groundwater recharge. The normal streamflow or rainfall during the wet period generate low and superficial infiltration but contribute to the wetting of the sediment. During the dry period, the dry sediment and probably the flashy character of the floods, limit the infiltration and therefore subsequent groundwater recharge. Therefore, two factors contribute to the seasonality of groundwater recharge: the magnitude of the streamflow events and the moisture conditions of the sediment. It was demonstrated that wet sediments may be orders of magnitude more favorable for deep percolation and recharge for a winter flow event compared with a summer flow event in dry sediments. In summary, this study demonstrated clear seasonality relations between streamflow magnitude compared with streamflow loss amounts and percolation depth magnitude, primarily caused by significantly higher streambed sediment moisture during winter and spring than summer. Finally, using analysis of sediment temperature patterns relative to moisture patterns, this study revealed a lateral recharge beneath the wadi derived from mountain-front recharge; this is a groundwater flow component rarely considered for semiarid and arid watersheds, that may contribute to intermittent stream flows along often dry stream channels.

Chapter 6: Conclusions

The present study was carried out in the mountain front of the High-Atlas Mountains. The main objectives of the study were: (i) The use of stable isotopes and groundwater levels to determine groundwater recharge sources in the mountain front of the central High-Atlas, (ii) use of major ions and stable isotopes de study the hydrochemical evolution of groundwater and the processes controlling its quality for human use, and (iii) test the use of heat as a tracer, combined with water content data, in estimating streamflow losses from an intermittent Atlasic wadi close to the mountain front of the central High-Atlas.

Groundwater recharge sources

We combined stable isotopes data and groundwater fluctuations to investigate the recharge sources in the mountain front of the High-Atlas. The Ourika watershed was chosen to address this goal, it is one of the most important watersheds in the Tensift basin in term of produced flow. Ninety-one (91) samples of meteoric water, surface water (streamflow, irrigation), groundwater (springs and wells) were collected in the mountain, mountain front and the plain from September 2017 to March 2018 spanning the dry and the wet seasons. Groundwater levels were measured twice in September 2017 (dry season) and March 2018 (wet season) in 50 wells in the mountain front and the plain.

An obvious altitude effect and seasonal effect was observed in the waters of the mountain, attesting of a close relationship between precipitations, surface water and groundwater in the High-Atlas. In the mountain front, an obvious isotopic contrast was observed and was concomitant with land use. The area around Ourika wadi and the area receiving more surface water for irrigation have depleted isotopic content and similar to this of surface water in the mountain. The area receiving less to no surface water have an enriched isotopic content reflecting the local rainfall signature. This two groups of isotopic signatures reflect the effect of diverting surface water for irrigation on recharging groundwater. Looking closely to the depleted group in the irrigation area, three isotopic signatures can be distinguished geographically, the isotopic content tend to depletion from the upstream to downstream. This was attributed to the effect of the traditional irrigation system which favorites upstream over downstream. This results on upstream receiving water most of time especially snowmelt water during spring and summer (highest isotopic content among surface water samples of the Ourika wadi), and the downstream being recharged exclusively during high-flow events characterized by depleted isotopic content.

Groundwater fluctuations between dry and wet season showed that most of seasonal recharge occurred in the irrigated area beneath the seguias then close to the wadis highlighting

the importance of irrigation recharge. Groundwater levels rose by up to 3.5 m in the irrigation area and fall by almost 1 m. These results are in good agreement with isotopic and irrigation diversion data, and allowed as to construct a conceptual model of seasonal groundwater recharge in the mountain front of the High-Atlas. Irrigation leakage beneath seguias and fields is the most important recharge source, followed by in-channel infiltration within the wadis and a finally a potential mountain block and/or direct infiltration of rainfall in the mountain foothills.

Hydrochemical evolution and water quality

The hydrochemical characteristics of groundwater can give insights about the origin and mixing of groundwater. Concentrations of elements can also allow the assessment of water quality, which is used for both domestic and irrigation supplies in the mountain front without any treatment, making it a potential health risk if its quality is deteriorated. To this objective, we used the results of 90 samples all analyzed for major ions and ^{18}O.

Water in the mountain have Ca-HCO3 facies with low EC with excellent quality. Surface water and groundwater tends to be enriched in element with decreasing altitude due to the contact with the rocks. In the mountain front, groundwater facies evolve from Ca-HCO3 to Ca-Cl-Mg due to the longer residence time, and the dissolution of halite developed an Na-Cl facies in the right side of the Ourika wadi. However, most of the samples in the study area have low salinity and have good to excellent quality making them suitable for drinking and irrigation uses.

Water-rock interactions are the main mechanism governing water formation according to Gibbs diagram, a slight potential effect of evaporation can also be seen in irrigation area. The water-rock interactions occur via several processes such as carbonates and evaporates dissolution, silicates withering and ion exchanges. Mountainous water plays an important role in the dilution of the groundwater salinity in the mountain front via seasonal recharge. The ecological agriculture practiced in the study area plays also an important role in reducing the anthropogenic effect on groundwater quality.

Stream losses from an intermittent wadi

Streamflow losses in ephemeral streams is considered the main source of groundwater recharge in arid and semiarid areas. In the Tensift basin, the atlasic wadis are believed to be the main recharge source for the alluvial aquifer. We used sediment temperature and water content to estimate infiltration from the Rheraya wadi and study its dynamics, thus evaluate

groundwater recharge from atlasic wadis. In addition, we test the heat tracing method widely used in ephemeral streams in a large intermittent wadi with special traditional irrigation practices.

Shallow-sediment temperature was used to detect the presence and duration of streamflow in the study site. The perturbations of temperature induced by streamflow presence were obvious and was successful to detect the presence and duration of streamflow when combined with streamflow at Tahanaout gaging station and rainfall in Rheraya watershed. Out of 31 thermal anomalies, 11 correspond to floods, 04 to normal flow and 16 others can be due to local rain events or ungauged flow from downstream tributaries of Rheraya wadi.

Sediments temperature and water content data were qualitatively analyzed to determine the recharging events. 12 events out of the 16 detected were considered as recharging events while infiltrating water from 04 of the events, two of them are summer flash floods, did not reach 3-meter depth. This means that even floods cannot induce recharge when some factors are present such as the initial state of sediment moisture, evaporation and the clogging layer. Temperature data was used in 1-D heat transport modeling using VS2DI, results showed that the infiltration is generally low when compared to similar contexts, and that the infiltration rates are influenced by both water levels in the wadi and the duration of the event.

Overall, the present study has set the ground for further investigations in the mountain-front of the High-Atlas, and its results can be useful for water managers and incorporated into future management strategies.

Chapter 7: Résumé substantiel en Français

I. Introduction

L'eau souterraine est la plus importante ressource en eau douce pour le développement sociale et économique de l'être Human (Holland et al, 2015), surtout dans les zones arides et semi-arides caractérisées par des ressources en eau de surface limitées (Custodio, 2002; Massuel et al., 2013). L'eau souterraine est utilisée à la fois dans l'approvisionnement en eau potable, l'agriculture et l'industrie (Aeschbach-Hertig and Gleeson, 2012). Les eaux souterraines sont en dégradation quantitative et qualitative, sous l'effet de plusieurs facteurs tels que la croissance démographique, l'industrialisation et le changement climatique (Vörösmarty et al., 2010 ; Arnell and Lloyd-Hughes, 2014).

Les zones arides et semi-arides couvrent plus de 30% de la surface du globe (Dregne, 1991). En plus des problèmes qui font face aux ressources en eau cités ci-dessus, les zones arides et semi-arides sont caractérisées par une demande évaporative importante, des précipitations faibles et des zones non saturées épaisses, ce qui limite la recharge des eaux souterraines (Izbicki et al., 2000 ; Walvoord et al., 2002). Par conséquent, le nombre des personnes ayant des difficultés d'accès à l'eau potable est en croissance (WHO, 2003).

Les hautes montagnes reçoivent des volumes importants d'eau par précipitations due aux effets orographiques. Ces montagnes, qui actent comme des châteaux d'eau, alimentent les plaines adjacentes avec de l'eau qui s'écoule en période de pluie et de fonte de neige dans des oueds et talwegs (Viviroli et al., 2003). Cette eau est directement exploitée par la population riveraine ou recharge indirectement les eaux souterraines (Blasch and Bryson, 2007 ; Wahi et al., 2008 ; Liu and Yamanaka, 2012 ; Martinez et al., 2017 ; Bresciani et al., 2018). Récemment, Berghuis et al. (2014) ont montré que la fraction de la neige par rapport au précipitation totale à diminué en faveur de la pluie au niveau des Etats-Unis. La fonte des neiges qui s'accumulent dans les hautes altitudes alimente les activités agricoles dans les zones piémontaises pendant le printemps et le début de l'été. La diminution du couvert neigeux implique la diminution des volumes d'eau qui s'écoule dans les oueds, par conséquent le décalage du débit vers des périodes plus courtes dans l'hiver. Cela va profondément influencer le développement socio-économique des communautés qui dépendaient depuis toujours de cette eau (Malek et al., 2020). L'établissement des stratégies de gestion efficaces pour faire face à ces problèmes nécessite une bonne compréhension des interactions eaux de surface - eaux souterraines notamment les processus de la recharge.

Le Maroc est situé dans une région jugée vulnérable au changement climatique. Il est caractérisé dans sa grande partie, par un climat semi-aride avec une forte variabilité interannuelle au niveau des précipitations et des périodes de sécheresse fréquentes (Hertig and Jacobeit, 2008a). Dans les deux dernières décennies, la croissance démographique, le développement industriel et l'expansion des périmètres irrigués ont augmenté, d'une façon dramatique, la pression sur les eaux souterraines (Ait Kadi and Ziyad, 2018). Le bassin du Tensift, localisé dans le centre du Maroc, est l'un des plus grands bassins hydrauliques du pays. Il héberge la plaine du Haouz, l'une des plus grandes plaines agricoles au Maroc. Ce bassin est dépourvu de ressources d'eau de surface pérennes naturelles. Il dépend en grande partie des ressources en eau souterraine, et en autre partie sur les eaux de barrages. Le pompage excessif et persistant des eaux de l'aquifère alluvial du Haouz a conduit à une sévère diminution du niveau de l'eau qui peut atteindre 2 m/an (Fakir et al., 2015).

II. Objectifs et structure de la thèse

Le présent travail vise à répondre à certaines questions concernant les sources et les processus de la recharge de l'eau souterraine dans le piémont du Haut-Atlas. L'objectif principal de cette étude est d'explorer les potentialités du traçage environnemental en combinaison avec d'autres méthodes dans l'investigation de la recharge. Les objectifs spécifiques sont :

- Détermination des sources de la recharge dans le piémont du Haut-Atlas par l'usage des isotopes stables de l'eau et le niveau de l'eau souterraine.
- Étude de l'évolution de l'hydrochimie des eaux souterraines et l'identification des processus mis en jeu.
- Caractérisation de l'infiltration dans lit d'un oued atlasique intermittent dans le piémont en utilisant la température comme traceur.
- En plus de la contribution de la présente thèse à l'avancement des connaissances sur les interactions entre les eaux souterraines et les eaux de surface dans le piémont du Haut-Atlas, ces résultats contribuent à l'approfondissement des connaissances générales sur les sources de recharge des eaux souterraines, en présentant les résultats d'un cas d'étude spécial dans une zone semi-aride ou la recharge naturelle interfère avec la recharge induite par les activités anthropiques. A l'échelle global, cette étude contribue au débat scientifique internationale sur les sources de recharge et leurs contributions dans les zones semiarides.

Cette dissertation se compose de six chapitres :

- Chapitre 1 : Introduction générale au contexte de l'étude, les questions scientifiques, les objectifs et la structure de la thèse.
- Chapitre 2 : Ce chapitre présente la zone d'étude, le Haouz central et les bassins versants Haut-Atlasiques de Ourika et Rheraya, où les études sont effectuées. Les caractéristiques géologique, morphologique, hydrologique et hydrogéologique de la zone d'étude sont présentés.
- Chapitre 3 : Ce chapitre présente un cas d'étude dans le piémont du Haut-Atlas, autour de l'oued Ourika, où nous avons utilisé les isotopes stables de l'eau et la piézométrie pour déterminer les sources de la recharge des eaux souterraines (Bouimouass et al. 2020).
- Chapitre 4 : Dans ce chapitre, d'une part, nous avons étudié l'évolution spatio-temporelle de l'hydrochimie des eaux de surface de la montagne et les eaux souterraines de la montagne et de piémont, et d'autre part nous avons déterminer les mécanismes responsables de la chimie des eaux.
- Chapitre 5 : Ce chapitre s'articule autour d'une expérimentation qui s'étend sur une année (Novembre 2013 – Novembre 2014) sous le lit de l'oued Rheraya. L'objectif de cette expérimentation était de caractériser l'infiltration des eaux pendant les périodes d'écoulement en utilisant les données de température de surface de l'oued, des sédiments et l'humidité des sédiments.
- Chapitre 6 : Ce chapitre présente les conclusions générales de l'étude, ainsi que les perspectives et les recommandations pour les recherches futures.

III. Résumé de chaque chapitre

III.1. La zone d'étude

Le bassin du Tensift est l'un des plus grands bassins hydrauliques du Maroc. Il englobe la plaine du Haouz située sur le versant Nord du Haut-Atlas, elle couvre une superficie d'environ 6000 km^2 et considérée comme l'une de plus grandes plaines agricoles du royaume. Le bassin du Tensift est bordé du Sud par la chaine du Haut-Atlas, du Nord par le massif des Jbilets, de l'Est par le bassin d'Oum Erbia et de l'Ouest par l'océan atlantique. Il est drainé par l'oued Tensift qui s'écoule de l'Est vers l'Ouest, et qui est alimenté en grande partie par ses affluents sud provenant du Haut-Atlas. Le versant Nord du Haut-Atlas est composé de neuf bassins versants principaux, drainés par des oueds dites atlasiques (Figure 2-1). La Haouz peut être

divisé en trois parties : le Haouz Oriental, le Haouz central et le Haouz occidental. Notre zone d'étude se trouve dans le Haouz central (situé entre le bassin de Zat et le bassin de N'fis), exactement au niveau des bassins de l'Ourika et Rheraya.

Le climat dans le bassin du Tensift est semi-aride avec une variabilité spatiale marquée, et des périodes de sécheresse fréquentes (Fniguire et al., 2017). Au niveau du Haouz central, les précipitations moyennes annuelles à la station de Marrakech dans la période entre 1962 et 2015 est de 184 mm/an (Hajhouji, 2018). Par contre, les précipitations moyennes dans la station d'Aghbalou (985 m) située dans le bassin de l'Ourika est de 527 mm/an, et peuvent atteindre 700 dans les plus hautes altitudes (Saidi et al., 2010). Les oueds atlasiques se caractérisent par un régime hydrologique pluvio-nival. Ils sont permanant dans la partie amont situé dans les montages du Haut-Atlas, cependant, ils sont intermittents dans la partie centrale qui correspond au piémont avec la présence des écoulements durant la période de pluie et de fonte de la neige. La partie avale (la plaine) est caractérisée par un écoulement éphémère ou l'eau est présent en réponse aux averses orageuses. Le débit moyen des oueds Ourika et Rheraya est de 4.92 m^3/s (Bouimouass et al., 2020) et 1.15 m^3/s (Hajhouji et al., 2018), respectivement. Le Débit de l'oued Ourika est le plus important parmi les oueds atlasiques car il draine le bassin versant de l'Ourika, caractérisé par sa grande surface (579 km^2), pentes très fortes et des terrains relativement imperméables.

Le bassin du Haouz est un bassin sédimentaire d'origine tectonique, remplis par des dépôts détritiques issues du démantèlement de la chaine atlasique pendant le Néogène et le Quaternaire (Sinan, 2000). La géologie et la structure du massif du Haut-Atlas centrale est très compliquée, formée de terrains d'âge variant du précambrien jusqu'au quaternaire. Le Haut-Atlas est caractérisé par l'abondance des roches cristallines (granodiorites, amphibolite, granite …), évaporites de Trias et des carbonates du Cénozoïque (Eocène, Moi-Pliocène …).

La plaine de Haouz s'étends au-dessus d'un large aquifère alluvial libre avec une surface dépassant 6000 km^2. Quelques aquifères captifs sont aussi présents sous la plaine du Haouz, encaissés dans les calcaires de l'Eocène, le Cenomano-Turonien et le Jurassique (Moukhchane, 1993 ; Sinan, 2000) affleurant surtout dans le Haouz occidental. L'aquifère alluvial est considéré comme la plus importante source de l'eau douce dans le bassin du Tensift. Cette aquifère libre est formé par des alluvions, caractérisés par une grande hétérogénéité latérale et verticale, et un substratum formé par les marnes et les argiles du Trias. Verticalement, l'aquifère peut être schématisé par une multicouche avec des structures lenticulaires d'argiles et marnes en alternance avec des éléments plus grossiers. Latéralement, plusieurs structures existent au

niveau e l'aquifère du Haouz tels que les paléo-chenaux, paléo-reliefs, cônes d'éboulis … (Sinan, 2000).

La majeure partie de la demande en eau pour l'irrigation et l'approvisionnement en eau potable dépend des eaux souterraines de l'aquifère alluviale. Un large nombre de puits (plus de 24000) pompent l'eau souterraine d'une manière consistante (Le page et al., 2012), ce qui exerce une forte pression sur cette ressource. Afin de soutenir les eaux souterraines, un canal artificiel (Canal Rocade) qui amène de l'eau depuis le bassin d'Oum Erbia vers le bassin de Tensift. Le canal Rocade s'étend sur une longueur de 120 km et alimente les grands périmètres irrigués et la majeure partie de la demande en eau potable pour la ville de Marrakech. L'eau du barrage de Takerkoust, sur l'oued N'fis, est aussi utilisé pour l'irrigation du périmètre irrigué du N'fis, et alimente parfois la ville de Marrakech en eau potable.

Dans le piémont, les habitants profitent de l'eau des oueds atlasiques pour l'irrigation pendant les périodes de crues et de la fonte de neige. Cette eau est dérivée des oueds par un réseau de canaux appelés Séguias. Ces séguias sont gérés par les habitants selon un système de partage traditionnel ancestral (Bouimouass et al., 2020). Ce system d'irrigation favorise la zone de piémont dans l'accès à l'eau pendant les périodes d'écoulement alimenté par la fonte de la neige.

III.2. Les sources de recharge des eaux souterraines dans le piémont du Haut-Atlas

Dans les zones arides et semi-arides, la recharge directe diffuse est très limitée à cause de plusieurs facteurs notamment la demande évaporative élevée, les précipitations faibles …etc (Shanafield and Cook, 2014). Par contre, la recharge indirecte localisée dans les dépressions topographiques, tels que les oueds et les lacs, auxquelles il peut s'ajouter l'écoulement en subsurface depuis les massifs montagneux vers l'aquifère dans les bassins bordés par des montagnes qui reçoivent plus de précipitations grâce au effets orographiques (Wilson And Guan, 2004). Il est aussi connu que les zones de piémonts sont des zones de recharge pour les bassins aride et semiarides car ils reçoivent plus d'eau (Bresciani et al., 2018 ; Markovitch et al., 2019). Cependant, il est souvent difficile de distinguer ces sources de recharge et leurs contributions, ce qui est important pour une bonne connaissance et gestion de la ressource en eau (Bresciani et al., 2018).

En plus des sources de recharge naturelles des eaux souterraines, une autre source d'alimentation induite par les activités anthropiques peut aussi contribuer considérablement à la recharge. L'irrigation parfois constitue une source de recharge importante (Ochoa et al.,

2010 ; Fernald et al., 2014 ; Rotiroti et al., 2019). Dans le piémont du Haut-Atlas, par exemple, où l'irrigation par les eaux de surface est abondante, elle peut être une source importante de recharge.

Dans ce chapitre, nous avons combiné des données hydro-chimique et hydro-physique pour la caractérisation des sources de la recharge des eaux souterraines dans le piémont du Haut-Atlas. La présente étude a été réalisée au niveau du bassin versant de l'Ourika, depuis la montagne jusqu'à la plaine. Le bassin versant de l'Ourika a été choisi parce qu'il est l'un des principaux sous bassins du Haut-Atlas, considéré parmi les plus actifs de point de vue hydrologique et en termes de génération de débit.

Sur la période allant de Septembre 2017 jusqu'à Mars 2018, nous avons collecté 95 échantillons des différentes sources d'eaux (les eaux météoriques, les eaux de surface et les eaux souterraines) que ce soitdans la montagne, le piémont ou la plaine. Les paramètres physico-chimiques (pH, conductivité électrique et température) ont été mesurés sur terrain à l'aide d'un pH mètre et un conductivimètre portable. L'alcalinité a été mesurée en fin de journée à l'aide d'un DIGITAL TITRATOR (HACH). Les échantillons ont été collectés dans des bouteilles de 250 ml et conservés à froid jusqu'à l'analyse. Tous les échantillons ont été analysés pour les isotopes stables de l'eau (^{18}O et ^{2}H) à l'aide d'un Picarro Analyser L 2130-I.

Deux campagnes piézométriques ont été réalisées sur 50 puits durant la période allant de Septembre 2017 jusqu'àMars 2018. La campagne de Septembre 2017 représente les basses eaux et la campagne de Mars 2018 représente les hautes eaux.

L'analyse des données des prélèvements des Séguias de l'oued Ourika depuis Septembre 2000 jusqu'à décembre 2016 ont montré que les séguias captent plus de 65% des volumes d'eau qui s'écoule dans l'oued Ourika dans la zone du piémont. Les Seguias du piémont dévient la totalité des volumes d'eau de l'oued pendant les périodes de l'écoulement normale. Les Séguias en aval ne reçoivent que pendant les périodes de débits élevés. Par exemple, les Séguias Tassoultant et Taoualt qui captent l'eau depuis le piémont dévient, respectivement, un volume mensuel moyen de 1,326,986 m^3 (14.4% du volume total dévié) et 557,286 m^3 (6.1% du volume total dévié). La Séguia Cherrifia, plus en aval, dévie un volume mensuel moyen de 45,228 m^3 (0.5% du volume total dévié). Temporellement, les prélèvements des Séguias montre deux pics pendant l'année hydrologique, un pic en Novembre coïncidant avec la période de pluie et un pic en avril coïncidant avec la période de la fonte de neige. Ces données montrent que le pic de d'Avril à diminuer ce qui indique une réduction au niveau de la fonte de la neige.

La différence entre les profondeurs de l'eau mesurées en Septembre 2017 et Mars 2018 a montré que le niveau de la nappe a augmenté jusqu'à 3.5 m dans la rive gauche de l'oued qui correspond à la zone irriguée par les séguias, et a diminué de 1 m dans la zone non-irriguée (non-irriguée ici réfère à l'irrigation par les eaux de surface).

Les résultats des analyses isotopiques ont révélé un contraste isotopique très marquée dans la zone d'étude. Les valeurs varient du -18.1‰ à 3.4‰ pour $\delta^{18}O$ et de -126‰ à -19‰ pour $\delta^{2}H$. Tous les échantillons tombent en dessus de la ligne météorique internationale indiquant l'absence de l'effet d'évaporation sur la composition isotopique des eaux de la zone d'étude. Les isotopes stables des précipitations montrent un effet d'altitude très clair. Les valeurs isotopiques de la pluie varient de -9.2‰ à -3.4‰ pour $\delta^{18}O$ et de -47‰ to -19‰ for ^{2}H dans la plaine, et varient de -12.4‰ à -5.5‰ pour $\delta^{18}O$ et de -111‰ à -31‰ pour ^{2}H dans le piémont, et de -18.1% à -8.2‰ pour $\delta^{18}O$ et -126 to -51 ‰ pour ^{2}H dans le Haut-Atlas. Ce même effet est présent aussi au niveau des eaux de surface et des eaux souterraines attestant d'une forte connectivité entre les précipitations, les eaux souterraines et les eaux de surface dans le Haut-Atlas. Les valeurs des isotopes stables dans les eaux de surface dans la montagne varient de -9.3‰ à -7.5‰ pour $\delta^{18}O$ et de -60‰ à -48‰ pour $\delta^{2}H$. Un échantillon collecté pendant une crue en Mars 2018 à l'oued Ourika au niveau de la plaine est le plus appauvrie en isotopes stables parmi les eaux de surface (-9.3‰ pour $\delta^{18}O$ et -60‰ pour $\delta^{2}H$). Deux échantillons collectés de l'oued Igerifrouan et l'oued Elmaleh, deux affluents avals de l'oued Ourika, pendant la même crue ont des valeurs de -8.1‰ et -6.9‰ pour δ18O et -49‰ et -41‰ pour δ2H, respectivement. Ce contraste isotopique est dû à l'effet d'altitude car l'oued Ourika draine les hautes altitudes, l'oued Igerifrouan draine des altitudes moyennes et l'oued Elmaleh draine des altitudes pluies faibles. Les valeurs de δ18O et δ2H des eaux des sources (Sp1 and Sp2) varient de -8.6‰ à -5.9‰ et de -54‰ à -36‰, respectivement, avec un enrichissement depuis Sp1 vers Sp2. En plus de l'effet d'altitude sur les eaux de surface des sources, un effet saisonnier est aussi observé. Cet effet est traduit par un appauvrissement en isotopes depuis la saison sèche vers la saison humide. Cela indique une forte connectivité entre les eaux météoriques, les eaux de surface et les eaux souterraines dans la montagne. Les précipitations et la fonte de la neige alimentent, en grande partie l'oued Ourika, pendant l'hiver et le printemps.

Les signatures isotopiques des eaux souterraines dans le piémont et la plaine montrent une variabilité spatiale claire, alors que la variabilité temporelle n'est pas marquée. Les valeurs isotopiques varient de -8.4‰ à -6‰ pour $\delta^{18}O$ et de -54‰ à -35‰ pour $\delta^{2}H$, avec une moyenne de −7.6‰ pour $\delta^{18}O$ et −49‰ pour $\delta^{2}H$. Les isotopes stables sont plus appauvries dans la zone

irriguée (une moyenne de -7.9‰ pour $\delta^{18}O$ et -51‰ pour $\delta^{2}H$) que dans la zone non irriguée (une moyenne de : -6.4‰ pour $\delta^{18}O$ et −38‰ pour $\delta^{2}H$). Selon la distribution spatiale de la composition isotopique, on peut distinguer deux grands groupes et six sous-groupes:

- Le groupe 1 composé de 41 échantillons, appauvris en isotopes stables, il couvre la zone autour de l'oued Ourika et la zone irriguée par les séguias. Ce groupe peut être divisé en trois sous-groupes :
  - Sous-groupe G1-1 : Situé dans la rive gauche de l'oued Ourika, il est caractérisé par l'abondance des séguias. Ce sous-groupe est le plus enrichi en isotopes stables.
  - Sous-groupe G1-2 : Situé dans la zone localisée autour de l'oued Ourika. Ce sous-groupe est relativement plus appauvri en isotopes stables que le sous-groupe G1-1.
  - Sous-groupe G1-3 : Situé en aval de la zone d'étude dans la rive gauche de l'oued. Ce sous-groupe est le plus appauvri en isotopes parmi les eaux collectés dans les puits et il est similaire aux eaux souterraines et de surface de la haute montagne.
- Le groupe 2 composé de 06 échantillons, enrichie en isotopes stables, il représente la zone non irriguée et les collines du piémont. Ce groupe peut être aussi divisé en 02 sous-groupes :
  - Sous-groupe G2-1 : Situé au niveau de la zone des collines, il est le plus enrichi en isotope stable dans cette étude.
  - Sous-groupe G2-2 : il représente la rive droite de l'oued Ourika ou le réseau des séguias est très limité et considérée comme une zone non-irriguée par les eaux de surface, ce sous-groupe est relativement moins enrichi que le sous-groupe G2-2.

Le sous-groupe G1-1 a une composition isotopique similaire à celle de l'oued Ourika et les sources (surtout ceux des moyennes et faibles altitudes) en dehors des périodes de pluies. Cependant la composition isotopique du sous-groupe G1-3 est similaire à celle de de l'oued Ourika et les sources en périodes de pluie et en hautes altitudes. La composition du sous-groupe G1-2 est intermédiaire entre les deux autres sous-groupes. Cela peut être expliqué par l'impact du système d'irrigation traditionnel (séguia). La zone du sous-groupe G1-1 bénéfice exclusivement d'eau pendant la période sèche ou l'écoulement est faible, d'où la similarité isotopique avec les eaux de surface de la même période. Le sous-groupe G1-3 situé dans l'aval de la zone d'étude profite de l'eau exclusivement pendant les crues, d'où la similarité avec les eaux de surface en hautes altitudes et en périodes humide. On note aussi que ce groupe est similaire isotopiquement à l'échantillon collecté pendant la crue du Mars 2018. En ce qui

concerne le sous-groupe G1-2, géographiquement situé entre les deux autres sous-groupes, il bénéficie des eaux de crues et occasionnellement des eaux d'écoulement normale.

Le groupe G2 situé dans la zone non-irriguée est plus enrichie en isotopes stables que le groupe G1. Ce groupe reflète la signature originale du piémont, influencé par les pluies locales enrichie en isotopes à cause de l'effet d'altitude. La composition isotopique de ce groupe tend à s'appauvrir de l'amont vers l'aval, similaire au groupe G1 est contraire à l'effet d'altitude dans la montagne. Cela reflète l'effet du système d'agriculture typique à ces zones semi-arides au Maroc, et surtout dans le piémont du Haut-Atlas. L'irrigation traditionnelle ne se limite pas seulement à détourner l'eau de l'oued et le distribue le long d'un réseau ramifié de séguias vers les champs et les parcelles, mais aussi selon un système de distribution ancestral qui favorise l'amont sur l'avale et le plus proche de la source d'eau qui profite le premier et le plus, notamment durant les périodes de sécheresse ou la rareté de l'eau fait reculer et diminuer les surfaces irriguées et par conséquent créer des problèmes sociaux.

Cette étude nous a permis d'établir un modèle conceptuel de la recharge des eaux souterraines dans le piémont du Haut-Atlas. L'irrigation par les eaux de surface, l'infiltration le long de lit de l'oued sont les sources de recharges les plus importants de recharge, auxquelles il s'ajoute l'infiltration directe des eaux de pluie et l'écoulement depuis le bloc montagneux vers l'aquifère au niveau des reliefs de faibles altitudes dans le piémont.

III.3. Evolution hydrochimique et qualité de l'eau

L'eau souterraine constitue la source principale de l'alimentation en eau potable et l'irrigation dans la zone rurale du piémont du Haut-Atlas. Cette eau est pompée de la nappe et directement utilisée pour les usages domestiques sans traitement, sauf des traitements occasionnels au chlore. L'eau souterraine des aquifères alluviaux peut être sujet de contamination d'origine naturelle ou anthropique. La contamination naturelle peut être due aux interactions eau-roche qui peuvent induire un enrichissement en éléments dépassant les limites des standards de qualité, alors que la contamination anthropique peut être due à l'application des engrais chimiques, des déchets industriels et des déchets domestiques.

La chimie de l'eau permet de comprendre les processus hydrologiques en renseignant sur le temps de séjour dans l'aquifère et les formations géologiques parcourus par l'eau pendant l'écoulement souterrain. La chimie de l'eau dans la zone piémontaise pourrait enregistrer l'impact des interactions entre l'eau provenant de la montagne, l'eau souterraine locale et l'activité humaine. Dans le présent travail, nous avons utilisé les ions majeurs pour l'étude des

mécanismes de formation de la chimie de l'eau souterraine dans la montagne et le piémont du Haut-Atlas, et pour évaluer sa qualité.

Nous avons utilisé les mêmes échantillons collectés entre Septembre 2017 et Mars 2018 pour étudier les sources de recharge dans le piémont du Haut-Atlas au niveau du bassin de l'Ourika. Dans cette étude nous avons détaillée l'évolution des teneurs en ions majeurs à l'échelle spatiale et temporelle. Pour cet objectif, un total de 88 échantillons d'eau a été utilisés (dont 67 d'eau souterraine, 16 de surface et 05 de précipitations). Ces échantillons ont été analysés pour les ions majeurs et l'oxygène-18.

Les données ont été analysés à l'aide de représentations graphiques (diagrammes binaires, diagramme de Piper, Diagramme de Gibbs …) afin de déterminer les mécanismes qui contrôlent la chimie de l'eau. La qualité de l'eau a été évaluée à l'aide d'indices basés sur la concentration des ions majeurs.

Dans la montagne, les eaux de surface et les eaux souterraines sont en relation étroite avec les eaux météoriques, cette relation est traduite par un faciès chimique bicarbonaté calcique (Ca-HCO3) et une faible salinité (moyenne = 273 µS/cm). En allant de l'amont vers l'aval, la teneur en éléments augmente à cause du contact avec les formations géologiques riches en silicates et carbonates. En piémont, la majorité des échantillons sont de faciès bicarbonaté calcique typique aux eaux douces avec une faible salinité (moyenne = 807 µS/cm). Cela est dû à la recharge des eaux souterraines au piémont par les eaux issues de la montagne et qui s'infiltre le long de l'oued Ourika et ses affluents et au niveau des champs irrigués. Les eaux souterraines dans le piémont sont plus enrichies en éléments que ceux de la montagne et montre 2 faciès secondaires, un faciès chloruré calcique et magnésien et un faciès chloruré sodique. Cela peut être expliqué par le temps de séjour plus long ou l'effet de l'évaporation dû au climat semi-aride qui caractérise notre zone d'action. Les résultats des analyses de Cl^- et ^{18}O ont montré un léger effet potentiel de l'évaporation dans la zone irriguée. Les eaux souterraines sont enrichies par la dissolution des minéraux (l'halite et les carbonates), l'hydrolyse des silicates et les échanges ioniques.

En générale, la qualité des eaux souterraines varie entre bonne à excellente, mais le lessivage des dépôts triasiques riches en évaporites, surtout l'halite, peut détériorer la qualité de l'eau surtout dans la rive droite de l'oued Ourika la rendant non utilisable pour l'usage domestique. La bonne qualité de l'eau souterraine dans le piémont du Haut-Atlas est due à

l'impact de l'irrigation traditionnelle, l'usage des fertilisants organiques, et la recharge par des eaux de surface d'excellente qualité.

III.4. Infiltration dans les lits des oueds

Dans les zones arides et semi-arides où l'infiltration directe de l'eau de la pluie est très limitée et les ressources en eau de surface pérennes sont presque inexistantes, la recharge des eaux souterrains s'opère surtout le long des oueds éphémères pendant l'écoulement en réponse aux averses orageuses dans les montagnes adjacentes (Shanafield and Cook, 2014). Cependant, ce type de recharge peut être limité par des facteurs morphologiques et lithologique (Schwartz, 2016). La nature des sédiments, l'épaisseur de la zone non saturée, la forte demande évaporative et l'existence d'une couche de matériaux fins à la surface de lit du l'oued sont tous des facteurs qui peuvent limités l'infiltration, et par conséquent, la recharge.

Plusieurs méthodes d'estimation de l'infiltration depuis la surface des lits des oueds existent dans la littérature, et ils sont présenté en détails dans plusieurs revues bibliographiques (Scanlon et al., 2002 ; Kalbus et al., 2006 ; Shanafield et al., 2014). Malgré tous les progrès et le développement achevé en termes d'acquisition de données, il reste difficile d'acquérir des données fiables et en continuité suffisante pour caractériser et quantifier l'infiltration. L'imprédictibilité et la nature sporadique des crues dans les zones arides et semi-arides rendent difficile l'accès aux site expérimentaux, et leur nature destructive endommage souvent les équipements installés sur place. La mesure de la température des sédiments (Constantz et al., 1994 ; Constantz and Thomas, 1997; Ronan et al., 1998 ; Stonestrom and Constantz, 2003; Goodrich et al., 2004, Hoffmann et al., 2007 ; Kulongoski and Izbicki, 2008, Rau et al., 2017) et de leur teneur en eau (Dahan et al., 2007 ; Dahan et al., 2008 ; Schwartz, 2016) ont été utilisés dans l'étude et la quantification de la dynamique de la recharge dans les oueds éphémères dans plusieurs zones arides et semiarides des Etats Unies et l'Australie. Pourtant, l'application de ces techniques dans des contextes d'écoulement intermittent reste très limité.

Dans la présente étude, nous avons utilisé une base de données de température et de la teneur en eau durant une année (Novembre 2013 – Novembre 2014) au niveau d'un site localisé dans la zone aval du piémont du Haut-Atlas de l'oued Rheraya. Un profil de sondes de température et d'humidité couvrant toute la zone non saturée depuis la surface a été mis en place afin d'étudier la dynamique de l'infiltration et la recharge des eaux souterraines depuis l'oued Rheraya.

Le site d'étude se situe dans la partie piémontaise du Haut-Atlas, dans le lit de l'oued Rheraya à 8 km de l'exutoire du bassin versant de Rheraya. 04 sondes thermiques ont été installées sur le lit de l'oued (60 m de largeur) à 50 cm en dessous de la surface afin de détecter la présence et la durée de événements hydrologiques. 12 autres sondes thermiques ont été installées verticalement sur un profile de 5.5 m couvrant la zone non saturée, avec un espacement de 50 cm entre eux. 04 sondes d'humidité en été installées chaque 1 m depuis la surface. Ces sondes enregistrent la température et l'humidité des sédiments chaque 30 minutes depuis 01//11/2013 jusqu'au 21/11/2014.

Les données des sondes installées à travers l'oued ont été compléter par des données de pluie et de débit, afin de déterminer la présence et la durée des écoulements dans l'oued. Les données de la teneur en eau et de la température des sédiments ont été analysées et discutées qualitativement à l'aide de représentations graphiques afin de déterminer les évènements qui rechargent la nappe parmi les événements détectées. En plus, les données de température des sédiments ont été utilisées pour la modélisation unidimensionnelle du transport de l'énergie à l'aide de VS2DI, afin de calculer les taux d'infiltration pendant les périodes d'écoulements.

La présence de l'eau influence la température des sédiments de la surface du lit de l'oued, qui se traduit par des variations brusques de température (baisses ou des hausses). Ces perturbations peuvent être inspecté visuellement sur les thermographes qui représentent la variation de la température en fonction de temps. Dans notre cas, 31 perturbations de température ont été détectés. Après la comparaison avec les données de pluie de débit de la station de Tahanaout, 04 de ces perturbations correspond un écoulement normal, 11 correspond aux crues, les autres 16 perturbations ne coïncidaient pas avec un écoulement mesuré à la station de Tahanaout. Ils peuvent être dues à l'effet de pluie, ou des écoulements induits par des affluents avales. En outre, la température peut détecter la présence et les durées des événements dans les sites ou le déploiement des équipements de mesure de débit est difficile.

Les thermographes du profil vertical de sondes ont une forme sinusoïdale à l'échelle journalière et saisonnière dans les sondes peu profondes, alors qui les sondes profondes sont relativement stable le long de la période de mesure. La présence de l'écoulement provoque des baisses brusques de température qui diffèrent en termes de magnitude et de durée d'un évènement à l'autre. L'évolution de la teneur en eau des sédiments pendant la période d'étude permet de distinguer deux états d'humidité : le premier où toutes les sondes sont sous-saturées, depuis 11/2013 jusqu'au 02/2014 et depuis 07/2014 jusqu'au 11/2014, et une période où les

deux sondes installées à 3 et 4 m sont saturées pendant toute la période entre 02/2014 et 07/2014.

Parce que la nappe a remonté jusqu'à 3 m de profondeur, comme indiqué par la teneur en eau, les événements dont l'eau infiltré dépasse les trois mètres de profondeur sont considérées comme des évènements rechargeant. La combinaison de la température et la teneur en eau a permis de déterminer 12 événements rechargeant parmi les 31 événements potentiels détectés au début. Deux crues d'une courte durée (5.5h et 6h) le 27 et le 29 Aout 2014 n'ont pas induit une recharge car l'infiltration de l'eau de ces crues n'a pas dépassé les deux mètres. Cela est peut-être due à l'évaporation élevée et au dépôt d'une couche fine à la surface de lit de l'oued qui peut limiter l'infiltration, et remis en question de la recharge par les crues.

Concernant la simulation du transport de l'énergie dans la zone non-saturée, nous avons utilisé 1DTemPro qui représente l'interface graphique du programme VS2DH, un modèle de simulation de transport en milieu sous-saturé. La simulation a été effectuée à l'aide des données de la température et des propriétés physiques et thermiques des sédiments. La conductivité hydraulique a été estimée à l'aide de l'analyse granulométrique des échantillons pris de différentes profondeurs du site, la porosité efficace a été calculée à partir des données de la teneur en eau, et les paramètres thermiques sont pris de la littérature. Les flux calculés par le modèle varient entre 0.03 et 4.65 mm/h avec une moyenne de 1.7 mm/h. Les flux les plus élevés correspond à la crue du 21/11/2014, alors que les plus faibles correspond à l'événement d'écoulement normale du 16/02/2014.

IV. Conclusion

La présente étude a pour objectif d'investiguer et d'enquérir les sources de recharge des eaux souterraines et les interactions des eaux de surface-eaux souterraines dans le piémont du Haut-Atlas central. Nous avons combiné plusieurs techniques et données (traçage isotopique, ions majeurs, fluctuations piézométriques, température et humidité) pour distinguer les différents types de recharge et caractériser l'infiltration des eaux dans les lits des oueds.

La combinaison entre les isotopes stables et les fluctuations piézométriques a permis de distinguer deux sources de recharge importantes dans le piémont du Haut-Atlas, la recharge par les eaux des oueds destinés à l'irrigation, et l'infiltration au niveau des lits des oueds. Cette étude a montré aussi un impact anthropique important sur la recharge due au système traditionnel de distribution des eaux d'irrigation. Ce système favorise l'amont à l'aval ce qui induit une concentration de la recharge au niveau de piémont et dans les zones ou les seguias

sont abondantes. La distribution spatiale des signatures isotopiques des eaux souterraines suggère la présence d'une troisième source de recharge qui est l'infiltration directe des eaux de pluie ou l'écoulement de subsurface depuis le block montagneux vers le bassin.

La relation étroite entre les eaux de surface et les eaux souterraines dans le piémont du Haut-Atlas à profondément influencé l'hydrochimie de ces derniers. La majorité des eaux souterraines sont de faible salinité similairement aux eaux du Haut-Atlas, avec un faible enrichissement en élément en allant vers l'aval. Ces eaux sont de bonne qualité chimique. Les caractéristiques hydrochimiques des eaux souterraines reflètent l'impact de la recharge par les eaux de surface de bonne qualité provenant du Haut-Atlas, et aussi l'impact de l'agriculture écologique pratiqué depuis des siècles dans la zone.

Les mesures in-situ de la température et l'humidité des sédiments en dessous d'un oued atlasique ont permis de caractériser la dynamique de l'infiltration des eaux et de la recharge par les eaux de surface. La majorité des évènements qui recharge la nappe arrive dans la saison humide (Janvier-Mai) et la saison des pluies (Novembre-Décembre). La recharge dans les lits des oueds est limitée par plusieurs facteurs tels que la durée des événements, l'état de saturation initiale des sédiments et l'évaporation.

References

Abourida, A. (2007). Approche hydrogéologique de la nappe du Haouz (Maroc) par télédétection, isotopie, SIG et modélisation. Université Cadi Ayyad Faculté des sciencesSemlalia. Marrakech. 146p.

Aeschbach-Hertig, W., & Gleeson, T. (2012). Regional strategies for the accelerating global problem of groundwater depletion. Nature Geoscience, 5(12), 853–861.

Aji, K., Tang, C., Song, X., Kondoh, A., Sakura, Y., Yu, J., & Kaneko, S. (2008). Characteristics of chemistry and stable isotopes in groundwater of Chaobai and Yongding River basin, North China plain. Hydrological Processes: An International Journal, 22(1), 63–72.

Alcalá, F. J., & Custodio, E. (2008). Using the Cl/Br ratio as a tracer to identify the origin of salinity in aquifers in Spain and Portugal. Journal of Hydrology, 359(1-2), 189-207.

Alyamani MS, Sen Z (1993) Determination of hydraulic conductivity from complete grain-size distribution curves. Ground Water, 31(4), 551–555

Anderson, M. P. (2005). Heat as a ground water tracer. Ground water, 43(6), 951-968.

Arnell, N. W., & Lloyd-Hughes, B. (2014). The global-scale impacts of climate change on water resources and flooding under new climate and socio-economic scenarios. *Climatic Change*, *122*(1-2), 127-140.

Baba, M. W., Gascoin, S., Jarlan, L., Simonneaux, V., & Hanich, L. (2018). Variations of the Snow Water Equivalent in the Ourika catchment (Morocco) over 2000–2018 using downscaled MERRA-2 data. Water, 10(9), 1120.

Baudron, P., Barbecot, F., Aróstegui, J. L. G., Leduc, C., Travi, Y., & Martinez-Vicente, D. (2014). Impacts of human activities on recharge in a multilayered semiarid aquifer (Campo de Cartagena, SE Spain). Hydrological Processes, *28*(4), 2223-2236.

Bartarya, S. K. (1993). Hydrochemistry and rock weathering in a sub-tropical Lesser Himalayan river basin in Kumaun, India. Journal of Hydrology, 146, 149-174.

Bennetts, D. A., Webb, J. A., Stone, D. J. M., & Hill, D. M. (2006). Understanding the salinisation process for groundwater in an area of south-eastern Australia, using hydrochemical and isotopic evidence. Journal of Hydrology, 323(1-4), 178-192.

Berghuijs, W. R., Woods, R. A., & Hrachowitz, M. (2014). A precipitation shift from snow towards rain leads to a decrease in streamflow. *Nature Climate Change*, *4*(7), 583-586.

Besbes, M., Delhomme, J. P., & De Marsily, G. (1978). Estimating recharge from ephemeral streams in arid regions: a case study at Kairouan, Tunisia. Water resources research, 14(2), 281-290.

Bethune, M. (2004). Towards effective control of deep drainage under border-check irrigated pasture in the Murray–Darling basin: A review. Australian Journal of Agricultural Research, 55(5), 485–494.

Bethune, M. G., Selle, B., & Wang, Q. J. (2008). Understanding and predicting deep percolation under surface irrigation. Water Resources Research, 44, W12430.

Biron, P. E. (1982). Le Permo-Trias de la région de l'Ourika (Haut-Atlas de Marrakech, Maroc): lithostratigraphie, sédimentologie, tectonique et minéralisations (Doctoral dissertation, Université Scientifique et Médicale de Grenoble).

Blasch, K. W., Fleming, J. B., Ferre, P. A., & Hoffmann, J. P. (2000). One-and two-dimensional temperature and moisture-content profiling of an ephemeral stream channel in a semiarid watershed [abs]: EOS. Transactions, American Geophyical Union, 81, F50.

Blasch, K. W., Ferré, T., & Hoffmann, J. P. (2004). A statistical technique for interpreting streamflow timing using streambed sediment thermographs. Vadose Zone Journal, 3(3), 936-946.

Blasch, K. W., & Bryson, J. R. (2007). Distinguishing sources of ground water recharge by using δ2H and δ18O. Groundwater, 45(3), 294–308.

Boudhar, A., Hanich, L., Boulet, G., Duchemin, B., Berjamy, B., & Chehbouni, A. (2009). Evaluation of the snowmelt runoff model in the Moroccan high Atlas Mountains using two snow-cover estimates. Hydrological Sciences Journal, 54(6), 1094–1113.

Bouimouass H, Fakir Y, Tweed S, Leblanc M. Groundwater recharge sources in semiarid irrigated mountain fronts. Hydrological Processes. 2020;1–18.

Boukhari, K., Fakir, Y., Stigter, T. Y., Hajhouji, Y., & Boulet, G. (2015). Origin of recharge and salinity and their role on management issues of a large alluvial aquifer system in the semi-arid Haouz plain, Morocco. Environmental Earth Sciences, 73(10), 6195–6212.

Bresciani, E., Cranswick, R. H., Banks, E. W., Batlle-Aguilar, J., Cook, P. G., & Batelaan, O. (2018). Using hydraulic head, chloride and electrical conductivity data to distinguish between mountain-front and mountain-block recharge to basin aquifers. Hydrology & Earth System Sciences, 22(2), 1629–1648.

Carol, E. S., Kruse, E. E., Laurencena, P. C., Rojo, A., & Deluchi, M. H. (2012). Ionic exchange in groundwater hydrochemical evolution. Study case: the drainage basin of El Pescado creek (Buenos Aires province, Argentina). Environmental Earth Sciences, 65(2), 421-428.

Celestino, A. E. M., Leal, J. A. R., Cruz, D. A. M., Vargas, J. T., Josue, D. L. B., & Ramírez, J. M. (2019). Identification of the hydrogeochemical processes and assessment of groundwater quality, using multivariate statistical approaches and water quality index in a wastewater irrigated region.

Chehbouni, A., Escadafal, R., Duchemin, B., Boulet, G., Simonneaux, V., Dedieu, G., ... & Merlin, O. (2008). An integrated modelling and remote sensing approach for hydrological study in arid and semi-arid regions: The SUDMED Programme. International Journal of Remote Sensing, 29(17-18), 5161-5181.

Chen, J., He, D., & Cui, S. (2003). The response of river water quality and quantity to the development of irrigated agriculture in the last 4 decades in the Yellow River Basin, China. Water Resources Research, 39(3).

Chourasia, L. P., & TELLAM, J. H. (1992). Determination of the effect of surface water irrigation on the groundwater chemistry of a hard rock terrain in central India. Hydrological sciences journal, 37(4), 313-328.

Chowdhury, A. H., Uliana, M., & Wade, S. (2008). Ground water recharge and flow characterization using multiple isotopes. Groundwater, 46(3), 426–436.

Clark, I. D., & Fritz, P. (1997). Tracing the Hydrological Cycle. Environmental Isotopes in Hydrogeology (pp. 35–60). CRC Press, Florida.

Cody, K. C. (2018). Upstream with a shovel or downstream with a water right? Irrigation in a changing climate. Environmental Science & Policy, 80, 62–73.

Constantz, J., & Thomas, C. L. (1997). Streambed temperature profiles as indicators of percolation characteristics beneath arroyos in the middle Rio Grande Basin, USA. Hydrological Processes, 11(12), 1621-1634.

Constantz, J., Stonestorm, D. A., Stewart, A. E., Niswonger, R., & Smith, T. R. (2001). Analysis of streambed temperatures in ephemeral channels to determine streamflow frequency and duration. Water Resources Research, 37(2), 317-328.

Constantz, J., & Stonestrom, D. A. (2003). Heat as a tool for studying the movement of ground water near streams. US Geol Surv Circ 1260.

Constantz, J. (2008). Heat as a tracer to determine streambed water exchanges. Water Resources Research, 44(4).

Custodio, E. (2002). Aquifer overexploitation: what does it mean?. Hydrogeology journal, *10*(2), 254-277.

Cuthbert, M. O., Acworth, R. I., Andersen, M. S., Larsen, J. R., McCallum, A. M., Rau, G. C., Tellam, J. H. (2016). Understanding and quantifying focused, indirect groundwater recharge from ephemeral streams using water table fluctuations. Water Resources Research, 52, 827–840.

Craig, H. (1961). Isotopic variations in meteoric waters. Science, 133(3465), 1702–1703.

Dahan, O., Shani, Y., Enzel, Y., Yechieli, Y., & Yakirevich, A. (2007). Direct measurements of floodwater infiltration into shallow alluvial aquifers. Journal of Hydrology, 344(3-4), 157-170.

Dahan, O., Tatarsky, B., Enzel, Y., Kulls, C., Seely, M., & Benito, G. (2008). Dynamics of flood water infiltration and ground water recharge in hyperarid desert. Groundwater, 46(3), 450-461.

Dahan, O., Talby, R., Yechieli, Y., Adar, E., Lazarovitch, N., & Enzel, Y. (2009). In situ monitoring of water percolation and solute transport using a vadose zone monitoring system. Vadose Zone Journal, 8(4), 916–925.

Deverel, S. J., & Gallanthine, S. K. (1989). Relation of salinity and selenium in shallow groundwater to hydrologic and geochemical processes, western San Joaquin Valley, California. Journal of Hydrology, 109(1-2), 125-149.

Duncan, R. A., Bethune, M. G., Thayalakumaran, T., Christen, E. W., & McMahon, T. A. (2008). Management of salt mobilisation in the irrigated landscape–A review of selected irrigation regions. Journal of Hydrology, 351(1-2), 238-252.

Dregne, H. (1991). A new assessment of the world status of desertification. *Desertification Control Bull*, *20*, 6-29.

El Fels, A. E. A., Alaa, N., Bachnou, A., & Rachidi, S. (2018). Flood frequency analysis and generation of flood hazard indicator maps in a semi-arid environment, case of Ourika watershed (western High Atlas, Morocco). Journal of African Earth Sciences, 141, 94-106.

Elango, L., & Ramachandran, S. (1991). Major ion correlations in groundwater of a coastal aquifer. J. Indian Water Resour. Soc, 54-57.

Elfarkh, J., Ezzahar, J., Er-Raki, S., Simonneaux, V., Ait Hssaine, B., Rachidi, S., ... & Jarlan, L. (2020). Multi-Scale Evaluation of the TSEB Model over a Complex Agricultural Landscape in Morocco. Remote Sensing, 12(7), 1181.

Fakir Y., Berjamy B., Le Page M., Sghrer F., Nasah H., Jarlan L., Er Raki S., Simonneaux V., Khabba S. (2015). Multi-modeling assessment of recent changes in groundwater resource: Application to the semi-arid Haouz plain (Central Morocco). EGU General Assembly, Vol. 17, EGU2015-14624.

FAO. 2013. Organic supply chains for small farmer income generation in developing countries – Case studies in India, Thailand, Brazil, Hungary and Africa. Rome.

Feng, Z. Z., Wang, X. K., & Feng, Z. W. (2005). Soil N and salinity leaching after the autumn irrigation and its impact on groundwater in Hetao Irrigation District, China. Agricultural Water Management, 71(2), 131-143.

Fernald, A., Guldan, S., Boykin, K., Cibils, A., Gonzales, M., Hurd, B., … Rodriguez, S. (2015). Linked hydrologic and social systems that support resilience of traditional irrigation communities. Hydrology and Earth System Sciences, 19(1), 293–307.

Fernald, A., Tidwell, V., Rivera, J., Rodríguez, S., Guldan, S., Steele, C., …Cibils, A. (2012). Modeling sustainability of water, environment, livelihood, and culture in traditional irrigation communities and their linked watersheds. Sustainability, 4(11), 2998–3022.

Fisher, R. S., & Mullican III, W. F. (1997). Hydrochemical evolution of sodium-sulfate and sodium-chloride groundwater beneath the northern Chihuahuan Desert, Trans-Pecos, Texas, USA. Hydrogeology journal, 5(2), 4-16.

Flint, A. L., Flint, L. E., Hevesi, J. A., D'Agnese, F., & Faunt, C. (2000). Estimation of regional recharge and travel time through the unsaturated zone in arid climates. GMS, 122, 115-128.

Fniguire, F., Laftouhi, N. E., Saidi, M. E., Zamrane, Z., El Himer, H., & Khalil, N. (2017). Spatial and temporal analysis of the drought vulnerability and risks over eight decades in a semi-arid region (Tensift basin: Morocco). Theoretical and Applied Climatology, 130(1-2), 321-330.

Gao, J., Zou, C., Li, W., Ni, Y., Liao, F., Yao, L., ... & Vengosh, A. (2020). Hydrochemistry of flowback water from Changning shale gas field and associated shallow groundwater in Southern Sichuan Basin, China: Implications for the possible impact of shale gas development on groundwater quality. Science of The Total Environment, 713, 136591.

Gleick, P. H. (2003). Global freshwater resources: Soft-path solutions for the 21st century. Science, 302(5650), 1524–1528.

Goodrich, D. C, Williams, D. G., Unkrich, C. L, Hogan, J. F., Scott, R. L, Hultine, K. R., Pool, D., Coes, A. L, Miller, S. N. 2004. Comparison of Methods to Estimate Ephemeral Channel Recharge, Walnut Gulch, San Pedro River Basin, Arizona. In Recharge and Vadose Zone Processes: Alluvial Basins of the Southwestern United States, ed. by F.M. Phillips, J.F. Hogan, and B. Scanlon, Water Science and Application 9, Washington, DC, American Geophysical Union, p. 77-99. 2004.

Gunda, T., Turner, B. L., & Tidwell, V. C. (2018). The influential role of sociocultural feedbacks on community-managed irrigation system behaviors during times of water stress. Water Resources Research, 54(4), 2697-2714.

Guo, X., Feng, Q., Liu, W., Li, Z., Wen, X., Si, J., … Jia, B. (2015). Stable isotopic and geochemical identification of groundwater evolution and recharge sources in the arid Shule River basin of northwestern China. Hydrological Processes, 29(22), 4703–4718.

Green, C. T., Liao, L., Nolan, B. T., Juckem, P. F., Shope, C. L., Tesoriero, A. J., & Jurgens, B. C. (2018). Regional variability of nitrate fluxes in the unsaturated zone and groundwater, Wisconsin, USA. Water Resources Research, 54(1), 301-322.

Hajhouji, Y., Simonneaux, V., Gascoin, S., Fakir, Y., Richard, B., Chehbouni, A., & Boudhar, A. (2018). Modélisation pluie-débit et analyse du régime d'un bassin versant semi-aride sous influence nivale. Cas du bassin versant du Rheraya (Haut Atlas, Maroc). La Houille Blanche, 3 (2018), 49–62.

Hajhouji Y., Fakir Y., Simonneaux V., Gascoin S., Bouras E.H., Chehbouni A. (2020) Effects of Climate Change at the 2040's Horizon on the Hydrology of the Pluvio-Nival Rheraya Watershed Near Marrakesh, Morocco. In: El Moussati A., Kpalma K., Ghaouth Belkasmi M., Saber M., Guégan S. (eds) Advances in Smart Technologies Applications and Case Studies. SmartICT 2019. Lecture Notes in Electrical Engineering, vol 684. Springer, Cham. https://doi.org/10.1007/978-3-030-53187-4_48

Haj-Amor, Z., Tóth, T., Ibrahimi, M. K., & Bouri, S. (2017). Effects of excessive irrigation of date palm on soil salinization, shallow groundwater properties, and water use in a Saharan oasis. Environmental Earth Sciences, 76(17), 590.

Hamilton, P. A., & Helsel, D. R. (1995). Effects of agriculture on ground-water quality in five regions of the United States. Groundwater, 33(2), 217-226.

Healy, R. W., & Ronan, A. D. (1996). Documentation of computer program VS2DH for simulation of energy transport in variably saturated porous media: Modification of the US Geological Survey's computer program VS2DT. US Geological Survey.

Healy, R. W. (2010). Estimating groundwater recharge. Cambridge University Press.

Heppner, C. S., Nimmo, J. R., Folmar, G. J., Gburek, W. J., & Risser, D. W. (2007). Multiple methods investigation of recharge at a humid-region fractured rock site, Pennsylvania, USA. Hydrogeology Journal, 15(5), 915-927.

Hertig, E., & Jacobeit, J. (2008). Downscaling future climate change: Temperature scenarios for the Mediterranean area. *Global and Planetary Change*, *63*(2-3), 127-131.

Hill, M. J. (1996). Nitrates and nitrites in food and water (Vol. 7). CRC Press.

Hu, Q., Yang, Y., Han, S., & Wang, J. (2019). Degradation of agricultural drainage water quantity and quality due to farmland expansion and water-saving operations in arid basins. Agricultural Water Management, 213, 185-192.

Hock, R., Rasul, G., Adler, C., Cáceres, B., Gruber, S., Hirabayashi, Y., ... & Zhang, Y. (2019). High Mountain Areas: In: IPCC Special Report on the Ocean and Cryosphere in a Changing Climate.

Hoffmann, J. P., Blasch, K. W., Pool, D. R., Bailey, M. A., & Callegary, J. B. (2007). Estimated infiltration, percolation, and recharge rates at the Rillito Creek focused recharge investigation site, Pima County, Arizona. In Ground-water recharge in the arid and semiarid southwestern United States (pp. 185-220).

Holland, J. E., Luck, G. W., & Finlayson, C. M. (2015). Threats to food production and water quality in the Murray–Darling Basin of Australia. Ecosystem services, 12, 55-70.

Immerzeel, W. W., Van Beek, L. P., & Bierkens, M. F. (2010). Climate change will affect the Asian water towers. Science, 328(5984), 1382-1385.

Immerzeel, W. W., Lutz, A. F., Andrade, M., Bahl, A., Biemans, H., Bolch, T., ... & Emmer, A. (2020). Importance and vulnerability of the world's water towers. Nature, 577(7790), 364-369.

Izbicki, J. A., Radyk, J., & Michel, R. L. (2000). Water movement through a thick unsaturated zone underlying an intermittent stream in the western Mojave Desert, southern California, USA. Journal of Hydrology, 238 (3–4), 194–217.

Jacks, G. (1973). Chemistry of ground water in a district in Southern India. Journal of Hydrology, 18(3-4), 185-200.

Jarlan, L., Khabba, S., Er-Raki, S., Le Page, M., Hanich, L., Fakir, Y., ... & Kharrou, M. H. (2015). Remote sensing of water resources in semi-arid Mediterranean areas: The joint international laboratory TREMA. *International Journal of Remote Sensing*, *36*(19-20), 4879-4917.

Jarlan, L., Khabba, S., Szcypta C., Lili-Chabaane Z., Driouech M., Le Page, M.; Hanich, L., Fakir, Y., BOONE A., Boulet G. (2016). Water resources in South Mediterranean catchments, Assessing climatic drivers and impacts. The Mediterranean Region under Climate Change, IRD ÉDITIONS, Sub-chapter 2.3.2, p: 303-308. ISBN : 978-2-7099-2219-7

Jia, H., Qian, H., Zheng, L., Feng, W., Wang, H., & Gao, Y. (2020). Alterations to groundwater chemistry due to modern water transfer for irrigation over decades. Science of The Total Environment, 717, 137170.

Johansson, O., Aimbetov, I., & Jarsjö, J. (2009). Variation of groundwater salinity in the partially irrigated Amudarya River delta, Uzbekistan. Journal of Marine Systems, 76(3), 287-295.

Kadi, M. A., & Ziyad, A. (2018). Integrated water resources management in Morocco. In *Global water security* (pp. 143-163). Springer, Singapore.

Kalbus, E., Reinstorf, F., & Schirmer, M. (2006). Measuring methods for groundwater? Surface water interactions: A review. Hydrology and Earth System Sciences Discussions, 10(6), 873–887.

Kao, Y. H., Liu, C. W., Wang, S. W., & Lee, C. H. (2012). Estimating mountain block recharge to downstream alluvial aquifers from standard methods. Journal of Hydrology, 426, 93–102.

Kendy, E., & Bredehoeft, J. D. (2006). Transient effects of groundwater pumping and surface-water-irrigation returns on streamflow. Water Resources Research, 42, W08415.

Kim, K. (2002). Plagioclase weathering in the groundwater system of a sandy, silicate aquifer. *Hydrological processes*, *16*(9), 1793-1806.

Knowles, N., Dettinger, M. D., & Cayan, D. R. (2006). Trends in snowfall versus rainfall in the western United States. Journal of Climate, 19(18), 4545-4559.

Koch, F. W., Voytek, E. B., Day-Lewis, F. D., Healy, R., Briggs, M. A., Lane Jr, J. W., & Werkema, D. (2016). 1DTempPro V2: New features for inferring groundwater/surface-water exchange. Groundwater, 54(3), 434-439.

Kulongoski, J. T., & Izbicki, J. A. (2008). Simulation of fluid, heat transport to estimate desert stream infiltration. Ground water, 46(3), 462-474.

Kurylyk, B. L., Irvine, D. J., & Bense, V. F. (2019). Theory, tools, and multidisciplinary applications for tracing groundwater fluxes from temperature profiles. WIREs Water, https://doi.org/10.1002/wat2.1329

Kruse, E. G., Bucks, D. A., & von Bernuth, R. D. (1990). Comparison of irrigation systems. In B. A. Steward & D. R. Nielsen (Eds.), Irrigation of agricultural crops (pp. 475–508). Madison, Wis: American Society of Agronomy.

Lambs, L. (2004). Interactions between groundwater and surface water at river banks and the confluence of rivers. Journal of Hydrology, 288 (3–4), 312–326.

Landon, M.K. , Rus, D.L. & Harvey, F.E. (2001). Comparison of Instream Methods for Measuring Hydraulic Conductivity in Sandy Streambeds. Papers in Natural Resources, 154. https://digitalcommons.unl.edu/natrespapers/154.

Le Page, M., Berjamy, B., Fakir, Y., Bourgin, F., Jarlan, L., Abourida, A., ... & Simonneaux, V. (2012). An integrated DSS for groundwater management based on remote sensing. The case of a semi-arid aquifer in Morocco. Water resources management, 26(11), 3209-3230.

Leduc, C., Pulido-Bosch, A., & Remini, B. (2017). Anthropization of groundwater resources in the Mediterranean region: processes and challenges. Hydrogeology Journal, 25(6), 1529-1547.

Li, P., Wu, J., & Qian, H. (2013). Assessment of groundwater quality for irrigation purposes and identification of hydrogeochemical evolution mechanisms in Pengyang County, China. Environmental Earth Sciences, 69(7), 2211-2225.

Li, P., Zhang, Y., Yang, N., Jing, L., & Yu, P. (2016). Major ion chemistry and quality assessment of groundwater in and around a mountainous tourist town of China. Exposure and Health, 8(2), 239-252.

Liu, Y., & Yamanaka, T. (2012). Tracing groundwater recharge sources in a mountain–plain transitional area using stable isotopes and hydrochemistry. Journal of Hydrology, 464, 116–126.

Liu, F., Zhao, Z., Yang, L., Ma, Y., Li, B., Gong, L., & Liu, H. (2020). Phreatic Water Quality Assessment and Associated Hydrogeochemical Processes in an Irrigated Region Along the Upper Yellow River, Northwestern China. Water, 12(2), 463.

Liu, F., Wang, S., Yeh, T. C. J., Zhen, P., Wang, L., & Shi, L. (2020). Using multivariate statistical techniques and geochemical modelling to identify factors controlling the evolution of groundwater chemistry in a typical transitional area between Taihang Mountains and North China Plain. Hydrological Processes, 34(8), 1888-1905.

Malek, K., Reed, P., Adam, J., Karimi, T., & Brady, M. (2020). Water rights shape crop yield and revenue volatility tradeoffs for adaptation in snow dependent systems. Nature communications, 11(1), 1-10.

Manning, A. H., & Solomon, D. K. (2005). An integrated environmental tracer approach to characterizing groundwater circulation in a mountain block. Water Resources Research, 41, W12412.

Marchane, A., Jarlan, L., Hanich, L., Boudhar, A., Gascoin, S., Tavernier, A., … Berjamy, B. (2015). Assessment of daily MODIS snow cover products to monitor snow cover dynamics over the Moroccan atlas mountain range. Remote Sensing of Environment, 160, 72–86.

Marghade, D., Malpe, D. B., & Rao, N. S. (2019). Applications of geochemical and multivariate statistical approaches for the evaluation of groundwater quality and human health risks in a semi-arid region of eastern Maharashtra, India. Environmental Geochemistry and Health, 1-21.

Markovich, K. H., Manning, A. H., Condon, L. E., & McIntosh, J. C. (2019). Mountain-block recharge: A review of current understanding. Water Resources Research, 55, WR025676.

Martinez, J. L., Raiber, M., & Cendón, D. I. (2017). Using 3D geological modelling and geochemical mixing models to characterise alluvial aquifer recharge sources in the upper Condamine River catchment, Queensland, Australia. Science of the Total Environment, 574, 1–18.

Massuel, S., George, B. A., Venot, J. P., Bharati, L., & Acharya, S. (2013). Improving assessment of groundwater-resource sustainability with deterministic modelling: a case study of the semi-arid Musi sub-basin, South India. *Hydrogeology Journal*, *21*(7), 1567-1580.

McCord, J. T., Gotway, C. A., & Conrad, S. H. (1997). Impact of geologic heterogeneity on recharge estimation using environmental tracers: Numerical modeling investigation. Water Resources Research, 33(6), 1229-1240.

Mendez, G. (2005). Evaluation of two low-flow releases from Big Tujunga Reservoir, Los Angeles County. U.S. Geological Survey Scientific Investigation Reports, 5003, 1-53.

Merchán, D., Causapé, J., Abrahão, R., & García-Garizábal, I. (2015). Assessment of a newly implemented irrigated area (Lerma Basin, Spain) over a 10-year period. II: Salts and nitrate exported. Agricultural Water Management, 158, 288-296.

Merchán, D., Sanz, L., Alfaro, A., Pérez, I., Goñi, M., Solsona, F., ... & Casalí, J. (2020). Irrigation implementation promotes increases in salinity and nitrate concentration in the lower reaches of the Cidacos River (Navarre, Spain). Science of The Total Environment, 706, 135701.

Meredith, E., & Blais, N. (2019). Quantifying irrigation recharge sources using groundwater modeling. Agricultural Water Management, 214, 9–16.

Michard, A., Westphal, M., Bossert, A., & Hamzeh, R. (1975). Tectonique de blocs dans le socle atlaso-mesetien du Maroc; une nouvelle interpretation des donnees geologiques et paleomagnetiques. Earth and Planetary Science Letters, 24(3), 363-368.

Mirzavand, M., Ghasemieh, H., Sadatinejad, S. J., & Bagheri, R. (2020). An overview on source, mechanism and investigation approaches in groundwater salinization studies. International Journal of Environmental Science and Technology, 1-14.

Moore, S. J. (2007). Streamflow, infiltration, and recharge in Arroyo Hondo, New Mexico (No. 1703-F). Geological Survey (US).

Moukhchane, M. (1983). Contribution à l'étude des réservoirs profonds de la bordure nord de l'Atlas entre Demnate et Imintanoute (Maroc). France: Besançon.

Nativ, R., & Smith, D. A. (1987). Hydrogeology and geochemistry of the Ogallala aquifer, Southern High Plains. Journal of Hydrology, 91(3-4), 217-253.

Niswonger, R. G., & Prudic, D. E. (2003). Modeling heat as a tracer to estimate streambed seepage and hydraulic conductivity: Heat as a tool for studying the movement of ground water near streams (pp. 81-89).

Niswonger, R. G., Prudic, D. E., Fogg, G. E., Stonestrom, D. A., & Buckland, E. M. (2008). Method for estimating spatially variable seepage loss and hydraulic conductivity in intermittent and ephemeral streams. Water Resources Research, 44, W05418.

Ochoa, C. G., Fernald, A. G., Guldan, S. J., & Shukla, M. K. (2009). Water movement through a shallow vadose zone: A field irrigation experiment. Vadose Zone Journal, 8(2), 414–425.

Ochoa, C. G., Fernald, A. G., Guldan, S. J., Tidwell, V. C., & Shukla, M. K. (2012). Shallow aquifer recharge from irrigation in a semiarid agricultural valley in New Mexico. Journal of Hydrologic Engineering, 18(10), 1219–1230.

Pahud, D. (2002). Geothermal energy and heat storage. Cannobio: SUPSI DCT LEEE. Scuola Universitaria Professionale della Svizzera Italiana.

Panda, B. R., Chidambaram, S., Ganesh, N., Adithya, V. S., Prasanna, M. V., Pradeep, K., & Vasudevan, U. (2018). A hydrochemical approach to estimate mountain front recharge in an aquifer system in Tamilnadu, India. Acta Geochimica, 37(3), 465-488.

Parkhurst, D. L., & Appelo, C. A. J. (1999). User's guide to PHREEQC (Version 2): A computer program for speciation, batch-reaction, one-dimensional transport, and inverse geochemical calculations. Water-resources investigations report, 99(4259), 312.

Partington, D., Shanafield, M., Turnadge, C. (2020). Comparing methods of identifying non-598 stationary, non-linear processes from stream temperature time series data. Earth and Space 599 Science Open Archive, https://doi.org/10.1002/essoar.10504201.1

Pérez-Sirvent, C., Martınez-Sanchez, M. J., Vidal, J., & Sánchez, A. (2003). The role of low-quality irrigation water in the desertification of semi-arid zones in Murcia, SE Spain. Geoderma, 113(1-2), 109-125.

Proust, F. (1961). Etude stratigraphique, pétrographique et structurale du bloc oriental du Massif ancien du Haut-Atlas (Maroc) (Doctoral dissertation).

Qin, D., Qian, Y., Han, L., Wang, Z., Li, C., & Zhao, Z. (2011). Assessing impact of irrigation water on groundwater recharge and quality in arid environment using CFCs, tritium and stable isotopes, in the Zhangye Basin, Northwest China. Journal of Hydrology, 405(1–2), 194–208.

Rajmohan, N., & Elango, L. (2004). Identification and evolution of hydrogeochemical processes in the groundwater environment in an area of the Palar and Cheyyar River Basins, Southern India. Environmental Geology, 46(1), 47-61.

Rau, G. C., Andersen, M. S., McCallum, A. M., Roshan, H., & Acworth, R. I. (2014). Heat as a tracer to quantify water flow in near-surface sediments. Earth-Science Reviews, 129, 40-58.

Rau, G. C., Halloran, L. J.S., Cuthbert, M. O., Andersen, M. S., Acworth, R. I. & Tellam J. H. (2017). Characterising the dynamics of surface watergroundwater interactions in intermittent and ephemeral streams using streambed thermal signatures. Advances in Water Resources, doi: 10.1016/j.advwatres.2017.07.005.

Reid, M. I., Dreiss, S. J. (1990). Modeling the effects of unsaturated, stratified sediments on groundwater recharge from intermittent streams. Journal of Hydrology, (114), 149-174.

Ronan, A. D., Prudic, D. E., Thodal, C. E., & Constantz, J. (1998). Field study and simulation of diurnal temperature effects on infiltration and variably saturated flow beneath an ephemeral stream. Water Resources Research, 34(9), 2137-2153.

Rotiroti, M., Bonomi, T., Sacchi, E., McArthur, J. M., Stefania, G. A., Zanotti, C., … Fumagalli, L. (2019). The effects of irrigation on groundwater quality and quantity in a human-modified hydro-system: The Oglio River basin, Po plain, northern Italy. Science of the Total Environment, 672, 342–356.

Sadat-Noori, S.; Ebrahimi, K.; Liaghat, A. Groundwater quality assessment using the Water Quality Index and GIS in Saveh-Nobaran aquifer, Iran. Environ. Earth Sci. 2014, 71, 3827–3843.

Saidi, M. E. M., Daoudi, L., Aresmouk, M. E. H., Fniguire, F., & Boukrim, S. (2010). The Ourika floods (high atlas, Morocco), extreme events in semi-arid mountain context: Eventos extremos num contexto semiárido montanhoso. Comunicações Geológicas, 97, 113–128.

Scanlon, B. R., Healy, R. W., & Cook, P. G. (2002). Choosing appropriate techniques for quantifying groundwater recharge. Hydrogeology Journal, 10(1), 18–39.

Scanlon, B. R., Jolly, I., Sophocleous, M., & Zhang, L. (2007). Global impacts of conversions from natural to agricultural ecosystems on water resources: Quantity versus quality. Water resources research, 43(3).

Schmadel, N. M., Neilson, B. T., & Stevens, D. K. (2010). Approaches to estimate uncertainty in longitudinal channel water balances. Journal of Hydrology, 394(3–4), 357–369.

Schoeller, H. Qualitative Evaluation of Groundwater Resources. Methods and Techniques of Groundwater Investigations and Development; UNESCO: Paris, France, 1965; Volume 5483.

Schwartz (2016). Factors affecting channel infiltration of floodwaters in Nahal Zin basin, Negev desert, Israel. Hydrological Processes, DOI: 10.1002/hyp.10826

Sefiani, S., El Mandour, A., Laftouhi, N., Khalil, N., Chehbouni, A., Jarlan, L., ... & Nassah, H. (2019). Evaluation of Groundwater Quality and Agricultural use Under a Semi-arid Environment: Case of Agafay, Western Haouz, Morocco. Irrigation and Drainage, 68(4), 778-796.

Shanafield, M., & Cook, P. G. (2014). Transmission losses, infiltration and groundwater recharge through ephemeral and intermittent streambeds: A review of applied methods. Journal of Hydrology, 511, 518–529.

Simmers, I. (2003). Understanding water in a dry environment: Hydrological processes in arid and semi-arid zones (No. 23). AA Balkema Publisher.

Sinan, M. (2000). Méthodologie d'identification, d'évaluation et de protection des ressources en eau des aquifères régionaux par la combinaison des SIG, de la géophysique et de la géostatistique: Application à l'aquifère du Haouz de Marrakech (Maroc). Ecole Mohammadia d'Ingénieurs, Maroc.

Sinan, M., & Razack, M. (2006). Estimation du champ de transmissivité d'un aquifère alluvial fortement hétérogène à partir de la résistance transversale. Application à la nappe du Haouz de Marrakech (Maroc). Revue des sciences de l'eau. Journal of Water Science, 19(3), 221–232.

Sorman, A. U., & Abdulrazzak, M. J. (1993). Infiltration-recharge through Wadi beds in arid regions. Hydrological Sciences Journal, 38(3), 173–186.

Stadler, S., Osenbrück, K., Knöller, K., Suckow, A., Sültenfuß, J., Oster, H., ... & Hötzl, H. (2008). Understanding the origin and fate of nitrate in groundwater of semi-arid environments. Journal of Arid Environments, 72(10), 1830-1842.

Stewart-Deaker, A. E., Stonestrom, D. A., & Moore, S. J. (2007). Streamflow, infiltration, and ground-water recharge at Abo Arroyo, New Mexico: Ground-water recharge in the arid and semiarid southwestern United States. Professional Paper, 83-105.

Stigter, T. Y., Dill, A. C., Ribeiro, L., & Reis, E. (2006). Impact of the shift from groundwater to surface water irrigation on aquifer dynamics and hydrochemistry in a semi-arid region in the south of Portugal. Agricultural water management, 85(1-2), 121-132.

Stonestrom, D. A., & Constantz, J. 2003. Heat as a tool for studying the movement of ground water near streams: US Geological Survey Circular, 1260, 96.

Stonestrom, D. A., Prudic, D. E., Walvoord, M. A., Abraham, J. D., Stewart-Deaker, A. E., Glancy, P. A., et al. (2007). Focused ground-water recharge in the Amargosa Desert basin: Chapter E in Ground-water recharge in the arid and semiarid southwestern United States. Professional Paper, 1703 (No. 1703-E, pp. 107-136). US Geological Survey.

Taylor, R. G., Koussis, A. D., & Tindimugaya, C. (2009). Groundwater and climate in Africa—A review. Hydrological Sciences Journal, 54(4), 655–664.

Talib, M. A., Tang, Z., Shahab, A., Siddique, J., Faheem, M., & Fatima, M. (2019). Hydrogeochemical characterization and suitability assessment of groundwater: A case study in Central Sindh, Pakistan. International journal of environmental research and public health, 16(5), 886.

Turner, B., Tidwell, V., Fernald, A., Rivera, J., Rodriguez, S., Guldan, S., … Cibils, A. (2016). Modeling Acequia irrigation systems using system dynamics: Model development, evaluation, and sensitivity analyses to investigate effects of socio-economic and biophysical feedbacks. Sustainability, 8(10), 1019.

Tweed, S., Leblanc, M., Cartwright, I., Favreau, G., & Leduc, C. (2011). Arid zone groundwater recharge and salinisation processes; an example from the Lake Eyre Basin, Australia. Journal of Hydrology, 408(3-4), 257-275.

Van Steenbergen, F., Haile, A. M., Alemehayu, T., Alamirew, T., & Geleta, Y. (2011). Status and potential of spate irrigation in Ethiopia. Water Resources Management, 25(7), 1899–1913.

Vincy, M. V., Brilliant, R., & Pradeepkumar, A. P. (2015). Hydrochemical characterization and quality assessment of groundwater for drinking and irrigation purposes: a case study of Meenachil River Basin, Western Ghats, Kerala, India. Environmental monitoring and assessment, 187(1), 1-19.

Viviroli, D., Weingartner, R., & Messerli, B. (2003). Assessing the hydrological significance of the world's mountains. Mountain Research and Development, 23(1), 32–40.

Viviroli, D., Dürr, H. H., Messerli, B., Meybeck, M., & Weingartner, R. (2007). Mountains of the world, water towers for humanity: Typology, mapping, and global significance. Water resources research, 43(7).

Viviroli, D., Archer, D. R., Buytaert, W., Fowler, H. J., Greenwood, G. B., Hamlet, A. F., ... & Lorentz, S. (2011). Climate change and mountain water resources: overview and recommendations for research, management and policy. Hydrology and Earth System Sciences, 15(2), 471-504.

Viviroli, D., Kummu, M., Meybeck, M., Kallio, M., & Wada, Y. (2020). Increasing dependence of lowland populations on mountain water resources. Nature Sustainability, 3(11), 917-928.

Vörösmarty, C. J., McIntyre, P. B., Gessner, M. O., Dudgeon, D., Prusevich, A., Green, P., ... & Davies, P. M. (2010). Global threats to human water security and river biodiversity. *nature*, *467*(7315), 555-561.

Wahi, A. K., Hogan, J. F., Ekwurzel, B., Baillie, M. N., and Eastoe, C. J. Geochemical Quantification of Semiarid Mountain Recharge, Ground Water, 46, 414–425.

Walvoord, M. A., Plummer, M. A., Phillips, F. M., & Wolfsberg, A. V. (2002). Deep arid system hydrodynamics 1. Equilibrium states and response times in thick desert vadose zones. Water Resources Research, 38(12), 44-1–44-15.

Wang, X., Chen, F., Hasi, E., & Li, J. (2008). Desertification in China: An assessment. Earth-Science Reviews, 88(3–4), 188–206.

Wheeler, T., & Von Braun, J. (2013). Climate change impacts on global food security. Science, 341(6145), 508-513.

World Health Organization (WHO) (2011) Guidelines for drinking water quality, 4th edn. World Health Organization, Geneva, 978-92-4-154815-1

WHO (2017) Guidelines for drinking water quality: fourth edition incorporating the first addendum. World Health Organization, Geneva

Willis, T. M., Black, A. S., & Meyer, W. S. (1997). Estimates of deep percolation beneath cotton in the Macquarie Valley. Irrigation Science, 17(4), 141–150. Wilson, J. L., & Guan, H. (2004). Mountain-block hydrology and mountain front recharge. Groundwater Recharge in a Desert Environment: The Southwestern United States, 9, 113–137.

Wilson, J. L. and Guan, H. Mountain-block hydrology and mountain-front recharge, in: Groundwater Recharge in a Desert Environment: The Southwestern United States, edited by: Hogan, J. F., Phillips, F. M., and Scanlon, B. R., American Geophysical Union, Washington, D.C., 113–137, 2004.

Yang, Q., Wang, L., Ma, H., Yu, K., & Martín, J. D. (2016). Hydrochemical characterization and pollution sources identification of groundwater in Salawusu aquifer system of Ordos Basin, China. Environmental Pollution, 216, 340-349.

Yechieli, Y., & Wood, W. W. (2002). Hydrogeologic processes in saline systems: playas, sabkhas, and saline lakes. Earth-Science Reviews, 58(3-4), 343-365.

Xiao, J., Wang, L., Deng, L., & Jin, Z. (2019). Characteristics, sources, water quality and health risk assessment of trace elements in river water and well water in the Chinese Loess Plateau. Science of the Total Environment, 650, 2004-2012.

Zaidi, F. K., Nazzal, Y., Jafri, M. K., Naeem, M., & Ahmed, I. (2015). Reverse ion exchange as a major process controlling the groundwater chemistry in an arid environment: a case study from northwestern Saudi Arabia. Environmental Monitoring and Assessment, 187(10), 607.

Zhang, B., Song, X., Zhang, Y., Han, D., Tang, C., Yu, Y., & Ma, Y. (2012). Hydrochemical characteristics and water quality assessment of surface water and groundwater in Songnen plain, Northeast China. Water research, 46(8), 2737-2748.

Zhang, Q., Xu, P., & Qian, H. (2020). Groundwater Quality Assessment Using Improved Water Quality Index (WQI) and Human Health Risk (HHR) Evaluation in a Semi-arid Region of Northwest China. Exposure and Health, 1-14.

Zhang, Y., Xiong, Y., Chao, Y., Fan, R., Ren, F., Xu, B., & Liu, Z. (2020). Hydrogeochemistry and quality assessment of groundwater in Jinghui canal irrigation district of China. Human and Ecological Risk Assessment: An International Journal, 1-18.

Zhu, B. Q., Ren, X. Z., & Rioual, P. (2018). Is the groundwater in the Hunshandake Desert (northern China) of fossil or meteoric water origin? Isotopic and Hydrogeochemical evidence. Water, 10(11), 1515.

Zkhiri, W., Tramblay, Y., Hanich, L., & Berjamy, B. (2017). Regional flood frequency analysis in the High Atlas mountainous catchments of Morocco. Natural Hazards, 86(2), 953-967.

Appendix 1: Stable isotopes and major ions data

Samples	Date	Type	EC (uS/cm)	HCO_3^-	Cl^- (mg/L)	NO_3^- (mg/L)	SO_4^{--} (mg/L)	Na^+ (mg/L)	K^+ (mg/L)	Mg^{++} (mg/L)	Ca^{++} (mg/L)	$\delta^{18}O$ (‰ VSMOV)	δ^2H (‰ VSMOV)
Sp1S	9/2017	Spring	92	34	4.0	2.8	8.9	4.1	0.4	2.9	8.9	-8.1	-52
Sp2S	9/2017	Spring	318	151	14.6	3.9	14.3	9	1.7	6.4	44.9	-7.6	-51
Sp3S	9/2017	Spring	943	371	79.9	5.0	55.2	55.4	3.6	21.5	113.5	-5.9	-36
St1S	9/2017	Streamflow	194	83	10.6	0.5	12.1	7	0.9	5.7	22.1	-7.8	-52
St2S	9/2017	Streamflow	563	256	30.3	1.7	22.5	24.6	2.1	15.2	69.7	-7.5	-49
W2S	9/2017	Well	763	327	51	11.2	30.6	35.1	1.2	27.8	85.6	-7.6	-50
W4S	9/2017	Well	709	224	93.8	7.3	22.3	50.1	1.6	13.1	70.4	-7.9	-52
W21S	9/2017	Well	463	189	35.4	7.1	14.3	25.0	0.7	11.1	50.9	-8.2	-54
W6S	9/2017	Well	1041	227	193.8	4.1	33.2	91.0	2.4	15.6	87.7	-7.6	-50
W5S	9/2017	Well	1458	323	282.3	8.3	41.8	124.0	2.1	23.6	129.8	-7.6	-50
W7S	9/2017	Well	1007	244	171.3	7.3	33.9	73.6	2.1	17.7	96.2	-7.8	-51
W25S	9/2017	Well	1363	295	276.8	3.0	29.6	92.6	0.7	39.5	111.4	-7.0	-45
W8S	9/2017	Well	1087	371	126.5	19.1	39.2	79.3	2.9	24.8	105.7	-7.8	-51
W9S	9/2017	Well	918	317	114.3	12	29.0	95.5	1.2	23.9	63.3	-7.6	-50
W12S	9/2017	Well	591	229	60.9	2.8	16.4	28,81	1.2	12.1	70.5	-7.9	-51
W26S	9/2017	Well	1200	399	175.8		31.8	120.4	1.1	37.5	79.7	-7.1	-47
W15S	9/2017	Well	820	262	113.5	7.6	27.9	51.1	2.1	18	76.5	-7.9	-52
W14S	9/2017	Well	588	224	56.3	8.6	15.9	33.6	1.1	13.3	65.6	-6.6	-40
W18S	9/2017	Well	592	188	69.4	12.3	21.0	45.4	1.2	12.5	55.3	-7.9	-52
W17S	9/2017	Well	2580	278	719.3	4.0	78.2	414.0	2.3	28	90.6	-6.1	-37
W22S	9/2017	Well	293	128	19.7	4.1	11.0	19.2	0.7	6.9	30.4	-8.4	-54
St1N	11/2017	Streamflow	154	63	5.7	1.1	10.7	5.0	0.7	4.2	16.9	-7.8	-51
St2N	11/2017	Streamflow	385	146	2.3	1.8	21.8	20.6	1.9	12.5	31.5	-7.4	-48
Sp1N	11/2017	Spring	77	32	2.4	1.9	5.6	2.6	0.2	1.9	7.4	-8.2	-51
Sp2N	11/2017	Spring	321	150	10.1	3.3	16.2	8.6	1.8	6	42.9	-7.5	-49
Sp3N	11/2017	Spring	653	215	55.6	3.5	56.4	42.1	2.7	15.6	65.0	-5.9	-35
W1N	11/2017	Well	913	315	65.2	48.9	49.1	41.3	0.6	46.7	57.8	-5.3	-30
W2N	11/2017	Well	869	161	172.6	9.4	31.8	63.7	2.9	16.2	68.8	-7.4	-48
W6N	11/2017	Well	672	256	46.6	14	37.8	34.2	1.0	26.2	54.4	-7.5	-48
W5N	11/2017	Well	650	200	71.5	13.8	27	40.0	1.4	12.3	69.0	-7.9	-50
W12N	11/2017	Well	434	143	46.9	1.2	14.9	22.9	0.8	9.6	38.3	-7.9	-50
W16N	11/2017	Well	617	155	71.3	17.5	35.2	32.2	0.8	15.7	45.4	-7.9	-51
W14N	11/2017	Well	345	132	26.7	5.7	11.6	18.2	0.4	7.7	30.5	-6.7	-39
W18N	11/2017	Well	400	112	42.8	10.6	18.3	30.2	0.9	8.8	30.9	-7.9	-51
W17N	11/2017	Well	2620	201	677.9	6.3	93.1	425.5	1.9	22.3	39.6	-6.0	-35
W20N	11/2017	Well	565	227	50.1	7.2	22.8	38.1	0.7	17.1	51.3	-7.9	-51
W21N	11/2017	Well	452	176	32.5	7.8	16.2	24.7	0.7	10.9	55.5	-8.1	-52
W13N	11/2017	Well	739	265	75.3	12.6	25.9	63.0	0.8	22.6	49.7	-7.5	-48
W3N	11/2017	Well	258	132	7.7	8.6	2.5	10.2	0.2	9.4	27.0	-5.1	-30

Rn2N	11/2017	Rain	23	9	0.8		0.7	0.6	0.6	0.1	2.8	-10.5	-74
St1D	12/2017	Streamflow	179	72	7.9	2.6	13.9	6.2	0.9	5.1	19.4	-7.8	-51
St2D	12/2017	Streamflow	423	174	23.8	1.8	24.1	18.6	1.8	10.7	43.8	-7.5	-49
Sp1D	12/2017	Spring	101	27	4.5	3.7	9.6	4.4	0.4	3.1	8.8	-8.2	-52
Sp2D	12/2017	Spring	311	146	10.5	2.3	17.2	8.3	1.6	6.0	42.9	-7.6	-50
W1D	12/2017	Well	912	329	67	50.5	50.7	42.2	0.6	46.9	65.3	-5.3	-31
W2D	12/2017	Well	751	215	100.9	6.5	35.2	76	2.8	12.3	51.5	-7.4	-48
W6D	12/2017	Well	795	342	47	14.5	39.1	34.1	1.0	26.0	83.6	-7.5	-48
W5D	12/2017	Well	757	244	87.0	12.6	30.4	48.5	2.2	14	76.9	-7.8	-50
W10D	12/2017	Well	735	223	94.5	8.0	27.8	46.7	1.3	14.1	66.1	-7.8	-50
W12D	12/2017	Well	586	217	55.6	4	21.1	27.7	1.5	11.5	69.1	-7.7	-49
W16D	12/2017	Well	708	210	79.0	19.2	38.4	34.7	1.0	16.9	81.9	-7.8	-50
W18D	12/2017	Well	539	168	56.5	12.1	22.8	37.1	1	10.7	45.5	-7.8	-50
W20D	12/2017	Well	681	288	49.5	4.0	27.8	47.3	1.0	19.7	57.9	-7.9	-51
W21D	12/2017	Well	440	185	29.3	6.8	14.4	23.8	0.8	11.0	37.7	-8.2	-53
W27D	12/2017	Well	1201	227	262.6	12	47.3	14.6	1.8	26.6	53.9	-6.8	-42
W3D	12/2017	Well	426	218	13.10	13.5	4.7	13.1	1.2	1.5	50.4	-4.8	-28
W13D	12/2017	Well	1020	183	155.7	2.4	149.8	80.6	2.9	27.4	86.0	-6.2	-43
Rn1D	12/2017	Rain	58	27	1.5	1.1	1,4	1.1	0.3	0.4	10.1	-15.3	-111
St1J	1/2018	Streamflow	166	66	6.8	3.7	12.7	5.4	0.8	4.7	18.1	-8.3	-54
St2J	1/2018	Streamflow	422	144	32.2	6.0	27.0	24.1	2.0	8.3	44.5	-7.7	-48
Sp1J	1/2018	Spring	98	34	4.4	3.6	9.5	4.2	0.4	3.0	8.2	-8.8	-53
Sp2J	1/2018	Spring	312	137	11.1	3.7	19.3	8.1	1.5	6.1	43	-7.8	-50
Rn3J	1/2018	Rain	54	18	5.2	1.2	1.8	3.6	0.4	0.5	5.3	-9.2	-48
St1F	2/2018	Streamflow	143	54	5.4	6.1	10.8	4.4	0.5	3.9	15.4	-9.2	-59
St2F	2/2018	Streamflow	271	109	12.5	8.1	16.7	9.6	1.3	6.3	31.0	-8.7	-55
Sp1F	2/2018	Spring	102	34	5.2	5.8	10.4	4.3	0.4	3.1	10.2	-8.6	-54
Sp2F	2/2018	Spring	322	140	10.8	7.1	20.0	8.7	1.5	6.6	44.3	-8.4	-54
Ir1F	2/2018	Irrigation	260	99	12.8	8.7	16.1	9.6	1.2	5.5	30.6	-8.8	-56
Rn1F	2/2018	Rain	20	11	0.7		1.4	1.2	0.2	0.2	2.8	-18.1	-126
Rn2F	2/2018	Rain	11	5	0.9		0.5	0.4	0.1	0,1	1.5	-12.4	-82
Sn1F	2/2018	Snow	7	4	0.2	0.2	0.05	0.1	0.1	0,04	0.9	-15.5	-104
Sn2F	2/2018	Snow	19	9	0.7	0.05	0.1	0.5	0.7	0.1	1.5	-17.1	-117
Sn3F	2/2018	Snow	35	21	0.3	0.1	0.1	0.2	0.2	0.1	5.9	-15.5	-106
St1M	3/2018	Streamflow	104	49	3.2	1.3	6.9	3.3	0.5	3.0	11.4	-9.3	-59
St3M	3/2018	Streamflow	176	61	10.3	9.0	10.5	7.2	1.3	3.8	18.0	-9.3	-60
St5M	3/2018	Tributary	1651	81	532.4	5.5	54.6	246.1	3.0	12.4	99.1	-7.0	-41
St6M	3/2018	Tributary	225	87	9.8	8.8	15.0	9.4	1.5	5.0	26	-8.1	-49
Ir2M	3/2018	Irrigation	242	88	15.6	4.1	13.4	11.5	1.5	4.8	26.0	-8.1	50
Sp1M	3/2018	Spring	98	37	4.4	4	9.1	4.2	0.4	3	9.8	-8.7	-54
Sp3M	3/2018	Spring	847	340	55,65	2.5	70.4	51.3	3.2	19.8	88.0	-6.7	-40
W24M	3/2018	Well	703	293	39.4	16.3	37.8	55.1	0.6	34.9	33.0	-6.0	-35
W2M	3/2018	Well	381	129	28.3	7.5	24.2	26.3	1.7	7.2	35.2	-8.1	-50

W10M	3/2018	Well	1094	301	187.3	11.2	33.2	118.3	0.9	30.5	61.8	-7.5	-48
W16M	3/2018	Well	682	207	70.1	22.1	37.8	30.6	0.9	17.5	77.0	-7.9	-50
W15M	3/2018	Well	818	239	119.5	15.2	42.9	47.3	1.6	22.2	85.6	-7.7	-49
W21M	3/2018	Well	442	181	27.8	9.6	16.0	23.0	0.8	11.1	47.8	-8.1	-52
W22M	3/2018	Well	296	122	17.4	7.2	13.1	18.1	0.6	6.6	30.5	-8.1	-52
W3M	3/2018	Well	409	193	12.5	22.1	3.8	10.8	0.5	12.6	52.1	-5.0	-29
W19M	3/2018	Well	726	220	85.6	22.4	31.1	41.7	1.2	17.9	66.7	-7.6	-48
W11M	3/2018	Well	635	272	47.1	16.2	6.9	36.0	1.2	17.0	56.0	-5.0	-29
W5M	3/2018	Well	763	217	109	10.3	29.6	58.9	1.5	12.6	70.7	-8.1	-51
W23M	3/2018	Well	803	321	67.9	11.8	33.5	87.2	1.1	24.6	42.7	-7.6	-48
Rn1	3/2014	Rain										-8.2	-51
Rn1	3/2014	Rain										-8.3	-51
Rn2	3/2014	Rain										-3.4	-30
Rn3	4/2014	Rain										-3.4	-19
Rn1	11/2014	Rain										-8.9	-61
Rn1	11/2014	Rain										-9.1	-63
Rn3	11/2014	Rain										-7.1	-42
Rn1	12/2014	Rain										-10.8	-77
Rn2	12/2014	Rain										-8.3	-55
Rn2	12/2014	Rain										-8.1	-51
Rn3	12/2014	Rain										-7.1	-43